Assessment of Hydrogeological Characterization and Modelling of Springsheds in a Changing Environment of Central Kashmir

Syed Rouhullah Ali
(2018-815-D)

Division of Soil and Water Conservation Engineering
College of Agriculture Engineering and Technology
Faculty of Horticulture
Sher-e-Kashmir University of Agricultural Sciences and Technology of Kashmir

2022

Assessment of Hydrogeological Characterization and Modelling of Springsheds in a Changing Environment of Central Kashmir

Syed Rouhullah Ali
(2018-815-D)

Thesis

Submitted to

College of Agricultural Engineering and Technology

Faculty of Horticulture

Sher-e-Kashmir
University of Agricultural Sciences and Technology of Kashmir
in partial fulfilment of requirement for the award of the degree of

Doctor of Philosophy in Agricultural Engineering

(Soil and Water Engineering)

2022

Dedicated

To My

Beloved Parents

Sher-e-Kashmir
University of Agricultural Sciences and Technology of Kashmir
Division of Soil & Water Conservation Engineering
College of Agriculture Engineering & Technology,
Faculty of Horticulture

Certificate – I

This is to certify that the thesis entitled **"Assessment of Hydrogeological Characterization and Modelling of Springsheds in a Changing Environment of Central Kashmir"** submitted in partial fulfilment of the requirements for the award of the degree of **Doctor of Philosophy in Agricultural Engineering (Soil and Water Engineering),** to the **College of Agricultural Engineering and Technology, FOH, Sher-e-Kashmir University of Agricultural Sciences and Technology of Kashmir** is a record of bonafide research work carried out by **Mr. Syed Rouhullah Ali (Regd. No. 2018-815-D)** under my supervision and guidance. No part of the thesis has been submitted for any other degree or diploma.

It is further certified that any help or information received during the course of investigation have duly been acknowledged.

(Dr. Junaid N. Khan)
Chairman
Advisory Committee

Endorsed

Head,
Division of Soil and Water Conservation Engineering

Sher-e-Kashmir
University of Agricultural Sciences and Technology of Kashmir
Division of Soil & Water Conservation Engineering
College of Agriculture Engineering & Technology,
Faculty of Horticulture

Certificate – II

We, the members of the Advisory committee of **Mr. Syed Rouhullah Ali (Regd. No. 2018-815-D)**, a candidate for the degree of **Doctor of Philosophy in Agricultural Engineering(Soil and Water Engineering)**, have gone through the manuscript of the thesis entitled, **"Assessment of Hydrogeological Characterization and Modelling of Springsheds in a Changing Environment of Central Kashmir"** and recommend that it may be submitted by the student in partial fulfilment of the requirements for the award of degree.

Advisory Committee

Chairman

Dr. Junaid N. Khan
Professor and Head,
Division of SWCE,
SKUAST-Kashmir, Shalimar

Members

Dr. Rohitashw Kumar
Professor and Associate Dean,
Division of IDE,
SKUAST-Kashmir, Shalimar

Dr. Farooq Ahmad Lone
Professor,
Division of EVS,
SKUAST-Kashmir, Shalimar

Dr. Shakeel Ahmad Mir
Professor,
Division of Agricultural Statistics, SKUAST-Kashmir, Shalimar

Dr. Imran Khan
Associate Professor,
Division of Agricultural Statistics, SKUAST-Kashmir, Shalimar
(Dean Nominee)

Sher-e-Kashmir
University of Agricultural Sciences and Technology of Kashmir
Division of Soil & Water Conservation Engineering
College of Agriculture Engineering & Technology,
Faculty of Horticulture

Certificate – III

This is to certify that the thesis **"Assessment of Hydrogeological Characterization and Modelling of Springsheds in a Changing Environment of Central Kashmir"** submitted by **Mr. Syed Rouhullah Ali (Regd. No. 2018-815-D)**, to the College of Agricultural Engineering and Technology, FOH, Sher-e-Kashmir University of Agricultural Sciences and Technology of Kashmir, in partial fulfilment of the requirements for the award of the degree of **Doctor of Philosophy in Agricultural Engineering (Soil and Water Engineering)** was examined and approved by the Advisory Committee and external examiner on 20/10/2022.

Chairman
Advisory Committee

External Examiner
Dr. Manzoor Ahmad Ahanger
Professor and Head
NIT, Srinagar

Head
Division of Soil and Water Conservation Engineering

Associate Dean,
College of Agricultural Engineering and Technology,
SKUAST-Kashmir

Sher-e-Kashmir
University of Agricultural Sciences and Technology of Kashmir
Division of Soil & Water Conservation Engineering
College of Agriculture Engineering & Technology,
Faculty of Horticulture

Name of the student	:	Syed Rouhullah Ali
Registration No.	:	2018-815-D
Major subject	:	Soil and Water Engineering
Minor subjects	:	Environmental Science/ Agronomy
Major advisor	:	**Dr. Junaid N. Khan** Professor and Head, Division of Soil & Water Conservation Engineering, SKUAST-Kashmir
Title of the Thesis	:	**"Assessment of Hydrogeological Characterization and Modelling of Springsheds in a Changing Environment of Central Kashmir"**

ABSTRACT

A study was planned to assess the effect of changing environment on springshed hydrology of Central Kashmir. A survey and assessment of hydrogeological characteristics were done to map the water resources of Central Kashmir viz. springs, wells, streams, lakes, etc. One hundred eighty-four (184) springs and two hundred eight (208) wells, including both bore-wells and dug-wells, were geotagged and further used for modelling purposes in the study area. Five springs among the surveyed springs were selected for periodic discharge measurement for 21 months. Considering the environmental change, future projections of the climate were generated using RCP 4.5 and 8.5 scenarios of HadGEM GCM data. Modelled data were corrected using the observed data of the same time period with the application of two simple methods, viz. modified difference approach and linear scaling method. The linear scaling method performed better than the modified difference approach with RMSE near the observed data after correction. The correction functions derived by the LS method were further used to generate the corrected future scenarios. The future scenarios

generated were divided into three time periods, viz. near future (NF), mid future (MF), and far future (FF). Future climate scenarios were compared with the baseline time period, which is the observed set of meteorological variables. The detailed mapping of the study area was done, and various thematic maps were prepared. These maps also served as input to the models. Land use and land cover change matrix were also defined between the two time periods, 2000 and 2017. The study area was analyzed for groundwater recharge potential and rainwater harvesting suitability to identify the potential and suitable zones in the area. Integrated catchment modelling was done with the help of the SWAT and MODFLOW models for the study area. The inputs like soil, LULC, weather data, aquifer properties, etc., were given to simulate the model for the study area under both the scenarios considered and compared with the baseline. The developed models were coupled using the SWAT-MODFLOW interface.

The results inferred that the climate projections for the 21st century showed an increase in average annual temperature under both scenarios and for both stations, AMFU Shalimar and IMD Srinagar. The maximum increase was predicted for the Shalimar station under both scenarios compared to the IMD Srinagar station, and the maximum increase was predicted under the RCP 8.5 scenario of 6.91 ^{o}C (FF) for AMFU, while 5.72 ^{o}C (FF) was predicted for the IMD station. The precipitation would increase throughout the future, and the maximum increase would be (47.29%) from the baseline under RCP 8.5 for Shalimar station. In the case of the IMD station, the precipitation would increase in the near future and then decrease in the mid and far future. The average streamflow in the Dal catchment is increasing, whereas, in other catchments, the streamflow shows a decreasing trend under the scenarios considered. The study region's flow budget indicated overall water extraction from the groundwater systems by -7001.23 and -11003.15 m^3/day during RCP 4.5 and 8.5, respectively, which resulted in a groundwater table drop/decline in Central Kashmir. Good areal coverage has been analyzed for groundwater recharging potential and rainwater harvesting suitability level, which may be used for recharging the local groundwater resources. The average discharge from treated and managed springs was almost constant throughout the recording period. Some of the springs and wells showed an increase in flow mainly due to the constructed water harvesting structures and fewer LULC changes in the nearby areas. Seasonal variation in spring discharge was also observed in the maximum of the springs under consideration. Forest class has shown the maximum negative change in the last two decades, which may concern the recharging in the higher Himalayan regions of Central Kashmir.

The study showed how GIS could leverage digital data to determine the optimum sites for groundwater and rain/snow water harvesting. A zonation helps manage water resources, especially springs in the studied region. Identification of groundwater recharge potential zones (GWRP) & water harvesting suitability levels (WHSL) in the region may effectively reduce the time, labor, and money

and consequently allows swift decision-making for sustainable water resources management, notably spring rejuvenation, to maintain water security in the water-scarce parts of the Central Kashmir Himalayas. As several sources of uncertainty are linked with the prediction of environmental change, the results reported here should be interpreted as trends and not as exact quantitative predictions of hydrological changes.

Key words: Central Kashmir, springshed, RCP 4.5, RCP 8.5, linear scaling, modified difference approach, SWAT, MODFLOW.

Signature of Student

Dated : _____

Signature of Major Advisor

Dated : _____

ACKNOWLEDGEMENT

In the name of Allah, who is the most Merciful, most compassionate, and most Gracious.

All praise Allah, who bestowed upon me the life then health, sense, and courage to go through this crucial juncture. Infinite peace, blessings, and salutes are upon the most revered Prophet Muhammad (PBUH), his family, and his companions.

Indeed, I take this opportunity to express my sincere and profound gratitude to Dr. Junaid N. Khan, Professor & Head, Division of Soil and Water Conservation Engineering, COAE&T, SKUAST-Kashmir, Shalimar, chairman of my advisory committee for his keen interest, benevolent guidance, valuable suggestions during the entire course of the investigation. His dynamic attitude, inspiring guidance, wholehearted encouragement, facile suggestions, and constructive criticism with a calm exposure led this uphill task to its successful completion and shall remain a lifelong gifted memory for me. I deem it my privilege to work under his able guidance.

With enormous gratification, I express my deep sense of gratitude to Dr. Rohitashw Kumar, Professor & Associate Dean; College of Agricultural Engineering & Technology, SKUAST-K, and co-chairman of my advisory committee for his constant and relentless guidance, sympathetic attitude, earned suggestions, insightful comments, and valuable discussion during the research. I am indebted to him for numerous clarifications and encouragement that helped me believe in myself while preparing this manuscript.

I am highly grateful for the constant and painstaking guidance, encouragement, suggestions, and sustained efforts of the other members of my advisory committee viz; Dr. Farooq Ahmad Lone, Professor, Division of Environmental Science; Dr. Shakeel Ahmad Mir, Professor, Division of Agricultural Statistics; Dr. Imran Khan, Associate Professor, Division of Agricultural Statistics, SKUAST Kashmir, (Dean P. G. Nominee), for their collaboration, guidance, wholehearted support, timely help and valuable suggestions during my research work.

It gives me great pleasure to place my deep sense of gratitude to the Division of Soil and Water Conservation Engineering, Division of Environmental Science, and College of Agricultural Engineering & Technology for providing me necessary facilities for the smooth conduct of my research work.

I extend my grateful thanks to all the staff members of the College of Agricultural Engineering & Technology, SKUAST-K, for their support and cooperation from time to time. I am also highly thankful to the Soil and Water Conservation Engineering Laboratory staff, with special reference to Mrs. Qazi Gousia, Junaid Mir & Abdul Rashid, who helped me with the field survey & experiments.

Completion of this work was only possible due to the cooperation and help of many people. I shall be failing in my duty if I do not record my indebtedness to my friends and colleagues, Mehraj ud Din Dar, Shakeel Ahmad Bhat, Sabah Prvaze, and other seniors and juniors for providing constant inspiration, moral encouragement, countless blessing, everlasting love and support without which I might not have succeeded at any phase of my life.

I am graciously thankful to ARIS and Library staff members of SKUAST-K for their constant encouragement, valuable suggestions, and generous help during the preparation of this manuscript.

I unfeignedly owe my parents tremendous filial respect and gratitude for their unending love and affection. They have been instrumental in every success that I have achieved. My family deserves all the credit and accolades earned by this achievement of this distinction. You are and will always remain my true energy and strength. I am colossally grateful to my parent's unconditional love and support, Mr.Syed Mohd Taqi and Mrs. Fatima Bano, and my beloved brothers, Mr. Syed Mudasir Ali and Mr. Syed Zaffer Ali, and other family members. Their presence in my life has been a solace of my eyes bestowed on me by my Lord, Allah, and the Almighty. My love increases for them with every passing day.

Last but not least, I thank all those who helped me anyway during the course of my study. I thank them one and all.

Syed Rouhullah Ali

Place: Shalimar, Srinagar

Dated:

CONTENTS

Chapter No.	Particulars	Page No.
1.	INTRODUCTION	1-5
2.	REVIEW OF LITERATURE	6-34
2.1	Climate change models	6-12
2.2	GIS applications for water resources management	12-14
2.3	Hydrogeological characterization and water demand of Himalayan regions	14-16
2.4	Integrated catchment modelling (Surface and groundwater simulation modeling)	16-26
2.5	Effect of changing environmental conditions on hydrology	26-34
3.	MATERIALS AND METHODS	35-72
3.1	Description of the study area	36-38
3.2	Materials used	38-41
3.3	Spring waterbody and well survey	41
3.4	Creating a monitoring system to collect data on spring discharge regularly	41-42
3.5	Future climate scenario generation	43-46
3.6	Comprehensive mapping and conceptual layouts	47-50
3.7	Land use/Land cover change detection/matrix	50-52
3.8	Identification of recharge areas and rainwater harvesting suitability	52-54

3.9	Geophysical exploration for lithological investigation and groundwater validation	54-56
3.10	Modelling of catchments (surface, groundwater modeling and coupling of models developed)	57-72
3.11	Measuring the impact of changing environment and suggesting the best measures for springshed management.	72
4.	EXPERIMENTAL FINDINGS	73-114
4.1	Bias computation and correction of modelled climate data	74-88
4.2	Future Climate Scenarios under RCP 4.5 and 8.5 scenarios for AMFU Shalimar	89
4.3	Future Climate Scenarios under RCP 4.5 and 8.5 scenarios for IMD Srinagar station	90
4.4	Land use and land cover (LU/LC) change detection in the Central Kashmir	91-93
4.5	Delineation of groundwater recharge potential zones of the Central Kashmir	93-94
4.6	Identification of rainwater harvesting suitability level of Central Kashmir	94-96
4.7	Vertical Electrical Sounding (VES) analysis of the subsurface layers of the Central Kashmir	96-99
4.8	Parameter sensitivity analysis, calibration, and validation of the model	99-101
4.9	Streamflow of various catchments of Central Kashmir under different RCP scenarios	101-103
4.10	Groundwater head and water-table depth of the various catchments of Central Kashmir under different RCP scenarios	103-106
4.11	Simulation of groundwater model and groundwater behavior for Central Kashmir	106-108

4.12	Spring discharge behavior during the reporting period	108-113
4.13	Effect of changing environmental conditions on springshed hydrology	113-114
5.	DISCUSSION	115-120
5.1	Climate change prediction	115-116
5.2	Hydrogeological investigation of the study area	116
5.3	Groundwater recharging potential and rainwater harvesting suitability with GIS approach	117
5.4	Streamflow behavior of the Central Kashmir	117-118
5.5	Groundwater behaviors of the Central Kashmir	118-119
5.6	Suggestive conservation measures	119-120
6.	SUMMARY AND CONCLUSION	121-125
	LITERATURE CITED	i-xxii

LIST OF TABLES

Table No.	Particulars	Page No.
3.1	Central Kashmir Himalaya geological formation stratigraphic sequence	38
3.2	Data sets and their sources used for the study	39
3.3	Details of the instruments used for the study	41
3.4	Climate models, resolution, and scenarios involved in the present study	43
3.5	RMSE and NRMSE values of different models selected for the study area	44
3.6	Datasets used for the LU/LC map generation	52
3.7	Material type and hydraulic conductivity (K) values used for different lithological units	68
3.8	Predicted average annual precipitation and computed recharge for the different scenarios for Central Kashmir	71
4.1	Correction functions using modified difference approach for modelled daily temperature and precipitation for AFMU SKUAST-Kashmir under RCP 4.5	78
4.2	Correction functions using modified difference approach for modelled daily temperature and precipitation for AFMU SKUAST-Kashmir under RCP 8.5	79
4.3	Corrections using linear scaling for modelled daily temperature and precipitation for AFMU SKUAST-Kashmir under RCP 4.5	80
4.4	Corrections using linear scaling for modelled daily temperature and precipitation for AFMU SKUAST-Kashmir under RCP 8.5	80
4.5(a)	Statistical parameters of the average annual AFMU SKUAST observed, modelled and model corrected T_{max}, T_{min}, and precipitation by modified difference and linear scaling method under RCP 4.5 Scenario	81
4.5(b)	Statistical parameters of the average annual AFMU SKUAST observed, modelled and model corrected T_{max}, T_{min}, and precipitation by modified difference and linear	82

	scaling method under RCP 8.5 Scenario	
4.6	Correction functions derived using modified difference approach for modelled daily temperature and precipitation for IMD Srinagar Station under RCP 4.5	83
4.7	Correction functions derived using modified difference approach for modelled daily temperature and precipitation for IMD Srinagar Station under RCP 8.5	84
4.8	Corrections derived using linear scaling for modelled daily temperature and precipitation for IMD Srinagar Station under RCP 4.5	85
4.9	Corrections derived using linear scaling for modelled daily temperature and precipitation for IMD Srinagar Station under RCP 8.5	85
4.10(a)	Statistical parameters of the average annual IMD Srinagar Station observed, modelled and model corrected T_{max}, $T_{min,}$ and precipitation by modified difference and linear scaling method under RCP 4.5 Scenario	86
4.10(b)	Statistical parameters of the average annual IMD Srinagar Station observed, modelled and model corrected T_{max}, $T_{min,}$ and precipitation by modified difference and linear scaling method under RCP 8.5 Scenario	87
4.11	Average annual based climate predictions for AFMU SKUAST Station using LS corrected modeled data	88
4.12	Average annual based climate predictions for IMD Srinagar Station using LS corrected modeled data	88
4.13	Land Use/Land Cover statistics from 2000 to 2017	93
4.14	Groundwater recharge potential zones and categorization	94
4.15	Rainwater harvesting suitability level and categorization of groups in Central Kashmir	95
4.16	Summary of VES model resistivity values and their corresponding thickness and depth for SKUAST Kashmir, Shalimar Campus	98
4.17	Summary of VES model resistivity values and their corresponding thickness and depth for SKUAST Kashmir,	98

	Shuhama Campus	
4.18	Summary of VES model resistivity values and their corresponding thickness and depth for KVK, Budgam	99
4.19	Summary of evaluation coefficients for calibration and validation	100
4.20	Average Streamflow (Cumec) for the period 2021-2095 during the different scenarios in Central Kashmir	103
4.21	Groundwater Head (m) during the different scenarios in Central Kashmir	105
4.22	Flow budgeting of Central Kashmir under different scenarios	108
4.23	Discharge of springs for different months in Budgam town	110
4.24	Discharge of spring for different months in SKUAST Shalimar	111
4.25	Discharge of spring for different months in Khag village	112
4.26	Discharge of spring for different months in Chatterhama village	113

LIST OF FIGURES

Fig. No.	Particulars	After Page No.
3.1	Location map of the Central Kashmir	41
3.2	Spring location map of Central Kashmir	41
3.3	Well location map of Central Kashmir	41
3.4	Various thematic maps generated using different datasets for Central Kashmir	50
3.5	Methodological steps for LU/LC change matrix	52
3.6	Methodology adopted for the identification of rainwater harvesting suitability	52
3.7	Methodology adopted for the identification of potential groundwater zonation	55
3.8	Working steps followed during geophysical groundwater resistivity investigation	55
3.9	Working principle of the groundwater resistivity meter	56
3.10	Methodological steps followed during interpretation of resistivity data	56
3.11	Framework for streamflow simulation using the QSWAT model	62
3.12	Framework for SWAT model calibration and validation	62
3.13	Framework of the groundwater modeling simulation using GMS software	66
4.1(a)	Biases in average modelled data of T_{max}	74
4.1(b)	Biases in average modelled data of T_{min}	74
4.1(c)	Biases in average modelled data of Precipitation	74

4.2	Change in average temperature from baseline in different time slices for AMFU Shalimar	74
4.3(a)	Average temperature trend during future under RCP 4.5 scenario for AMFU Shalimar	90
4.3(b)	Average temperature trend during future under RCP 4.5 scenario for AMFU Shalimar	90
4.4	Change in average annual precipitation from baseline in different time slices for AMFU Shalimar	90
4.5	Change in average temperature in different time slices in future for IMD Srinagar	90
4.6(a)	Average temperature trend during future under RCP 4.5 scenario for IMD Srinagar	90
4.6(b)	Average temperature trend during future under RCP 8.5 scenario for IMD Srinagar	90
4.7	Change in average annual precipitation from baseline in different time slices for IMD Srinagar	90
4.8(a)	LU/LC of Central Kashmir generated from LISS III 2000.	93
4.8(b)	Percentage area of LU/LC categories, 2000	93
4.9(a)	LU/LC of Central Kashmir generated from LISS III 2017	93
4.9(b)	Percentage area of LU/LC categories, 2017	93
4.10	Percentage change of LU/LC categories, 2000 & 2017	93
4.11	Analysis of conversion of different LU/LC categories of Central Kashmir	93
4.12(a)	Groundwater recharge potential zones of Central Kashmir	94
4.12(b)	Groundwater recharge potential zones and springs geotagged in Central Kashmir	94
4.13	Percentage area of groundwater recharge potential zones in Central Kashmir	94

4.14(a)	Rainwater harvesting suitability level map of Central Kashmir	95
4.14(b)	Rainwater harvesting suitability level map and springs geotagged in Central Kashmir	95
4.15	Percentage area of rainwater harvesting suitability level in Central Kashmir	95
4.16(a)	Observed and Simulated hydrographs for calibration of Dal catchment	102
4.16(b)	Observed and Simulated hydrographs for validation of Dal catchment	102
4.17(a)	Observed and Simulated hydrographs for calibration of Sindh catchment.	102
4.17(b)	Observed and Simulated hydrographs for validation of Sindh catchment	102
4.18(a)	Observed and Simulated hydrographs for calibration of Dudhganga catchment.	102
4.18(b)	Observed and Simulated hydrographs for validation of Dudhganga catchment	102
4.19(a)	Observed and Simulated hydrographs for calibration of Sukhnag catchment	102
4.19(b)	Observed and Simulated hydrographs for validation of Sukhnag catchment	102
4.20(a)	Streamflow of the Dal catchment in future under RCP 4.5 scenario	104
4.20(b)	Streamflow of the Dal catchment in future under RCP 8.5 scenario	104
4.21(a)	Streamflow of the Sindh catchment in future under RCP 4.5 scenario	104
4.21(b)	Streamflow of the Sindh catchment in future under RCP 8.5 scenario	104

4.22(a)	Streamflow of the Dudhganga catchment in future under RCP 4.5 scenario	104
4.22(b)	Streamflow of the Dudhganga catchment in future under RCP 8.5 scenario	104
4.23(a)	Streamflow of the Sukhnag catchment in future under RCP 4.5 scenario	104
4.23(b)	Streamflow of the Sukhnag catchment in future under RCP 8.5 scenario	104
4.24(a)	Dal catchment groundwater head (amsl) during baseline	106
4.24(b)	Dal catchment watertable depth (mbgl) during baseline	106
4.25(a)	Dal catchment groundwater head (amsl) during RCP 4.5 scenario	106
4.25(b)	Dal catchment watertable depth (mbgl) during RCP 4.5 scenario	106
4.26(a)	Dal catchment groundwater head (amsl) during RCP 8.5 scenario	106
4.26(b)	Dal catchment watertable depth (mbgl) during RCP 8.5 scenario	106
4.27(a)	Sindh catchment groundwater head (amsl) during baseline	106
4.27(b)	Sindh catchment watertable depth (mbgl) during baseline	106
4.28(a)	Sindh catchment groundwater head (amsl) during RCP 4.5 Scenario	106
4.28(b)	Sindh catchment watertable depth (mbgl) during RCP 4.5 scenario	106
4.29(a)	Sindh catchment groundwater head (amsl) during RCP 8.5 Scenario	106
4.29(b)	Sindh catchment watertable depth (mbgl) during RCP 8.5 scenario	106
4.30(a)	Dudhganga catchment groundwater head (amsl) during baseline	106

4.30(b)	Dudhganga catchment watertable depth (mbgl) during baseline	106
4.31(a)	Dudhganga catchment groundwater head (amsl) during RCP 4.5 scenario	106
4.31(b)	Dudhganga catchment watertable depth (mbgl) during RCP 4.5 scenario	106
4.32(a)	Dudhganga catchment groundwater head (amsl) during RCP 8.5	106
4.32(b)	Dudhganga catchment watertable depth (mbgl) during RCP 8.5	106
4.33(a)	Sukhnag catchment groundwater head (amsl) during baseline	106
4.33(b)	Sukhnag catchment watertable depth (mbgl) during baseline	106
4.34(a)	Sukhnag catchment groundwater head (amsl) during RCP 4.5 scenario	106
4.34(b)	Sukhnag catchment watertable depth (mbgl) during RCP 4.5 scenario	106
4.35(a)	Sukhnag catchment groundwater head (amsl) during RCP 8.5	106
4.35(b)	Sukhnag catchment watertable depth (mbgl) during RCP 8.5	106
4.36(a)	Groundwater head of Central Kashmir during baseline time period	108
4.36(b)	Groundwater head of Central Kashmir during RCP 4.5 scenario	108
4.36(c)	Groundwater head of Central Kashmir during RCP 8.5 scenario	108
4.37(a)	Discharge of Budgam-I spring and cumulative precipitation for different months in Budgam town	108
4.37(b)	Discharge of Budgam-II spring and cumulative precipitation for different months in Budgam town	114

4.37(c)	Discharge of SKUAST Shalimar spring and cumulative precipitation for different months	114
4.37(d)	Discharge of Khag spring and cumulative precipitation for different monthsal catchment groundwater head (amsl) during baseline	114
4.37(e)	Discharge of Chatterhama spring and cumulative precipitation for different months	114

LIST OF PLATES

Plate No.	Particulars	After page No.
1	Marksim DSSAT weather file generator screenshot for AMFU Shalimar.	44
2	Marksim DSSAT weather file generator screenshot for IMD Srinagar.	44
3	Field investigation of groundwater resistivity profiling in Central Kashmir	55
4	Interpretation of groundwater resistivity data using INTERPEX 1D software	56
5	SWAT-MODFLOW interface for creating a fully linked surface and groundwater model	56

LIST OF ABBREVIATIONS

UNESCO	United Nations Educational, Scientific and Cultural Organization
UNCCD	United Nations Convention to Combat Desertification
NDF	Nordic Development Fund
ICIMOD	International Centre for Integrated Mountain Development
GIS	Geographic Information System
IPCC	Intergovernmental Panel on Climate Change
GHG	Greenhouse Gases
SRES	Special Report on Emission Scenarios
CMIP	Coupled Model Intercomparison Project
HadCM3	Hadley Centre Coupled Model Version 3
GCMs	General Circulation Models
RCMs	Regional Climate Models
RCPs	Representative Concentration Pathways
SDSM	Statistical Downscaling Model
NCEP	National Centre for Environmental Prediction
HAD GEM-ES	Hadley Center Global Environment Model 2 - Earth System
IMD	Indian Meteorological Department
AMFU	Agricultural Meteorological Field Unit
NF	Near Future
MF	Mid Future
FF	End Future
GWRP	Groundwater Recharge Potential Zone
WHSL	Water Harvesting Suitability Level
GMS	Groundwater Modeling System

SWAT	Soil and Water Assessment Tool
HRUs	Hydrologic Response Units
SUFI	Sequential Uncertainty Fitting Algorithm
MCA	Multi Criteria Analysis
AHP	Analytic Hierarchy Process
WOP	Weighted Overlay Process
CWI	Standardized Compound Weight Index
LULC	Land Use Land Cover
DEM	Digital Elevation Model
ASTER	Advanced Space Borne Thermal Emission And Reflection Radiometer

Chapter-1

INTRODUCTION

Freshwater is one of the most limited resources on the planet and is essential to many areas of human existence. Furthermore, water is a scarce resource in India, especially in the Himalayan region. Because the country and Himalayan region generally have uneven rainfall distribution, which is the major factor of water scarcity. In addition, the growing demand for freshwater due to population growth, economic growth, urbanization, and water pollution magnifies the scarcity (Molobela and Sinha, 2011; Du Plessis, 2017). In many parts of the country, freshwater supplies are scarce or nonexistent. According to specific assessments (Molobela and Sinha, 2011), water shortage would grow more complicated owing to rising water demand and economic tensions. As a result, the country's water resources should be managed to ensure their optimum and smart usage without jeopardizing the needs of future generations.

Water has social, economic, and environmental values and is vital for development (UNESCO, 2011). Global changes affect water resources significantly. Population and economic expansion, climate change, land use/cover change, and environmental pollution contribute to freshwater scarcity (Dolman *et al*., 2003; Millennium Ecosystem Assessment, 2005; UNESCO, 2011 and UNCCD, 2017). Natural or anthropogenic factors cause environmental changes. Environmental change drivers are interconnected, according to reports. Variations in land use and land cover contribute to climate change, exacerbating freshwater shortages and ecosystem disturbances (Dolman *et al*., 2003). Population and economic growth influence land use/cover change.

According to experts, uncontrolled groundwater exploitation and inadequate aquifer recharge are the primary causes of groundwater depletion in many areas of India. In many places on the earth, groundwater is a significant drinking water supply and an essential irrigation water source. More than 95% of

the world's largest freshwater is buried under the earth's crust, at depths of up to 800 meters, with just a meager 1.5% found in surface water bodies like rivers and lakes. Thus, groundwater will continue to be the primary supply of fresh water in the future. However, the depletion of aquifers due to overuse and increasing groundwater contamination threatens a reliable supply of clean water and ecological sustainability (Famiglietti, 2014).

The water balance analysis of a catchment shows its inflow and outflow (Ahmad *et al.,* 2010; Entekhabi *et al.,* 2014). Freshwater, encompassing surface and groundwater, is a renewable resource whose distribution is determined by freezing and thawing, precipitation, runoff, and evapotranspiration (Shams *et al.*, 2013). Water balance allows us to assess and analyze water resources and anticipate their dynamics under environmental changes (Sokolov and Chapman, 1974). Due to spatial and temporal volatility, its distribution is vital in the hydrologic cycle (Ahmad *et al.,* 2010).

In the environment, springs serve as a natural discharge point for groundwater. Pressure is exerted on the water already in the aquifer when precipitation enters and recharges it. Water moves through fractures and tunnels in the aquifer as a result of this pressure. At springs, this water may flow out naturally to the ground surface. They supply baseflow for streams and are important isothermal water sources for trout streams. The different lithology and hydraulic properties of the rock types make some settings more likely for springs. Springsheds are locations within groundwater and surface water basins that contribute to spring discharge (Copeland, 2003). Groundwater springshed boundaries may not always match up with surface boundaries. They change as the groundwater level rises and falls. We must understand the geologic background and source of spring's water to conserve and safeguard them.

Many rural people in hilly locations, such as the Himalayas, rely on springs for agricultural and domestic water (Pandit *et al*., 2007; Vashisht and Sharma, 2007; NDF, 2014). Natural stresses (particularly climate change) and

poor watershed management have reduced many Himalayan spring's outputs (Agarwal *et al*., 2012). For example, Valdiya and Bartarya (1989) found a 40% decline in spring discharge in the Kumaun Himalaya region from 1951 to 1986, mainly due to land-use patterns and vegetation. They found that 75% of springs are dry, and the average streamflow is reduced by 40%. Mahamuni and Kulkarni (2012) found that approximately 8,000 settlements in the Himalayas have severe water shortages owing to springs drying up. ICIMOD (2015) found that in Nepal's mid-hill area, springs were drying up due to a combination of biophysical (climate variability, land-use change) and socioeconomic (spring maintenance) factors. Vashisht (2008) stated that managing springs and minor seepage canals in the Siwalik foothill regions of the Himalayas might prevent water scarcity. Drying springs and water shortage challenges highlight the need to better understand spring hydrology, particularly in the Himalayas. Negi (2002) reviewed micro and mesoscale research to help control Himalayan springs. Researchers Bruijnzeel and Bremmer (1989) and Alford (1992) determined that contemporary Himalayan hydrological processes are poorly understood, and management strategies based on limited knowledge would not address water scarcity. So spring research is needed. Watershed modifications have improved the water supply for rural populations in the Himalayas. Most operations ignored karst geology and favored aquifer routes (Agarwal *et al*., 2012). Rare are studies assessing the benefits and durability of these measures, particularly on spring discharge. As a result, these treatments have minimal influence on spring discharge. Inadequate research and a lack of synthesis of published and grey literature have hampered the understanding of Himalayan springs.

The Himalayan mountain springs act as the lifeline for both rural and urban communities. Out of the 5 million springs across India, 3 million, i.e., more than 60%, are in the Indian Himalayan region alone, as per the released "Report of Working Group 1" by the NITI Aayog (NITI Aayog, 2017). Over 200 million people in India depend on springs. Out of which, 50 million people are in the 11

States and 2 UTs of the IHR. Thousands of people rely on springs for water in the Kashmir Himalayas, yet their systems are unknown. Many rural people in the Himalayas are dependent on springs for agricultural and domestic water. Out of 6553 villages, 3313 have springs, with 50.6% of villages having springs in UT of J&K (NITI Aayog, 2017).

In the fragile Himalayan mountain ecosystems, the current trends reflect higher discharge rates than replenishment. High population expansion and urbanization are causing water competition in the Himalayan watershed. Timing and volume changes in rural water supply and irrigation affect water security and agricultural productivity (IPCC, 2001). Existing watershed management techniques are insufficient based on limited scientific field research and static policy guidelines. Himalayan watersheds require GIS-based water resource planning (Rana and Gupta, 2009). Recent innovations in watershed-based water management aim to develop a distributed hydrological model with 'what-if' scenario capabilities for planners employing spatial and non-spatial data sets for selected watersheds. Substantial efforts have been made to optimize water resource management and build decision support systems. For Himalaya to optimize water allocation strategy, seasonality of water sources and inaccessibility of perennial water resources must be considered.

Even though springs in J&K are an important natural source of water for the entire Himalayan belt of the UT, no serious efforts have been made to rejuvenate them. Instead, a massive plan for a centralized pipe water delivery system was implemented, but due to its poor maintenance and a lack of community participation in its management fell short of meeting local's needs. There is widespread agreement that rural residents in the Himalayas who live in inaccessible areas need to revive and improve traditional water sources water yield to meet their daily water demands.

Considering the points mentioned above, this study considered all the factors contributing to water harvesting and recharging of the groundwater

resources of Central Kashmir. The hydrogeological properties, modelling of springsheds, and regeneration techniques for springs in the Kashmir Himalayas, which have hardly been taken into account earlier, were investigated from a spring rejuvenation perspective. The current work aims to establish a springshed mapping and modelling technique in Central Kashmir, integrating climatic, surface, and groundwater models with remote sensing and GIS technology under the following objectives:

1. To generate future climate scenarios for the study area.
2. To simulate the surface and groundwater models for the study area.
3. To analyze the impact of changing environment on springshed hydrology.

Chapter-2

REVIEW OF LITERATURE

A comprehensive assessment of the literature review provides a pathway to strategize the work activities mainly to overcome barriers and identify research gaps. It provides an excellent overview of work carried out in the targeted research area and identification of future developments. The assessment and investigation expose the complications attached to the previous research activities and provides an opportunity for finding corrective measures. This chapter is devoted to analyzing the research work in assessing hydrogeological characterization and modeling of springsheds under changing environmental conditions. The available review of the present study has been organized and presented as follows:

2.1 Climate change models

Climate models are computer-based simulations of the climate system based on mathematical equations. Physical rules such as the conservation of mass, energy, and momentum inform these models based on a multitude of experimental evidence and research. To simulate and generate data on temperature, precipitation, and wind, regional climate models (RCMs) use "Emission scenarios" developed by an intergovernmental panel on climate change (IPCC). The model runs to derive atmospheric concentrations of greenhouse gases (GHG) (each run is different as the weather is partly a stochastic phenomenon). Observations of the atmosphere, oceans, cryosphere, and land surfaces are compared to model simulations regularly and in greater depth. The predictions must either undergo statistical downscaling or dynamic downscaling to integrate local topological factors and analyze potential regional implications on water resources and agriculture. Local bias correction procedures may still be necessary to address differences in magnitude and temporal trends in the downscaled data.

2.1.1 Emission Scenarios

Land use and land cover data, as well as GHG and pollutant concentrations from both natural and anthropogenic sources, are all accounted for in the emission scenarios. Over the years, various methods of climate research scenarios have been utilized, from simple representations of yearly percentage increases in global GHG concentrations to more detailed depictions of many gases and particles that impact the climate, resulting from extensive socio-economic and technological assumptions.

In 2000 that the Intergovernmental Panel on Climate Change (IPCC) released a special report on emissions scenarios that established the global and regional emission paths (SRES). Emission routes A1, B1, A2, and B2, were created based on various socio-economic development assumptions. According to IPCC climate models, these emission routes would lead to future climate change. In IPCC's Fourth Assessment Report, SRES-based emission scenarios and CMIP3 climate predictions were used to assess future climate change and its effects on society and ecosystems. The CMIP3 models have traditionally been used to make climate forecasts for India. From 1901 to 2098, surface temperature and monsoon rainfall in India was predicted using CMIP3 multi-model data (Kumar *et al*., 2011). An Indian high-resolution regional climate model has been used to downscale global climate data from the Hadley Centre Coupled Model (HadCM3), one of the CMIP3 models, to understand how climate change occurs entirely affects India in the long term. PRECIS was used for the baseline (1961–1990) and long-term climatology (2071–2100) for the SRES scenarios A2 and B2 by Kumar *et al.*, (2006). Additionally, under the SRES scenario A1B, Kumar *et al.*, (2011) employed the PRECIS model to predict regional climatology in India from 1961 to 2098. An ensemble of 17 members from HadCM3 was perturbed to produce three simulations, each of which was utilized to drive PRECIS over three time periods: short term (the 2020s), medium-term (2050s), and long term (30 years or more) (2080s). As far back as 1997, the IPCC had set the economic and policy assumptions for the SRES scenarios released in 2000, and about 15 years

old are SRES scenarios (Moss *et al.*, 2010). The scientific community established new emission scenarios known as representative concentration pathways (RCPs). There are no specific socio-economic narratives or scenarios in contrast to the force. The idea that a single radiative forcing route might arise from various socio-economic and technical development scenarios is central to the process.

RCPs (Representative Concentration Pathways) are sets of consistent estimates of only the radiative forcing components (change in the balance between incoming and outgoing radiation to the atmosphere caused by atmospheric composition) intended as input for climate modelling. Increased greenhouse gas and aerosol concentrations in the lower atmosphere increase radiative forcing (Wm-2). The four RCP scenarios are RCP 2.6, 4.5, 6.5, and 8.5. Each hypothesis represents stability, mitigation, and baseline emission levels. New climate predictions are based on the new RCP scenarios (IPCC, 2014).

2.1.2 General circulation models and downscaling

Global Climate Models, commonly known as General Circulation Models (GCMs), are the most complex climate models. They attempt to show the major elements of the climate system in 3D. The tool is used to conduct tests on the effects of climate change and then generate various future scenarios for climate change evolution. Global climate models are developed and maintained by several academic institutes worldwide. According to these models, temperature, rainfall, and wind are calculated in a three-dimensional array of grid cells encompassing the globe and spaced 100–400 km apart, with 40 layers spanning ocean depth and atmospheric height. These models are comparable in many aspects, but slight changes in grid features, geographical resolution, parameterization techniques, and model sub-components (e.g., some models include an atmospheric chemical representation while others do not) result in different climate simulations. The following is a summary of studies on several GCMs:

McGuffie and Henderson (1997) used an atmospheric and oceanic general

circulation model (GCM) based on fundamental physical rules, including models of land surfaces, snow and ice, and other ice-forming substances. Depending on the acronym, a model can be classified as purely atmospheric, purely oceanic, or as a coupled ocean-atmosphere model by adding a (A), (O), or (C).

Xu (2000) examined the current gap and strategies for minimizing the gap between GCMs ability and the need for hydrological modelers, as GCMs can't characterize local sub-grid-scale features and dynamics. This evaluation of this study emphasized several problems linked to current GCM capacity, downscaling technique, and hydrological modeling tools. According to the findings of this study, more advanced techniques must be required to develop climate scenarios.

Goyal and Ojha (2010) developed downscaling models employing direct, forward, backward, and stepwise linear regression. They used these models to downscale GCM outputs to estimate monthly precipitation in an arid area of India using SRES scenarios. They revealed that direct regression overtakes backward regression. The results were produced the same using backward regression followed by forwarding and stepwise regression methods.

Jalota *et al.*, (2012) used GCM to forecast rice-wheat crop production for 2020, 2050, and 2080 based on climate change. As a result, grid cell-scale GCM performance tends to be poor, although grid-scale or sub-grid-scale consequences of climate change, such as a hydrological catchment, a city, or an agricultural farm, may be relevant.

Chandhina and Kansal (2016) developed the Statistical Downscaling Model (SDSM) to downscale the daily rainfall in the Piperiya watershed in Chhattisgarh. They calibrated and validated the model with large-scale NCEP reanalysis data using daily rainfall data from 1961 to 1990 and 1991 to 2001. Monthly rainfall has been computed using forecasts from 2011 to 2040, 2041 to 2070, and 2081 to 2100 using GCM HadCM3 outputs for A2 and B2 scenarios. They identified SDSM as a valuable technique for forecasting rainfall monthly

using the A2 and B2 emission scenarios of the HadCM3 model.

Liu *et al.,* (2017) used SDSM to downscale the daily mean temperature at 32 stations from 1954 to 2014. They used this method to determine the daily mean temperature at each station. The mean climate model output for RCP 2.6, 4.5 & 8.5 scenarios was obtained from Meteorological Research Institute (MRI), Japan. They found a rise in the temperature of all seasons, except for spring in the 2020s.

2.1.3 Regional climate models

For instance, global general circulation models (GCMs) use more than 100 km grid spacings, often too coarse for catchment-based hydrological investigations. It is necessary to employ downscaling methods, which use coarse GCM information to construct horizontal distributions of climate parameters on a much smaller scale (Wilby and Wigley 1997). Regional climate models (RCMs) can be utilized for dynamical downscaling in addition to statistical approaches. The horizontal resolutions of these models typically range from 10 to 50 kilometres. They have the ability to disrupt essential processes that occur on a regional scale, such as the orographic lifting of air masses on complicated terrain and the development of clouds and precipitation that goes along with it. In either scenario, the output of GCMs or the results of global reanalyses have an effect on RCMs at the lateral limits of their domains. Hydrological models can employ the simulated climatic parameters (precipitation, near-surface air temperature, specific humidity, etc.). Nesting RCMs is a technology derived from numerical weather prediction, and the first RCMs for climate application was developed by the Weather Research and Forecasting Division (Dickinson *et al.,* 1989; Giorgi 1990). High-resolution RCMs are driven by beginning circumstances, time-dependent lateral meteorological factors, and surface boundary conditions when using the nested regional climate modelling approach. It is being used in a variety of climate applications, ranging from research on palaeoclimate (Hostetler *et al.*, 2000) to research on anthropogenic climate change. They can do multi-decadal climate simulations with high resolution (down to 10 to 20 km or less) and

describe climatic feedback processes at the regional scale. Recently, RCMs have been introduced to link atmospheric models with other climatic processes, such as hydrology, ocean, sea-ice, land-biosphere models, and chemical/aerosol models, to simulate the climate system.

2.1.4 Bias Correction

The raw output of climatic parameters from GCM/RCM models may not be directly applicable to the analysis of the climate system for future behavior, subsequent changes, and local impacts. The modeled daily rainfall and temperature errors may affect the monthly and annual time trends and magnitudes. Precipitation biases are more evident than temperature biases, Andreasson *et al.*, (2004). In order to remove model biases and downscale coarse-grid climate simulations to a finer spatial resolution of local interest, downscaling approaches, such as physical process-based dynamic downscaling or statistical downscaling, are required (Maurer and Hidalgo 2008). It is possible to simulate physical processes at fine scales using high-resolution GCMs and boundary conditions provided by coarse-resolution GCMs in the dynamic approach. The statistical approach translates coarse-scale climate projections into a finer scale that connects the climate at two spatial resolutions through trained transfer functions. Choosing predictor variables is critical in capturing the anthropogenic climate variation signal (Hewitson and Crane 2006). It is important that the selected predictors accurately reflect the atmospheric circulation dynamics and physical link between the predictant and the predictor. Methods for bias correction, such as statistical downscaling using cumulative distribution functions (CDFs), can also be used to correct errors in data (Ines and Hansen 2006; Piani *et al.*, 2010; Wood *et al.*, 2004). Both approaches have their benefits and drawbacks, which have been well documented (Fowler *et al.*, 2007; Wilby *et al.*, 2009). The statistical downscaling techniques are widely used in climate impact research because they require less computational power than dynamical model-based methods.

Dar *et al.*, (2018) reported that regional climate models (RCMs) produce

more credible findings for analyzing the regional effect of climate change, as there is a significant bias that must be rectified before they can be utilized in climate change research. In this study, two correction functions were applied using two methods for the local bias correction of maximum temperature, minimum temperature, and rainfall viz.., the modified difference approach and the linear scaling method. These correction functions were validated to reduce the bias between the modeled (HAD GEM2-ES-GCM) and observed climate data at Ludhiana, Punjab. For bias correction of meteorological data to bring it closer to observed values, the linear scaling technique yielded better correction functions for maximum, minimum temperature, and rainfall than the modified difference approach.

2.2 GIS applications for water resources management

Sarkar *et al.,* (2001) used thematic maps of drainage, lineament, lithology, slope, and land use to develop a groundwater potential map for a micro watershed. Multi criterion analysis was used to combine weights of each thematic map with the individual capability value (CV), which were transformed into capabilities values using Baysian statistics. It was multiplied by the map's relevant probability weight of each prospective CV value. Afterward, the groundwater supply site categorized six potentiality levels from excellent to very poor.

Rawat *et al.,* (2011) used remote sensing and GIS modelling to examine the dangers in the Himalayas and rising hydrological hazards in the Dhabka watershed in Nainital district, Kosi basin India. The GIS Database Management System (DMS) included land use, climate, hydro information, and hydrological hazard assessment were included. Deforestation, flash flooding, soil erosion, and other hydrological risks have all increased as a result of climate change.

Krios and Schulte (2013) used MCA, SCS-CN, and a GIS technique to identify RWH (terraces and bund systems) locations in the Ronquillo watershed in Peru. Findings from this study show that the Ronquillo watershed, which is most

suitable for RWH implementations (terraces and bund systems), is 44 percent terraceable and 24 percent bundable. Land use and management practices eventually influenced the RWH technique selection.

Dabiri *et al.,* (2016) used Analytic Hierarchy Process (AHP) to study the site selection of water harvesting systems in water-scarce Iran. The elements/factors included physiography, rainfall, vergation and soil, which they used to determine the criteria. The slope factor emerged as the most critical consideration in selecting RWH sites.

Mousavi *et al*., (2017) employed a probabilistic frequency ratio (PFR) and boosted regression tree models for springs in Torghabeh and Shandiz residential neighborhoods, Iran. To conduct the research, a total of 155 springs were selected. ArcGIS was used to create GIS-based maps of altitude, slope aspect, slope degree, slope length, plan curvature, profile curvature, distance from river, river index, topographic wetness index, distance from fault, fault density, land use, and lithology. BRT and FR models were used to create a groundwater spring potential map.

Suryabhgavan (2017) used remote sensing and GIS to identify the Bata river basin's (HP, India) groundwater potential zone (GWP). Geomorphology, soil and drainage, land use, and land cover maps were all created for the 288 km^2 research area. The weighted overlay index approach integrated all of the thematic layers to produce GWP zones. Each parameter was given a rank, and then weights were allocated based on its relevance. It was decided to divide the research area into five sections: extremely poor, poor, moderate to good, good, and very excellent.

Ghimire *et al.,* (2019) determined that the Melamchi Larke region of Central Nepal Himalayas has a prospective groundwater spring area and explored it using different geospatial approaches. The Melamchi-Larke region, located around 50 km northwest of Kathmandu, was chosen and surveyed for 412 springs.

For potential spring mapping, they used a statistical approach known as Weight of Evidence (WoE). Slope, aspect, land cover, elevation, and other types of geospatial maps were also prepared with the help of geospatial techniques.

2.3 Hydrogeological characterization and water demand of Himalayan regions

Valdiya and Bartarya (1989) studied the water flow in the Gaula watershed. The research focused on a 600 km^2 section of the Gaula River basin, with elevations varying from 500 to 2610 feet above sea level. The forest cover in the watershed area dropped by 13.1 percent between 1963 and 1985, according to their research. They discovered that spring discharges had decreased by 25 to 75 percent during the previous five to fifty years, which they termed a "perceptible drop." From 1951-60 to 1971-81, the average discharge of the Gaula River declined by 38.5% from 13,615 cumec/day to 5935.9 cumec/day.

Negi *et al.,* (2007) used hydrogeological and geomorphological aspects to describe springs, identify recharge zones, and propose conservation methods to increase spring discharge. Peak rainfall and peak outflow were synchronized, indicating rapid penetration into the area of an unconfined aquifer. They determined that smaller recharge zones are beneficial for enhancing spring discharge and are easier to safeguard and manage. They also found that rainfall, physiography, lithology, slope and aspect, land-use practices, vegetation, altitude, soil type, and anthropogenic interference all impacted the water quality of 12 Himalayan springs selected for the observation.

Singhal et al. (2010) conducted an analysis of groundwater depletion in the Indian state of Uttarakhan. Using a combination of geophysical techniques (resistivity profiles and electromagnetic surveys), isotope techniques (to determine the age and recharge of spring water), and well-monitoring data. According to the findings of the study, the existing rate of groundwater expansion cannot be maintained for very much longer; thus, it is suggested that a check dam be built in

order to increase spring discharge.

Tambe *et al.,* (2012) revealed a 50 percent decrease in spring discharge in Sikkim within a decade. The spring flow was also found to be increased by 230 percent as a result of the springshed development initiative. However, they observed that identifying recharge regions, creating local expertise, motivating rainwater harvesting systems in farmer fields, and obtaining public funds continue to be challenges for springshed development.

Parmar *et al.,* (2016) studied the Takoli Gad watershed in the Garhwal Himalayas by looking at the relationship between rainfall and spring discharge. Summer, winter, and monsoon flow rates of 15 springs were tracked during the 2007-2008 reporting period. Twelve springs are located in Phyllite terrain, while the other three are in Quartzite terrain. The research found that spring discharge was lowest in the summer and highest in the monsoon.

Chinnasamy and Prathapar (2016) examined the methods to study the hydrology of springs in the Himalayan area. They divided the methodologies into two categories: desk-based analytical and field-based empirical. Field-based empirical methods help us characterize hydrology, land-use patterns, geology, and climate, while desk-based analytical methods guide responses across watersheds and flux evaluation, which are potential inputs for developing hydrogeological maps, and conceptualizing processes that control groundwater movement and storage, and creating a mathematical model. The article examines existing literature and data before starting on expensive field experiments. The results of desktop analysis, hydrogeological maps, and field investigations are then used to develop a conceptual model, which can serve as the foundation for a numerical model.

Kumar and Sen (2020) assessed the potential of spring for sustainable agriculture. A spring in Tehri Garhwal district of Uttarakhand, behind the Mussoorie ridge in the Anglar watershed, was chosen for the investigation. Water

flow from springs was monitored from February 2014 to April 2016. On a daily basis, a variety of meteorological variables were observed. To determine the feasibility of spring for agricultural purposes, they evaluated crop water requirements and evapotranspiration. The monitored spring was determined to be capable of meeting the annual agricultural water needs of 6411.35 mm in the area.

2.4 Integrated catchment modelling (Surface and Groundwater simulation modeling)

Onta and Gupta (1995) used one-dimensional groundwater consolidation models to simulate piezometric levels and land subsidence in the lower Central Plains of Thailand. MODFLOW was used to develop the model based on data collected between 1955 and 1990. From 1991 to 2010, the reaction of the aquifer system to various pumping strategies was forecasted via the development of pumping strategies for likely future situations based on previous experience. According to the model predictions, if groundwater levels remain stable, the current pace of removal must be slowed. Groundwater management regulations, land subsidence control plans, and action programmes in Bangkok metropolitan area were changed as a result of the research.

Reeve *et al.,* (2001) undertook the groundwater flow simulations in the northern Minnesota Glacial Lake Agassiz Peatlands using three-dimensional groundwater modelling. A steady-state MODFLOW model covering 10,160 km^2 of the research region was built for groundwater modeling. According to numerical calculations, the Itasca Moraine, situated to the south of the peatlands, serves as a recharge location for the regional groundwater flow. Small flow networks dominate these peatlands hydrology with streamlines under 10 kilometers, and groundwater from far-off recharge sites has little or no influence.

Osman and Bruen (2002) found when the water table drops below the stream bed, seepage from the stream may partly infiltrate an unconfined aquifer. It was taken into account that a detached stream in the unsaturated region of the

aquifer might cause a change in seepage flow and fluctuations in the water table. MODFLOW was used to evaluate the approach, then compared to predictions from the widely-known SWMS 2D variably saturated model (model for simulating water flow and solute transport in two-dimensional variably saturated media). Seepage flow and local water table mounding were compared. It was found that the proposed results form the method applied were highly comparable to those of SWMS 2D.

Senthilkumar and Elango (2004) used a three-dimensional mathematical model in the Lower Palar River basin, southern India, to model the groundwater flow. An abundance of groundwater was drained for agricultural, industrial, and drinking water purposes in the research region. In addition to the riverbeds three primary pumping stations, other wells were scattered around the region. With 70 rows, 40 columns, and two layers, the model simulated groundwater movement across about 392 square miles. For the period from 1991 to 2001, the model simulated a transitory state. The aquifer system was found to be stable at the current pumping rate, except for a few spots along the coast where the groundwater head declines from 0.4 to 1.81 m below sea level during the dry seasons. As a result, the eastern portion of the region saw an increase in groundwater removal of 2 million gallons per day (MGD) at a large pumping station, resulting in a decrease in groundwater head of between 0.9 and 2.4 meters.

El-Yaouti *et al.,* (2008) employed a three-dimensional finite-difference groundwater flow model to study the unconfined aquifer of Bou-flow Areg's system behavior under various stresses. Groundwater Modeling System (GMS) modelling software MODFLOW was used in this study. Observed groundwater levels from 1990 to 2006 were used in both steady-state and transient simulations for the two strata. The modelling findings reveal that seasonal variations in recharge from natural infiltration of precipitation and irrigation are responsible for swings in hydraulic heads. It may also simulate the positive changes in the Bou-Areg aquifer's hydraulic heads and the varying reactions of the hydrogeological

system that result from those changes. Under different situations, several scenarios were used to forecast the response of the aquifer system.

Elango and Sivakumar (2008) conducted research in the coastal aquifer situated south of the city of Chennai, India. The aquifers in this region were under stress owing to the pumping of groundwater to supply the ever-increasing water requirements of the metropolis. The work was carried out to construct a numerical model for this region to understand the system behavior with the changes in hydrological stresses. The finite-difference computer algorithm MODFLOW (Modular 3D finite-difference flow) with Groundwater Modeling System (GMS) as pre-processor and post-processor was used to model the groundwater flow in this research.

Kim *et al.,* (2008) present a strategy for integrating SWAT and MODFLOW for Musimcheon Basin in Korea. Semi-distributed groundwater component of SWAT does not incorporate distributed parameters like hydraulic conductivity and storage coefficient. Calculating head distribution and pumping rate helped comprehend groundwater recharge. SWAT model HRUs were switched with MODFLOW model cells to overcome this problem. This HRU–cell conversion interface studied groundwater recharge and evapotranspiration. For boundary flow, examine the stream network and aquifer interaction and for river-aquifer interaction, River package of MODFLOW was used. The application illustrates how a SWAT–MODFLOW model can imitate groundwater recharge rates, aquifer evapotranspiration, and groundwater levels. It permits aquifer and channel contact. This interaction created groundwater outflow throughout the basin, especially at low flow. SWAT-improved MODFLOWs water transfer approach effectively recreated scattered decline and lowered streamflow. This model is beneficial for sustainable groundwater development, considering outflow to streams, springs, or marshes.

Setegn et al. (2008) utilised SWAT 2005 to replicate Lake Tana's water balance. This study evaluated the SWAT model's effectiveness and applicability

for projecting Basin streamflow. Gomera, Gilgel Abay, Megech, and Ribb rivers were utilised to calibrate and validate the model. Flow is more responsive to HRU definition criteria than subbasin demarcation. SUFI-2 and GLUE accomplished. All sources of uncertainty were incorporated by bracketing 60% of the measured river discharge. Baseflow (40-60% of total discharge) contributes more than surface runoff in the studied area. The calibrated model may be used to study climate, land-use, and management scenarios on streamflow and soil erosion.

Schuol *et al.,* (2008) utilized the semi-distributed hydrological model SWAT (Soil and Water Assessment Tool) to predict freshwater components at a subbasin level with a monthly resolution over the whole African continent. Prediction uncertainties were assessed at 207 discharge stations using SUFI-2 (Sequential Uncertainty Fitting Algorithm). The model and its results might be used in climate change, water, food security, and virtual water commerce studies. Although there is significant prediction uncertainty, the model outcomes are typically satisfactory. On the other hand, these uncertainties reveal the actual understanding of the modeled processes. Advanced investigations show that water scarcity indicators can be computed by taking these model-based uncertainties into account.

Ahmad and Umar (2009) performed groundwater flow modeling in the Yamuna-Krishni interfluve to simulate flow system dynamics and assess water balance. Different boundary packages in Visual MODFLOW, Pro 4.1 were used to apply the horizontal flows, seepage losses from unlined canals, recharging from rainfall, and irrigation return flows. The river boundary package was used to simulate the river-aquifer interaction. For various zones, hydraulic conductivity values varied between 9.8 and 26.6 m/day. Zones were allotted recharge and irrigation returns based on rainfall and irrigation returns. To replicate stress zones, pumping rates of 500, 1000, 1500, 2000, and 2500 m^3/day were used. From June 2006 to June 2007, the zone budget showed a deficit in water balance. The research region received a total recharge of 160.21 mcm. Pumping out 233.56

mcm of groundwater left a deficit balance of -73.35 mcm. The model sensitivity to these changes was evaluated as input parameters varied. Hydraulic conductivity and recharge factors were shown to have the greatest impact on the model performance. The model simulations for several scenarios showed that artificial groundwater recharging and combined surface and groundwater usage are necessary to minimize the drop in the water table.

Kushwaha *et al.,* (2009) used a conceptual groundwater modelling technique to develop a mathematical groundwater model for the northern half of the Mendha sub-basin in the semi-arid regions of northeastern Rajasthan. For this reason, GMS, which supports the MODFLOW-2000 code, was used. Source/ Sink Coverage; Recharge; Extraction; Return Flow; Soil; and Soil Coverage were all examined to simulate. Based on the present groundwater withdrawal and recharge rates, the model was run for 15 years, from 2006 to 2020. Groundwater storage decreased from 349.50 mcm to 222.90 mcm per year, while groundwater extraction grew from 258.69 mcm to 358.74 mcm per year, according to the water budget forecasts. It was also possible to make water table contour maps for 2007, 2015, and 2020.

Singh *et al.,* (2011) used SWAT to estimate the total quantity of water available in Cauvery river basin, India, and anticipate changes in land management practices on water availability in the research region. The measured Nash Sutcliffe coefficient was 0.93, while the computed coefficient of determination was 0.94. The current flow predicted in the model was 574 TMC, with 75 percent predictable flow and 60 percent agricultural land, and 35 percent forest area. Changing the land use circumstances resulted in a series of situations. The lowest flow achieved in the scenarios was 559 TMC with a land cover condition of 50 percent forest cover and 45 percent farmed land area. The greatest was 597 TMC for land conditions with 75% agricultural and 20% forest cover. The findings revealed that the basin's water supply is inversely related to the quantity of forest cover.

Setegn *et al.,* (2011) utilised GCM results to analyse water resource vulnerability in Ethiopia's Lake Tana Basin. 15 GCMs predicted the basin's monthly precipitation and temperature variations. GCMs predicted temperature rises but erratic rainfall. Temperature and precipitation changes impact streamflow and other hydrological components. They created daily climate projections by altering historical data sets to reflect GCM climatologies and calculated hydrological changes using the Soil and Water Assessment Tool (SWAT). SWAT was calibrated and validated using four Lake Tana streams. Four of the nine GCMs evaluated for the Special Report on Emissions Scenarios A2 scenario showed significant annual streamflow declines from 2080-2100. Human activities and climate change may affect Lake Tana's water balance during the next century, although the direction of change is unknown using current GCMs.

Gaur *et al.,* (2011) devised an approach for evaluating groundwater that combined the numerical model MODFLOW with spatial modelling via GIS in the Banganga River sub-basin in Rajasthan, India. There was a good deal of overlap between the groundwater flow vector map created from the numerical model and the thematic basin maps like geology and geomorphology to identify prospective groundwater zones. By altering the well discharge and suggesting the position of additional water collecting facilities, many scenarios were envisaged, and it was observed that increasing the discharge of wells in the prospective zones placed the aquifer under less stress. Structures for harvesting rainfall have been proposed to stabilize groundwater levels.

Siarkos and Latinopoulos (2012) conducted a groundwater quality assessment and delineation of wellhead zones in the N. Moudania watershed. A three-dimensional finite-difference model called MODFLOW simulates groundwater flow in the N. Moudania aquifer, while MODPATH, a post-processing tool for particle tracking, is used to draw boundaries around home water supply wells. A steady-state model was created for the flow model. A trial-and-error approach was used to improve the estimate of the hydraulic conductivity

distribution. Finally, recommendations were made for managing and controlling the identified possible pollution point sources, particularly if they were situated inside the protection zones of the analyzed water supply wells.

Xu *et al.,* 2012 used MODFLOW and the SWAP programme to model the regional groundwater flow problem in the Hetao irrigation area, upper Yellow River basin of North China. Net recharge flux and average water table level in each SWAP zone were sent to the SWAP programme through a three-dimensional groundwater flow model, MODFLOW 2000. They developed a SWAP module for the MODFLOW-2000 model to simulate groundwater recharge and evapotranspiration for shallow water problems. For this evaluation, MODFLOW-2000 and the SWAP software were used to simulate the flow of groundwater over a large area of dry land used for irrigation in northern China.

Chinnasamy (2012) calibrated and validated an HYDRUS code (Chinnasamy and Hubbart 2014a) and a MODFLOW code (Chinnasamy and Hubbart 2014b) for the Baskett study area, Ozarks Forests, Missouri, USA, which is characterized geologic context. Land use and recharge rates were identified using remotely sensed imagery, and meteorological data were gathered at "micro-climate stations." Predicting the gain/loss behavior and determining the proportion of streamflow losing water to the aquifer were both within the model's capabilities.

Doummar *et al.,* (2012) employed an integrated catchment model (MIKE SHE) to study the flow mechanisms in the Gallusquelle springs' large-scale karst geologic system (Southwest Germany). Their findings revealed that soil type had the greatest impact on groundwater recharge via regulating infiltration and evapotranspiration. Peak discharges were also found during the saturated condition of the soil.

Faramarzie *et al.,* (2013) studied climate change impact on African freshwater availability for 2020–2040. Future climate predictions from five GCMs

under four IPCC emission scenarios were input into an existing SWAT hydrological model to forecast the impact on water resources in Africa. According to the findings, mean water resources will rise. Subbasins and countries varied significantly. In several regions/countries, most climatic scenarios anticipated the same direction of change in water resources, showing high confidence in the projections. Future drought events and duration will rise basis on the amount and frequency of dry days. Dry regions have more uncertainty about water resource consequences than rainy regions—this challenges agriculture in arid locations where water is scarce, and irrigation will be needed to stabilize and boost crop yields.

Alam and Umar (2013) conducted research in the Hindon-Yamuna Interfluve Region. The flow system and zone budget were evaluated via groundwater flow modelling. This research uses Visual MODFLOW, pro 4.1, to model groundwater flow. The model has three layers, 58 rows and 37 columns, and simulates groundwater flow across around 1345 km^2. In Visual MODFLOW, v 4.1, multiple boundary packages were used to apply horizontal flows, seepage losses from unlined canals, recharge from rainfall, and irrigation return flows. The river boundary package was used to simulate the river-aquifer interaction. The pumping well package employed simulated pumping rates of 500, 1000, and 1500 m^3/day. The total annual direct recharge for the study region was calculated using the zone budget under steady-state conditions as 416.10 mcm. 416.63 mcm of groundwater is drained each year by pumping. The reaction of the aquifer system to varied circumstances was predicted using two alternative scenarios.

Kumar (2013) studied the modular three-dimensional groundwater flow model MODFLOW and found that groundwater models may be used to forecast the effects of new development scenarios and the interactions between surface water and groundwater. But if the model is poorly developed from the start, it might be a waste of time and money that could have long-term negative effects if the model doesn't effectively reflect the actual system being simulated.

Guzman *et al.,* (2015) assessed long-term anthropogenic influences on agro-ecosystems by simulating surface and groundwater interactions. SWATmf was developed to link and integrate the widely used surface watershed model SWAT with the groundwater model MODFLOW. The SWATmf dataset from Oklahoma Fort Cobb Reservoir links and dynamically simulates SWAT and MODFLOW. SWATmf can model surface and groundwater interactions depending on streamflow and groundwater levels, according to this research.

Miglani *et al.,* (2015a) investigated spatial and temporal patterns of water on the Sirhind Canal Tract of Punjab using PMWIN to simulate the groundwater model. GEC (1997) techniques were used to estimate the amount of water recharged by irrigation and rain. Hydraulic conductivity was shown to be less susceptible to the model sensitivity than specific yield. The study concluded using a simulated model, water resources may be managed more efficiently.

Bouaamlat *et al.,* (2016) created a tafilalet oasis system (TOS) groundwater model in the lower Ziz and Rheris valleys, southern Morocco. The Arc Hydro Groundwater tool with the MODFLOW-2000 code was used to run numerical simulations on a geographical database in a geographic information system. According to the steady-state and transient models run between 1960 and 2011, the water table is at an equilibrium between infiltration from the surface and evapotranspiration, which drains it. Hydraulic heads were more responsive to yearly fluctuations than seasonal fluctuations when the Hassan Addakhil dam was completed in 1971. Due to recurrent droughts, the most considerable water-level variations were seen in irrigated regions. Groundwater resources in the TOS may be managed using the paradigm. To preserve groundwater against overexploitation and degradation of water quality, it can predict the effect of alternative management strategies.

Sudhakar *et al.,* (2016) coupled the MODFLOW groundwater management and development software with the GIS (Geographic Information System) for groundwater conditions. GIS applications in groundwater hydrology

were outlined in two primary areas: subsurface flow and pollution modelling using GIS and artificial recharge site selection. Although they are still meager, success rates for groundwater investigations using these methods have grown dramatically in recent years. Using GIS and MODFLOW together can transform the way groundwater resources are monitored and managed in the future.

Zandi *et al.,* (2016) conducted the research to develop a model of the prospective map of groundwater spring occurrences. Using the information on spring locations and occurrence frequencies, a Logistic Regression (LR) model was developed. The possible zones for groundwater springs were divided based on the most statistically significant characteristics of spring occurrences. The statistical characteristics of the suggested model were assessed. Policymaker's strategic development planning allows for the low-cost use of groundwater resources.

Srinivas and Naik (2017) used spatial inputs, soil type, and slopes to create a continuous simulation-based hydrological model for the Musi river basin in India utilizing a distributed hydrological modelling technique. The hydrologic modelling technique involves rainfall-runoff modeling; sensitivity analysis were performed for the most sensitive parameterization of streamflow using the SWAT CUP Sequential Uncertainty domain parameter fitting (SUFI-2) algorithm. The model was calibrated for 2010 and 2011, then observed data was used to verify it for 2013. The Nash-Sutcliffe Coefficient (NSE), Percentage of Deviation Measures (Pbias), and RMSE-Observations Standard Deviation Ratio were used to assess the performance of the calibration and validation outcomes (RSR). At a 95 percent confidence level, the observed and modelled discharges were not statistically different (95PPU). After considering the model input uncertainties and sensitive parameterization, the model daily simulation results and monthly time series showed a good correlation and a very strong correlation.

Chapagain *et al.,* (2019) investigated the distribution, discharge, water consumption, and conservation of natural springs. 93% of the permanent springs

in Melamchi are at mid-elevation (1500–2500 m). One-fourth of springs are utilized for drinking, livestock, irrigation, and residential cleaning. 45% of springs offer drinking water for five households. They found that spring water volume has dropped 30% in a decade. Mid-elevation springs with less than 5 lpm discharge are more vulnerable to climate change and humans. 18% of springs instantly dried up just after the 2015 Nepal earthquake, according to the study.

2.5 Effect of changing environmental conditions on hydrology

Wilkinson and Cooper (1993) used an idealized aquifer/river system model to study the impacts of climate change on aquifer storage and groundwater flow to rivers. Based on the Chalk and Triassic sandstones in the UK, the generalized model can encompass geographical variations in transmissivity of aquifers and may also be extended to other aquifers across the world. A number of different climate change scenarios were used to modify the climatic inputs of the model, which were derived from historical recharge data and approximated using actual rainfall and potential evaporation measurements. Under larger evaporation change scenarios, baseflow simulations showed significant proportionate decreases at lower Chalk flows. Baseflow decreases were less severe and uniform in the slower-responding Triassic sandstone aquifer simulations. It was less affected for the low evaporation change scenario but still substantial for the Chalk aquifer hydrologic regime.

Rosenberg *et al.,* (1999) researched the Ogallala aquifer in the central United States to determine the influence of climate change on water output and groundwater recharge. Three distinct GCMs predict the temperature and CO_2 concentration variations. Recharge was lowered in all cases, with 77% depending on the simulated settings.

Sherif and Singh (1999) concluded there is some evidence that climate change may affect saltwater intrusion in coastal aquifers, where they used two coastal aquifers to evaluate the influence of climate change on seawater intrusion.

The melting of ice sheets and glaciers and changes in air pressure would all contribute to a rise in sea levels due to climate change. More saltwater intrusion is expected when sea levels rise due to the increased saline water heads imposed along the coast. Three climate change scenarios were examined. It was concluded that the Nile Delta aquifer is more susceptible to climate change and sea-level rise under these hypothetical scenarios. The Nile Delta aquifer would expand by 9.0 kilometers if the Mediterranean Sea rose by 50 centimeters. As sea levels increase in the Bay of Bengal, an additional 0.4 km of incursion will occur. Adding further pumping to the Nile Delta aquifer would have serious environmental consequences.

Limbrick *et al.,* (2000) employed GCM outputs created by the Headley Center in 1996 in a semi-distributed rainfall-runoff model to simulate the Kennet River in the United Kingdom. Under all scenarios, groundwater recharge and storage would be decreased because of a shorter recharge season and a decrease in the total annual runoff.

Loaiciga *et al.,* (2000) investigated the effects of climate change on a karst aquifer in south-central Texas (i.e., groundwater use). By comparing historical and future stream flows projected by connected general and regional climate models, runoff scaling factors were used to evaluate the influence of climate change on streambed recharging. According to the research, there is a greater risk of contaminating the aquifer due to human activity than climate change.

Neff *et al.,* (2000) conducted a statistical investigation of the historical link between groundwater levels and precipitation in Pennsylvania, US, to examine possible changes in groundwater levels owing to climate change. To account for changes in geology, the borehole groundwater level records were divided into "precipitation-based areas," and the hydrograph data was normalized. The groundwater levels in each of the five precipitation-based zones were averaged together. This statistical model, which links present groundwater levels to rainfall, was applied to two different GCM climate change scenarios to forecast future

groundwater levels.

Kirshen (2002) studied a highly permeable aquifer in the northeastern United States using the groundwater model MODFLOW. Precipitation and evapotranspiration were used to estimate groundwater recharge. Using both GCM-predicted and hypothetical adjustments to the input parameters, the recharge rates, and groundwater levels were greater, with no difference or much lower, depending on the climatic scenario.

Croley and Luukkonen (2003) evaluated the climate change's impact on groundwater levels in Lansing, Michigan. In order to determine groundwater recharge rates, an empirical streamflow model was calibrated using results from two GCMs. Groundwater levels are anticipated to rise or fall as a consequence of climate change, depending on the GCM employed in the research findings.

Eckhardt and Ulbrich (2003) studied a small watershed in Germany by determining the effects of climate change on groundwater recharge and streamflow. Based on simulations from five distinct GCMs, the input parameters of their hydrologic model were adjusted. According to the findings, increasing temperatures will result in more rain and snowfall in winter, raising recharge levels and stream flows in January and February. In March, the snowmelt-induced rise throughout recharge ceased, and recharge and streamflow might be lowered in the summer months.

Allen *et al.*, (2004) considered climate change in the Grand Forks Aquifer in the south-central region of British Columbia as an example of aquifer response to variations in recharge and river stage. According to the results, the groundwater system in the Kettle and Granby River valleys, which run through the valley, is less sensitive to changes in recharge to the aquifer under various climate change scenarios, according to the results, which were modelled under steady-state circumstances. The overall water table arrangement and groundwater flow direction changed slightly in all scenarios. The aquifer's water table rose by

around 0.05 meters and fell by about 0.025 meters as a consequence of models with high and low recharge rates. The water-table elevation rose by an average of 2.72 m and 3.45 m as a result of simulated changes in river-stage elevations of 20 and 50 percent, respectively. Lower-than-base flow simulations resulted in water table elevations dropping by an average of -0.48 m and -2.10 m, respectively when river stage elevations were reduced by 20% and 50%. According to the data, the present water table heights of the valley were in line with the typical river-stage elevation (between current base flow and peak-flow stages).

Brouyere *et al.,* (2004) investigated the influence of climate change on the hydrological cycle in typical Belgian water basins and created an integrated hydrological model (MOHISE) for the study area. Physically consistent hydrologic phenomena, such as groundwater flows represented using a geographically dispersed, finite-element technique, are considered in this model. The integrated system was used to assess the influence of climate change on the water cycle in Geer basi, Belgium using IPCC climate change scenarios. Climate change has an influence on groundwater levels and groundwater reserves, and the findings of a groundwater model were examined in depth. According to the results, groundwater levels and reserves were anticipated to fall in most scenarios based on the modelling done in the Geer Basin on a pluri-annual basis. On the other hand, tests conducted on this aquifer found no improvement in seasonal variations in groundwater levels.

Holman (2006) studied the groundwater recharge from East Anglia, UK, using an integrated method that considers climatic and socio-economic change. Future groundwater recharge is affected by various variables, including shifting precipitation and temperature patterns, coastal floods, urbanization, the creation of woodlands, and changes in cropping and rotational practices, among others. The findings have identified the most important causes of uncertainty and shortfalls in recharge estimates. To better understand the impact of future developments, socio-economic scenarios were emphasized. It is possible that soils of the future

may not have the same infiltration qualities present in today's soils. The possible ramifications of taking soil parameters as constant were discussed.

Ranjan *et al.,* (2006) studied the fresh groundwater resources, such as salt intrusion in coastal aquifers. For 2000-2099, they employed the Hadley Centre climate model, HadCM3, and the SRES A2 and B2 low and high emission scenarios. In both scenarios, annual fresh groundwater resource losses, there was a growing long-term tendency in all stressed locations except northern Africa/Sahara. They also discovered that precipitation and temperature were not strongly correlated with fresh groundwater loss when they were taken separately. A lack of fresh groundwater supplies will significantly influence the socio-economic activities of the country, particularly population growth and the amount of fresh groundwater per person.

Scibek and Allen (2006) predict the future effects of climate change on groundwater resources. An unconfined aquifer was used to test the technology close to Grand Forks, British Columbia, Canada. They used the Statistical Downscaling Model to bring climate change scenarios from CGCM1 model runs down to the regional level (SDSM). Therefore, four climate scenarios were simulated in one-year runs using a three-dimensional transient groundwater flow model included in MODFLOW (1961-1999 current, 2010, 2040-2069, and 2070-2099). For groundwater levels, the geographical distribution of recharge has a significantly greater influence on levels than the temporal fluctuation of recharge, as represented by an annual average. The downscaled CGCM1 model predicted for the Grand Forks area's future climate indicates that the unconfined aquifer will get higher recharge from spring into summer. But the total impact of recharge is limited because of the main river-aquifer interactions and river recharge.

Dams *et al.,* (2007) described a Kleine Nete sub-catchment of Belgium would see a decrease in groundwater volume and an increase in the overall hydrologic balance between 2000 and 2020 due to changes in land use. In this investigation, a land-use change model was coupled with water balance and

groundwater models. The CLUE-S model was used to predict how the land would be used in the future. It was determined that four different SRES scenarios (A1, A2, B1, and B2) would be employed in the land-use modelling. The WetSpass model was combined with a MODFLOW groundwater model to simulate components of the water balance, including groundwater level and baseflow. According to the findings, the average recharge dropped with time for all circumstances. Reduced groundwater levels and reduced total baseflow were also seen as a consequence of the expected drop in recharge, which ranged from 2.5 cm for scenario A1 to only 0.9 cm for scenario B2.

Jyrkama and Sykes (2007) evaluated climate change influence on groundwater recharge using a physical-based technique. To assess regional groundwater recharge potential with a high geographical and temporal resolution, the technique was based on the hydrologic model HELP3. The approach was utilized in their research to model the past and future circumstances of the Grand River watershed using 40 years of real meteorological data. The effect of climate change was simulated by changing the model input parameters based on climatic predictions for the area. According to the findings, climate change is expected to increase the total rate of groundwater recharge.

Woldeamlak *et al.,* (2007) studied the consequences of climate change on the groundwater systems of the Grote-Nete watershed, Belgium. They simulated the effects of wet (greenhouse), cold, or NATCC (North Atlantic Thermohaline Circulation Change) and dry climatic scenarios on an area of 525 km^2. For wet situations, low, middle, and high-temperature values were used. WetSpass simulated seasonal and yearly water balance components, including groundwater recharge, whereas MODFLOW was used to simulate mean annual groundwater elevations and outflow. WetSpass results for the wet scenarios showed that wet winters and drier summers were expected. In the high wet scenario, groundwater levels might rise by as much as 79 centimeters, impacting the distribution of meadows and the diversity of organisms found in them. Compared to the current

climate, cold scenarios showed drier winters and wetter summers. The dry scenarios foretold a year of sweltering weather. Due to high evapotranspiration rates by forests and minimal precipitation, there was no recharging in the summer. Groundwater levels in the eastern portion of the Campine Plateau have dropped by 0.5 m on a yearly basis, with a high of 3.1 m.

Toews and Allen (2009) explored the Oliver area of British Columbia, Canada, and built a regional-scale numerical groundwater model to evaluate the effects of future anticipated climate change on groundwater. According to the findings, recharge to the yearly water budget would grow in the future (2050s and 2080s) from its present levels to an expected 1.2 percent in the 2050s and 1.4 percent in the 2080s.

Allen (2010) studied historical groundwater levels for selected observation wells in British Columbia, Canada, to better understand historical patterns in the area. Most records show a downward trend in groundwater levels from 1976 to 1999, and this downward trend is linked to regional precipitation declines over the same time period, but the shorter time periods utilized in this research showed varying tendencies. For this investigation, a global climate model (CGCM1) forecasted future precipitation and temperature variations and was utilized as input for a model that simulates recharging. The daily weather data show the past environment and two possible futures (the 2020s and 2050s). Precipitation forecasts for this area of British Columbia were very unclear based on this specific global climate model predictions. Both positive and negative variations in yearly precipitation were anticipated using various global climate models.

Singh and Kumar (2011) investigated an area prone to drought and the effects of climate change on dynamic groundwater systems to manage and augment the basin's groundwater supply. The study focused on the databases, analysis, projected rainfall and temperature generation, recharge estimate, and groundwater modelling. Maps were created in ILWIS3.2, and required data was collected. The SRES GCM forecasts for the South-Asia area were used to

calculate future rainfall for the time-slice 2004-2039. The Visual HELP model required site-specific soil, plant, and climate data to be collected, and groundwater recharge estimates at twelve different sites in the basin were performed. Twelve zones were used to create the groundwater model in the water balance approach. A time slice from 2004 to 2039 was used to estimate the influence of climate change on groundwater recharge and levels.

Bokar *et al.,* (2012) conducted a collaborative effort on the impact of climate variability on groundwater resources in Kolondieba catchment basin, Sudanese climatic zone, Mali, where high evaporation demand and short recharge periods have contributed to groundwater level fluctuations. MODFLOW groundwater flow modelling indicated that groundwater is flowing into the river network; however, the transient flow model showed a reduction in water levels over time by an average groundwater drop of 2 to 15 cm per year between 1940 and 2008. A downscaling of the Climate Global Model data yielded accurate predictions of groundwater levels.

Kumar (2012) considers groundwater recharge and resources, soil moisture, and coastal aquifers for evaluating the influence of climate change on groundwater resources in India. He also considered contemporary research and methods. A summary of current research papers has been presented. WHI UnSat Suite and WetSpass were used to estimate the recharging of the groundwater table. Analyzed and modelled GCMs were used to build future predicted climate change datasets that included temperature, precipitation, and solar radiation.

Crosbie *et al.,* (2013) used 16 global climate models (GCMs) and three global warming scenarios to look at changes in groundwater recharge rates in the U.S High Plains region in 2050 relative to 1990. WAVES was used to simulate groundwater recharge for various soil and plant types in the High Plains region. A 2050 climate change estimate for the Northern High Plains showed an 8 percent increase in recharge, a 3 percent drop in the Central High Plains, and a 10 percent decline in the Southern High Plains, increasing the present north-to-south trend in

recharge. Both an increase and a drop in recharge rates were predicted for dry and wet future climatic scenarios, with a magnitude greater than 50% of present recharging. The sensitivity of recharge to changes in rainfall was related to the amount of current recharge and the amount of current precipitation sensitivity, and vice versa.

Blanco-Gomez *et al.*, (2019) investigated the implications of climate change on the Guajoyo River Basin water resources in El Salvador using the SWAT model. The expected future climate change by two climate change sceanrios (RCP 4.5 and 8.5) and five GCMs were studied. A considerable decline in Pepcipitation and an average annual temperature increase were expected between the middle and the end of the twenty-first century. The findings suggested a declining trend in the quantity of water available and more severe droughts for future climatic scenarios related to the base period (1975-2004).

Chapter-3

MATERIAL AND METHODS

This chapter provides an overview of the procedures and methodologies adopted to study the hydrogeological characterization and modeling of springsheds in the changing environment of Central Kashmir. To achieve the objectives of the study, ArcMAP 10.4.1, QSWAT 1.8, SWATCUP 5.2.1.1, SWAT-MODFLOW, and GMS 10.3 software were used to model the effects of changing environment. The research was undertaken at the College of Agricultural Engineering & Technology at SKUAST-K, Shalimar Campus, from 2018-2021.

Subsequent sections describe the study area and methodologies used to analyze the changing environmental conditions and their effects in Central Kashmir.

3.1 Description of the study area

3.2 Materials used

3.3 Spring waterbody and well survey

3.4 Creating a monitoring system to collect data on spring discharge regularly

3.5 Future climate scenario generation

3.6 Comprehensive mapping and conceptual layouts

3.7 Land use/Land cover change detection/matrix

3.8 Identification of recharge areas and rainwater harvesting suitability

3.9 Geophysical exploration for lithological investigation and groundwater validation

3.10 Modelling of catchments (surface, groundwater modeling, and coupling of models developed)

3.11 Measuring the impact of changing environment and suggesting the best measures for springshed management.

3.1 Description of the study area

3.1.1 Site

Central Kashmir falls in the central part of the Kashmir Valley, comprising three districts Srinagar, Budgam, and Ganderbal. The study area is located between 33°41′ - 34°28′ N Latitude and 74°23′ - 75°37′ E Longitude and the elevation ranges from 1560 to 5360 m amsl. The geographical area of the study area is 3290 km^2. The location map of the study area is shown in figure 3.1. The climate of the study area is temperate cum mediterranean type. The average monthly minimum temperature ranges from -1.8°C to 18.6°C and the average monthly maximum temperature ranges from 4.9°C to 30.6°C.

3.1.2 Physiography and Topography

The Pir Panjal mountain in the southwest and the Great Himalayan range in the northeast divide the Central Kashmir Valley into a relatively flat terrain. The valley terrain is mostly gentle, excluding the Karewas, little plateaus. The Pir Panjal side, i.e., the southwestern side, is more likely to have such plateaus than the north-eastern side. During its route through the valley, the Jhelum river flows north-westerly, obscuring the Karewas that lie along its banks along its path. The valley floor rises to 1585 m amsl on average. These mounds are located at an altitude of about 1620 m amsl. Marshes may be found in low-lying locations, particularly surrounding natural water sources.

3.1.3 Climate

Central Kashmir's weather and climate are inextricably tied to the subcontinent's weather system in general. The valley's high altitude (about 1600 m amsl) in the northwestern corner of the subcontinent is surrounded by high mountains, giving it a particular geographical character and climatic features. It has a climate that is temperate-to-mediterranean. The annual precipitation

averages 734-824 mm, with the majority of precipitation occurring during the winter months. Rainfall is caused by western disturbances throughout the winter (temperate cyclones). The Mediterranean Sea is the source of these disruptions. The rainfall brought on by these storms is widely distributed throughout the Alamgir region. During the winter season, from December to February, about 65% of the precipitation falls in the form of snow. The rainy months are March and April. The months of May through September are usually dry. Winter temperatures range from -1.8 to 18.6^{o}C, while summer temperatures hover around 35^{o}C.

3.1.4 Geology

Geologically, Central Kashmir valley represents rocks of all ages, from Precambrian to Holocene; however, a significant nature of rocks is in the record of Late Mesozoic rocks. In the valley basin, the Precambrian to early Jurassic rocks is well preserved, overlain by Plio-Pleistocene Karewa deposits overlain by alluvium of recent age. These rocks are widely used for lithostratigraphic and biostratigraphic correlation.

The bounding mountain ranges of Central Kashmir are generally composed of the oldest stratigraphic sequence of Precambrian Salkhalas, Cambrian Dogra slates, Permian Panjal volcanic, and Triassic Limestone rocks. The area has a complete stratigraphic record of rocks of all ages from Archean to Recent.

The lithological description of different stratigraphic horizons of the Kashmir Valley is described in table 3.1.

3.1.5 Soils

The soils are shallow to deep, mostly loamy skeletal, loamy sand, silt loam, and loamy sand. However, patches of fine and clayey skeletal soils are also met with. Soils are acidic to neutral, rich in organic carbon, and have low to high water holding capacity. Variations in slope, plant cover, parent material, and slope

aspect affect soil properties. The soils are usually mild to severely eroded and stony in specific areas; rock outcrops dominate these patches.

Table 3.1: Central Kashmir Himalaya geological formation stratigraphic sequence (Wadia, 1975; Bhatt, 1976, 1989)

Age	Group/ Formation	Thickness (meters)	Lithology
Recent	Recent Alluvium	150	Alluvium
Plio-Pleistocene	Karewa Group	1300-1800	Boulders, silt, clay sand, and loess-paleosols
Jurassic	Wuyan Formation	300	Limestone and Sandstone
Triassic	Khrew Formation	2000	Shale, limestone, and conglomerate
Permian	Zewan Formation	400	Tuffs, shale, slate quartzite, and basalt
Permo-Carboniferous	Panjal Volcanics	1800-2400	Basaltic and andesitic traps interbedded with shales.
Middle Carboniferous	Fenestella Shale	600	Shale, Sandstone, and conglomerate
Lower Carboniferous	Syringothyris Limestone	300	Limestone, Shales, and quartzites.
Devonian	Muth Quartzite	650	Quartizites
Silurian	NA	50	Slate, greywackes, and sandstone
Ordovician	NA	NA	Shales, Silt, and Limestones
Early Cambrian	Dogra Slate	1525	Slate, Sandstone, limestone, and shale
Pre-Cambrian	Salkhala Series	NA	Quartzite, phyllites, slates, shale, etc.,

3.2 Materials used

3.2.1 Secondary data collection of remote sensing and meteorological data

3.2.1.1 Remote sensing data used

The research used remote sensing data in the form of satellite imageries

available in digital format from various data sources. These data sources are outlined in table 3.2.

Table 3.2: Data sets and their sources used for the study

S No.	Data set	Parameter estimated	Source
1	LISS III (23.5 m)	LULC	https://bhuvan.nrsc.gov.in/
2	ASTER DEM (30 m)	Slope, Altitude, Drainage, Flow Accumulation, etc.,	https://search.earthdata.nasa.gov/search
3	Survey of India (Toposheets) Scale 1:50,000	Drainage	https://www.surveyofindia.gov.in/
4	Soil	Soil Class/Texture	https://www.nbsslup.in/
5	Precipitation	Precipitation	https://dsp.imdpune.gov.in/
6	Geology Map	Geology	https://geominjk.nic.in/ JK Dept. of Geology & Mining
7	Geomorphology	Geomorphology	https://bhuvan.nrsc.gov.in/
8	Lineament	Lineament density	https://bhuvan.nrsc.gov.in/

3.2.1.2 Weather Data

Long-term observed daily climate data ($T_{max,}$ $T_{min,}$ and precipitation) were

collected from Indan Meteorological Department (IMD) Srinagar station from 1989 to 2019 and Agricultural Meteorological Field Unit (AMFU), SKUAST-Kashmir, Shalimar, from 1985 to 2019.

The daily modelled data under RCP 4.5 and 8.5 was obtained from (MarkSim® GCM - DSSAT weather file generator) under GCM (HAD GEM2-ES-GCM) from 2010 to 2095.

3.2.2 Software used for mapping and modelling

The software's used for the research:

(a) Mapping and geospatial analysis

- ✓ ArcMap 10.4.1
- ✓ QGIS 2.6

(b) Model implementation

- ✓ QSWAT 1.8
- ✓ SWAT CUP 5.2.1.1
- ✓ SWAT-MODFLOW
- ✓ GMS 10.3 (Groundwater Modeling System)

(c) Others

- ✓ Interpex IX1D 2.21 (VES)
- ✓ Microsoft excel 2010

3.2.3 Instruments used

In the present study, various instruments were used for the collection and analysis of the data and to locate the geographical coordinates of the respective locations. The details of the instruments and implements used are summarized in Table 3.3.

Table 3.3: Details of the instruments used for the study

S No.	Instrument	Purpose
1	GPS receiver	Geographical coordinates/ground truthing
2	Measuring container and stopwatch	Measurement of Spring discharge
3	AIMIL resistivity meter	Subsurface and Lithological investigation and identification of Groundwater potential zones
4	Guelph Permeameter	Estimation of soil hydraulic characteristics

3.3 Spring waterbody and well survey

In Central Kashmir extensive survey was conducted in all three districts. From the three districts of Central Kashmir, 184 springs waterbodies (72 from Budgam, 63 from Srinagar, and 49 from Ganderbal District) were surveyed and geotagged. Five springs were selected for periodic discharge measurements from these surveyed spring waterbodies. Discharge of all springs was measured using a container of 1-liter capacity and stopwatch method for on-site sampling and surveying. The study area explored points of spring waterbodies are shown in Fig. 3.2. These geotagged point locations were input to the groundwater modelling system for flow budget computation.

Wells in the region, such as bore-wells, tube wells, hand pumps, and open wells, were also included in this research. A total of 208 wells in all three districts have been surveyed and collected from the annual reports of the CGWB. The discharge measurement of the few wells was taken and used for the model input in the flow budgeting of the research region. The surveyed wells in the study area are shown in Fig. 3.3.

3.4 Creating a monitoring system to collect data on spring discharge regularly

3.4.1 Spring Discharge Measurements

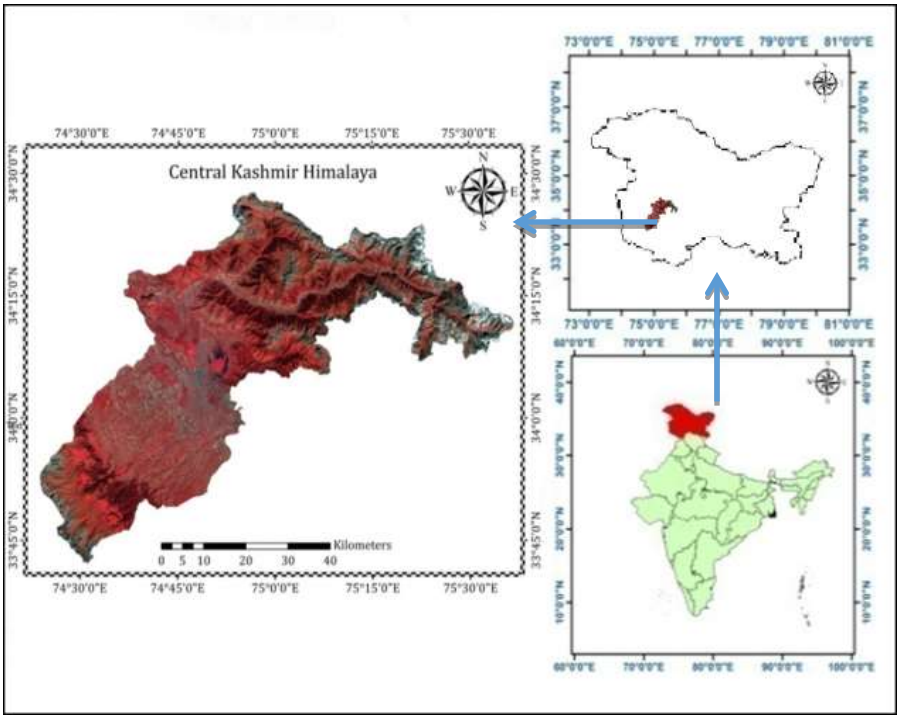

Fig. 3.1: Location map of the Central Kashmir

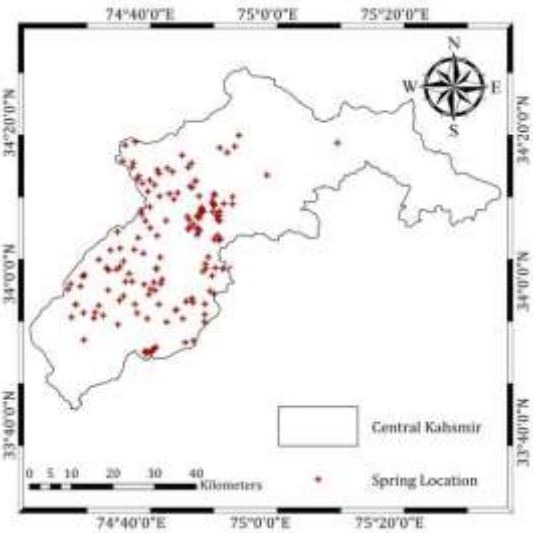

Fig. 3.2: Spring location map of Central Kashmir

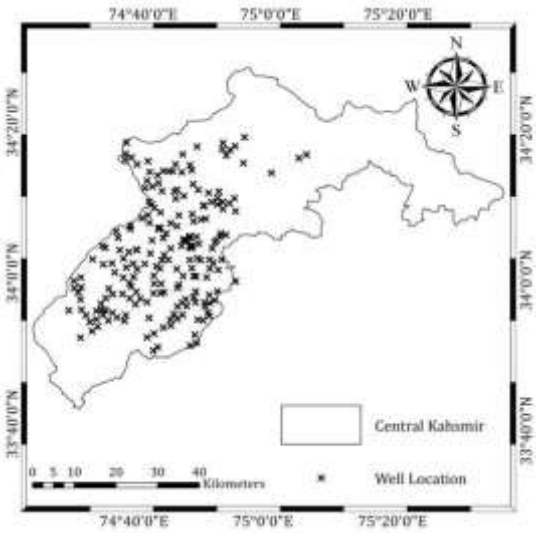

Fig. 3.3: Well location map of Central Kashmir

Discharge of the mountain springs is never constant; their variation is significant in different seasons. Also, spring discharge changes significantly throughout the season depending on different environmental conditions. Central Kashmir is among the affected regions of the Himalayas by water scarcity. Therefore it is required to adopt methodologies for testing and analyzing the spring discharge variation. Following is the method used for spring discharge measurement:

3.4.1.1 Time Volume Method

This method is mostly used for discharge pipes or other places where water can be collected directly into a container. This study selected these types of springs for easy discharge measurement. It is a simple and efficient method for lower discharge rates. It is not accurate for higher discharges. In this method, a container of known volume "V" is used to collect the water sample directly through the spring outlet. A timer is used for measuring the time "T" in which the container is filled with water. The discharge "Q" of the spring is calculated by using the following equation:

$$Q = \frac{V}{T} \qquad \textbf{(3.1)}$$

where,

Q - Discharge of the spring

V - Volume of the container that is filled with water

T - Time taken to fill the container by V volume

The time volume method was used to calculate the discharge of the springs of the study area. The discharge of each spring was taken at least three times, and the average of all the readings was noted as the discharge of the spring.

The five springs were selected for the periodic discharge measurements, and the monthly measurements were taken for 18 to 21 months.

3.5 Future climate scenario generation

3.5.1 Historical and future weather data (modeled data)

Using the MarkSim DSSAT weather generator, we were able to generate site-specific historical and future temperature and precipitation data from five GCMs, namely, Hadley Center Global Environment Model 2 - Earth System (HADGEM2-ES), GFDLESM-2M, CISRO MK 3-0, BCC-CSM 1-1, and GISS-E2R under the RCP 4.5 and 8.5 scenarios (Table 3.4) (Jones and Thornton 2013). The Marksim GCM downscales and generates daily data for a specified location from 2010 to 2095 using the geographical coordinates of the station (longitude and latitude). Data for the time slices representing periods 1985–2019 (baseline), near-future (NF) (2021-2045), mid-future (MF) climate change projection (2046–2070), and far-future (FF) projection (2071–2095) were used. After statistically evaluating RMSE and NRMSE (Table 3.5), HAD GEM2-ES was one of the best performers, with the least error, followed by BCC-CSM 1-1, and was utilized further for climate projections for the research area.

Table 3.4: Climate models, resolution, and scenarios involved in the present study

Model	Modelling Centre/Group	Resolution (Lat)-deg	Resolution (Long)-deg	Scenario Involved
BCC-CSM1-1	Beijing Climate Center, China Meteorological Administration	2.812	2.812	4.5 and 8.5
CSIRO-Mk3-0	Commonwealth Scientific and Industrial Research Organization in collaboration with Queensland Climate Change Centre of Excellence, Australia	1.895	1.875	4.5 and 8.5

GFDL-ESM-2M	NOAA Geophysical Fluid Dynamics Laboratory	2.000	2.500	4.5 and 8.5
GISS-E2-R	NASA Goddard Institute for Space Studies, USA	2.022	2.517	4.5 and 8.5
HadGEM2-ES	Met Office Hadley Centre, UK	1.250	1.875	4.5 and 8.5

Source: Chaturvedi *et al* (2012)

Table 3.5: RMSE and NRMSE values of different models selected for the study area

Model	RMSE	NRMSE
BCC-CSM1-1	4.71	0.283
CSIRO-Mk3-0	4.89	0.295
GFDL-ESM -2M	5.16	0.314
GISS-E2-R	4.89	0.298
HAD GEM2-ES	4.49	0.272

3.5.2 Working of Marksim DSSAT weather file generator

In the following sections, the Marksim DSSAT weather file generator is explained. Marksim DSSAT weather file generator snapshot can be seen in this section (Plate 1 & 2).

1. Using Google Earth, pinpoint your preferred location on the map and verify its latitude, longitude, and elevation (in mountainous areas, you may have to move very slightly to select the correct altitude).
2. Select the GCM combination you require, and 17 GCMs exist in the portal.
3. Choose an emissions scenario among four IPCC Concentration Pathways (RCP 2.6, 4.5, 6.0, and 8.5). RCPs are greenhouse gas concentration trajectories discussed in the fifth assessment report of IPCC.
4. Choose the year, and the data will imitate daily weather data from that year's statistical average.

Plate 1: Marksim DSSAT weather file generator screenshot for AMFU Shalimar.

Plate 2: Marksim DSSAT weather file generator screenshot for IMD Srinagar.

5. Replication determines how many DSSAT climate files you get (1 to n). They are labeled CLIM0101 through CLIMnn01; they are random duplicates of your chosen year.

6. View data via the visual interface below the map and download the zipped file for further processing.

3.5.3 Bias Correction of Climate Model Outputs

For local bias correction of T_{max}, T_{min}, and precipitation, two basic methods were used: the modified difference approach method (equations 3.1 & 3.2) and the linear scaling method (equations 3.3 & 3.4). The statistics of GCM variables like temperature and precipitation often show a noticeable bias due to restrictions in, for example, the incorporation of local topography and non-stationary phenomenon within the GCMs. Modelled climate data from MarkSim DSSAT was available from 2010 to 2095, and for the derivation of correction functions, the time slice of 2010-2019 was used for both observed and modeled climate variables.

3.5.3.1 Modified Difference Approach

Some statistical factors were introduced to the modified difference technique to enhance the corrective function. In temperature adjustment, for example, mean (μ) and standard deviation (σ) were introduced with the aim of shifting and scaling to modify the μ and variance (Leander and Buishand 2007). T (cor) is the corrected daily temperature, and P(cor) is the corrected precipitation.

$$\overline{T(cor)} = \overline{T(obs)} + \frac{\sigma(obs)}{\sigma(mod)} \times (T(mod) - \overline{T(obs)} + (\overline{T(obs)} - \overline{T(mod)}) \quad \textbf{(3.1)}$$

$$P_{cor} = (P_{mod} + (dx)) \times \left(\frac{\sigma P_{obs}}{\sigma P_{mod}}\right) \quad \textbf{(3.2)}$$

Where, (μ) mean, (σ) standard deviation, $T_{(cor)}$ corrected temperature, P_{cor} corrected precipitation, $T_{(mod)}$ and P_{mod} modelled/uncorrected daily temperature and precipitation for a scenario, $T_{(obs)}$ and $P_{(obs)}$ observed temperature and

precipitation obtained from the baseline scenario. Over bar represents the average over the time period under analysis. The averaged daily difference between observed and modelled values is represented by (dx).

3.5.3.2 Linear Scaling Method

The purpose of the linear scaling (LS) approach is to accurately match the monthly mean of corrected values with observed data (Lenderink *et al*., 2007). Adjustments are made monthly based on the magnitude of the discrepancy between the observed and raw data (in this case, the raw data from GCM simulations and models). Precipitation monthly corrections are normally multiplied by a factor, and temperature monthly corrections are added. In order to determine the multipliers and addends, linear scaling formulas are used (Equations 3.3 and 3.4).

$$T_{cor,\,m,d} = T_{mod,\,m,\,d} + \mu(T_{obs,m}) - \mu(T_{mod,\,m}) \quad \textbf{(3.3)}$$

$$P_{cor,m,d} = (P_{mod,m,d}) \times \left(\frac{\mu P_{obs,m}}{\mu P_{mod,m}}\right) \quad \textbf{(3.4)}$$

$P_{cor,m,d}$ and $T_{cor,m,d}$ are corrected precipitation and temperature on the d^{th} day of m^{th} month. $P_{mod,m,d}$ and $T_{mod,m,d}$ are the modelled/uncorrected precipitation and temperature on the d^{th} day of m^{th} month. μ(...) is the expectation operator; for example, ($P_{obs,m}$) is the mean value of observed precipitation for a particular month (m).

Model corrected data was divided into three-time slices near future (NF) climate change projection (2021–2045), mid future (MF) projection (2046–2070), and far future (FF) projection (2071–2095), and climate change extent was compared with baseline historical observed data (1989-2019).

3.6 Comprehensive mapping and conceptual layouts

3.6.1 Methodology for mapping

ASTER DEM was used to extract the boundary of the Central Kashmir Valley comprising three districts, viz. Srinagar, Budgam, and Ganderbal, and four major catchments like Dal, Sindh, Dudhganga, and Sukhnag Catchment. The details of datasets used for map generation were downloaded from various sources, and some were available from the concerned government agencies and are given in table 3.2.

The drainage network for the research region was digitized using the ArcGIS 10.4.1 platform and derived from the ASTER Global Digital Elevation Map (ASTER GDEM). The slope map was created using the Spatial Analysis tool and ASTER data. The rainfall map was created using data collected from Central Kashmir meteorological stations. The rainfall distribution map was created by spatially interpolating this data using the Inverse Distance Weighted (IDW) approach. This interpolation approach combines the ideas of closeness and progressive modification of the trend surface to follow Thiessen polygons. The line density analysis tool was used to develop the lineament density and drainage density maps. Thematic layers such as land use have been defined using satellite images from IRS LISS III satellite data at a scale of 1:50,000 (geo-coded, using UTM projection, spheroid, and datum WGS 84, Zone 43 North). The other maps created utilizing available datasets and then used for modelling are discussed below.

Slope: The change in elevation affects the runoff at a given location. Groundwater infiltration is inversely linked to the slope of the land. Groundwater infiltration is often facilitated by a break in the slope (i.e., a steep slope followed by a more gradual slope) (Saraf and Choudhary, 1998). A total of nine slope classes have been established in the research region based on the slope, i.e., <5%, 5-10%, 10-20%, 20-30%, 30-40%, 40-50%, 50-60%, 60-70%, and >70%. The

slope map of the study area [Fig. 3.4(a,b)] shows that a gentle slope of <10% dominates the area of the central and valley regions with 48% areal coverage. Higher ranges and mountainous areas have a 27% areal coverage with a steep slope of >40%.

Altitude: The recharge potential of an area is strongly influenced by its altitude. Water tends to collect at lower elevations rather than higher elevations. Groundwater potential decreases with elevation and vice versa (Gedebo *et al.*, 2006). The research region is divided into five groups [Fig. 3.4(c,d)]: 2000, 2000-3000, 3000-4000, 4000-5000, and >5000 m. The majority of the study area is within the lower altitude zone of 2000 m, with 45% of the study area within this zone. The Central Kashmir upper ranges have an altitude range of 2000-3000, 3000-4000, 4000-5000, and>5000 m, encompassing an area of 21%, 11%, 23%, and 0.23 %, respectively.

Drainage density: Permeability affects drainage density, and low drainage density increases recharge and GWP. Surface water features like rivers, ponds, etc., may operate as GWP recharge zones (Karanth, 1987). The resulting drainage density map of the area [Fig. 3.4(e,f)] was grouped into five classes such as <2 km/km^2, 2-6 km/km^2, 6-10 km/km^2, 10-14 km/km^2 and >14 km/km^2. Most of the area (85%) falls in a low drainage density of <2 km/km^2 occupying lower parts of the region. However, the mountainous regions and higher parts are covered by a drainage density range of 2-6 km/km^2, 6-10 km/km^2, 10-14 km/km^{2,} and >14 km/km^2 area of 15%.

Rainfall: The replenishment of groundwater and rainwater collection both rely heavily on rainfall as one of their primary sources. The high rainfall levels indicate a chance of significant groundwater recharging and harvesting, which results in high GWP zones. In contrast, low rainfall amounts suggest little groundwater recharge, which results in low GWP zones (Mwega *et al.*, 2013). Using the annual rainfall data, a spatial distribution map of rainfall was generated, and two rainfall zones were established using the data from two different stations

[Fig. 3.4(g),h)]. The average annual precipitation in the research region varies from 850 to 900 mm.

Geology: The geological formation of a region is one of the most important factors that determine the distribution and availability of groundwater (Krishnamurthy and Srinivas, 1995). The percolation of water and the features of the aquifer are both under the influence of lithology, which affects groundwater recharge (El-Baz *et al.,* 1995). There are seven geological types of alluvium: panjal trap, zewan formation, triassic jurassic limestone, Salkhala Series, Fenestella Shale, Syringothyris Limestone, and Muth Quartzite have been found. The study area is mainly dominated by alluvium, covering an area of 39% and occupying the mainly lower part of the valley with a gentle slope. The study region is covered by panjal traps and salkhala series, with an area of 47% in the higher reaches. Other geological types form 14% of the area, which mainly covers the mountain regions of Central Kashmir [Fig. 3.4(i,j)].

Geomorphology: Groundwater movement and storage are heavily influenced by geomorphology and landforms (Dinesh Kumar *et al.,* 2007). When geomorphological features and structures are combined with geological formations, groundwater quality, movement, and occurrence are all influenced. Understanding the occurrence of porous and permeable zones requires understanding the evolution of landforms in the area. Groundwater recharge involves considering the study area's geomorphology (Senanayake *et al.,* 2016). Fluvial, glacial, structural, lacustrine origin, and water bodies are the vital geomorphic features seen in the selected area [Fig. 3.4(k,l)].

Soil: The quality of the soil is the primary factor in determining the amount of groundwater available. Soil conditions highly influence water infiltration. Grain size has a significant impact on soil infiltration rates. The relationship between runoff and infiltration rates is used to determine GWP and RWHSL, and soil properties are used to establish such a relationship (Tesfaye, 2010). Nine major types of soil groups were identified in the study area, i.e.,

Aquic Hapludalfs, Lithic Udorthents, Typic Dystrochrepts, Fluventic Eutrochrepts, Typic Udorthents, Aeric Haplaquepts, Aeric Fluvaquents, Dystric Eutrochrepts, Lithic Cryorthents [Fig. 3.4(m,n)].

Land Use Land Cover: The quantity of precipitation that reaches the water table and recharges groundwater is influenced by LULC. Hydrology is significantly impacted by LULC changes such as forest cover changes, agricultural intensification, wetland drainage, and urbanization (De Roo *et al.*, 2001). Surface runoff volume and discharge rate often increase, whereas groundwater recharge and base flow decrease due to those changes (Moscrip and Montgomery, 1997). The study area was classified into seven LULC classes [Fig. 3.4(o,p)]: waterbodies/wetlands, glacier/snow, forests, agriculture, horticulture/plantation, and wasteland/barren and built-up/utility.

Lineament: Lineaments often indicate a permeable zone on a lineament density map, which measures the quantitative length of linear features per unit area rendered on a grid (Sitender, 2010). Identifying GWP zones has proven easy using lineament analysis (Rao *et al.*, 2004). GWP may benefit from areas with a high density of lineaments (Haridas *et al.*, 1998). Infiltration is increased when the lineament density is high, but runoff is increased when the lineament density is low (Kumar *et al.*, 1999). Lineament density ranged from 0.5 km/km^2 to 9 km/km^2 in the studied region [Fig. 3.4(q,r)].

Flow Accumulation: The flow accumulation operation counts the total number of pixels that drain into the outlets. The flow accumulation was divided into two classes, ranging from 0-5000 and >5000. The flow accumulation map for the study area is given in figure 3.4(s).

3.7 Land use/Land cover change detection/matrix

This section covers the detailed analysis of Land use/land cover change detection in Central Kashmir Himalayas. A comprehensive methodological framework was adopted for this study to analyze the LU/LC for which various

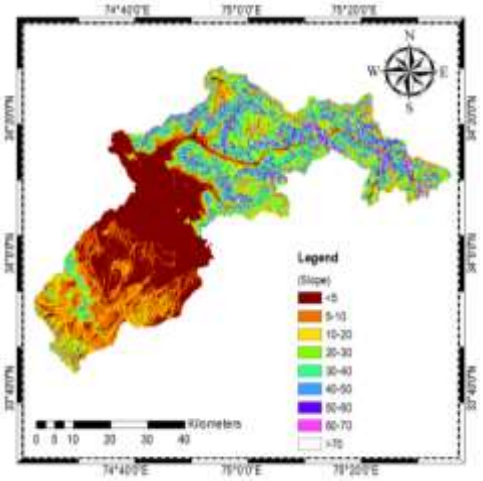

a. Slope map (%)

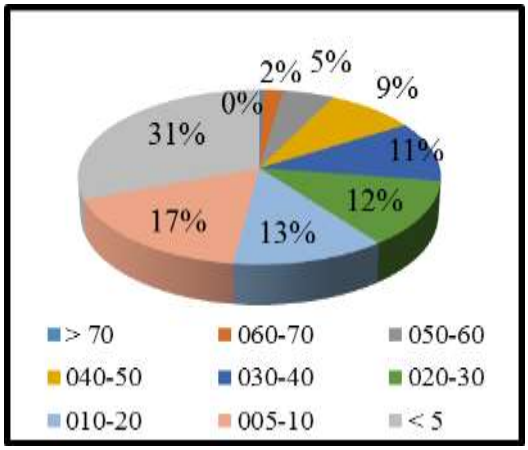

b. Areal distribution of Slope (%)

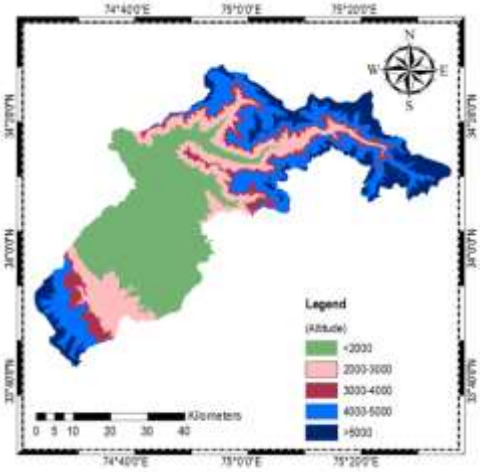

c. Altitude map (m)

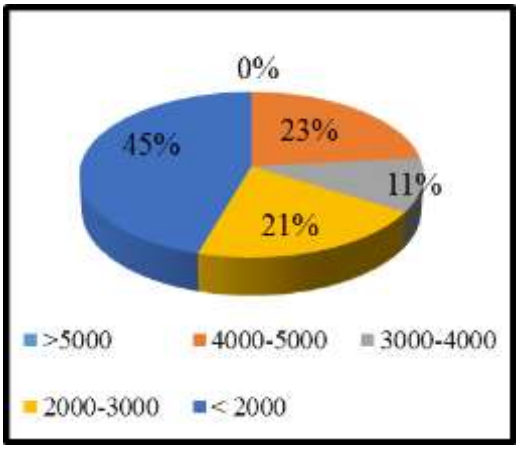

d. Areal distribution of Altitude (%)

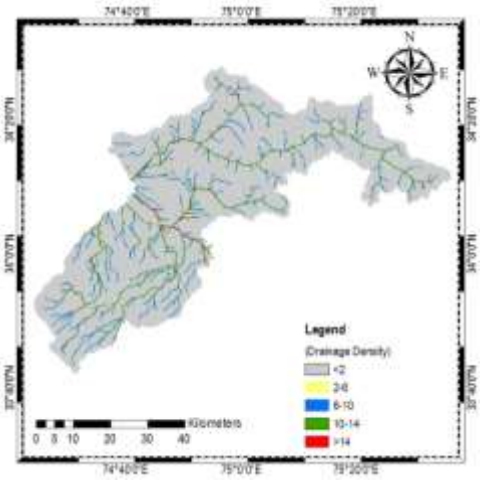

e. **Drainage density map (km/km^2)**

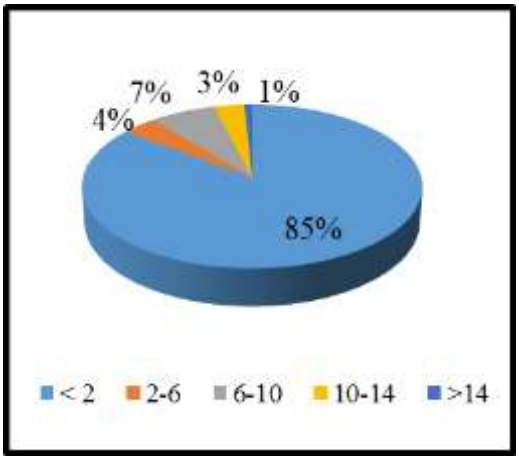

f. **Areal distribution of D density (%)**

g. **Precipitation map (mm)**

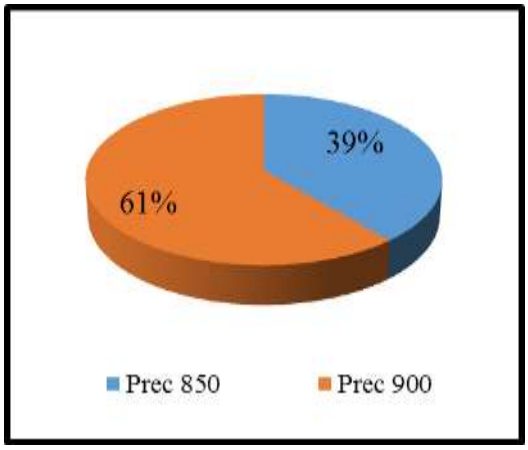

h. **Areal distribution of Precipitation (%)**

i. Geology map

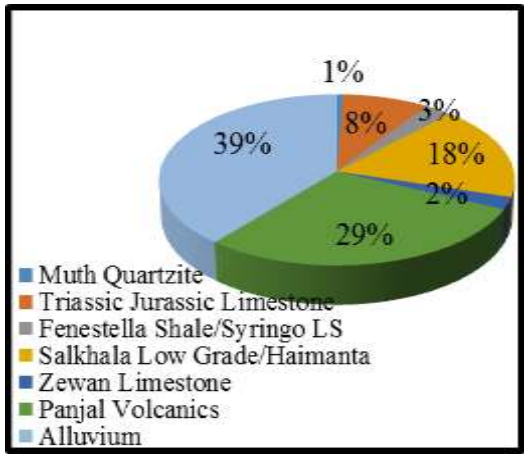

j. Areal distribution of Geology (%)

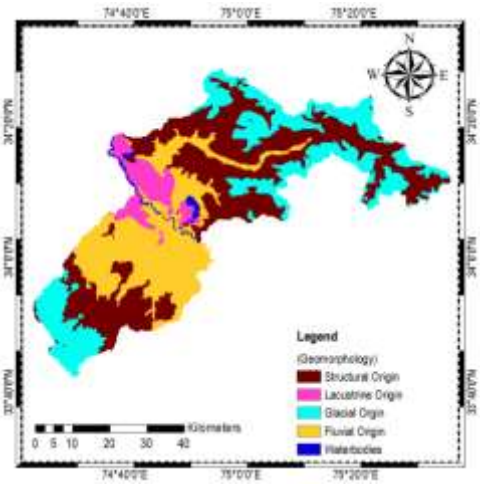

k. Geomorphology map

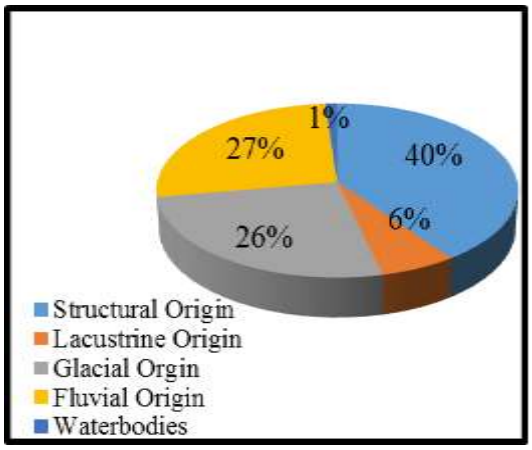

l. Areal distribution of Geomorphology (%)

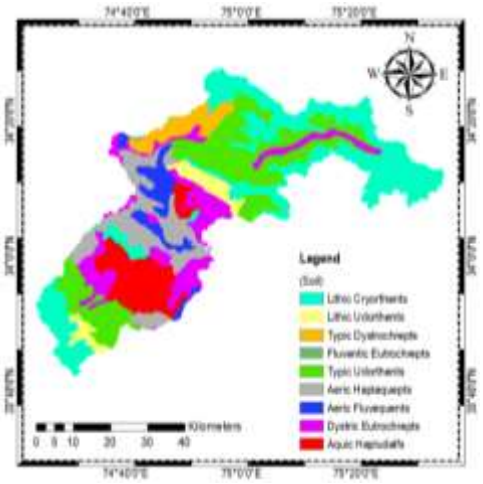

m. Soil map

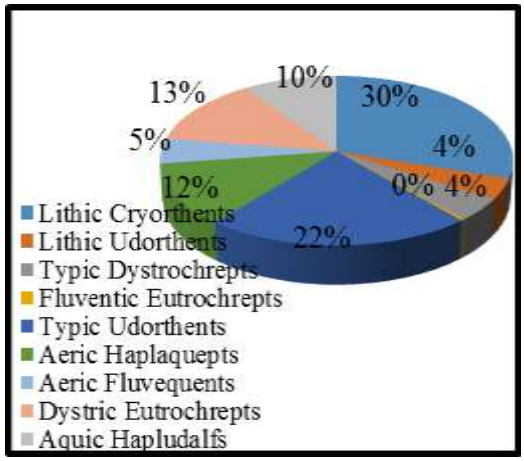

n. Areal distribution of Soil groups (%)

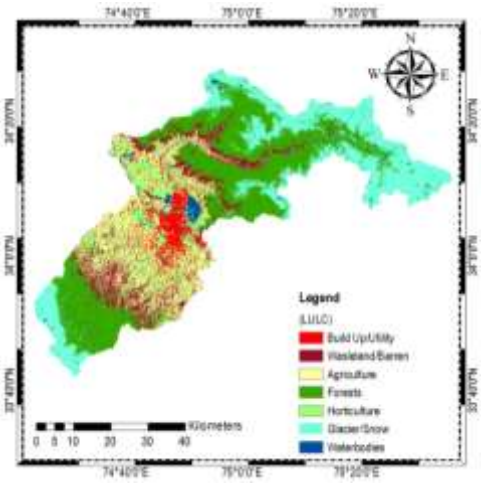

o. LU/LC Map

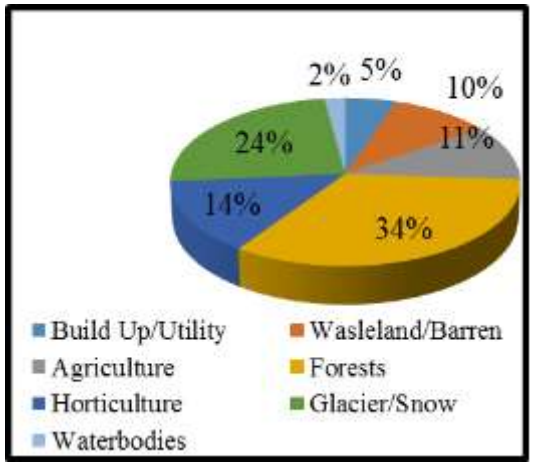

p. Areal distribution of LU/LC classes (%)

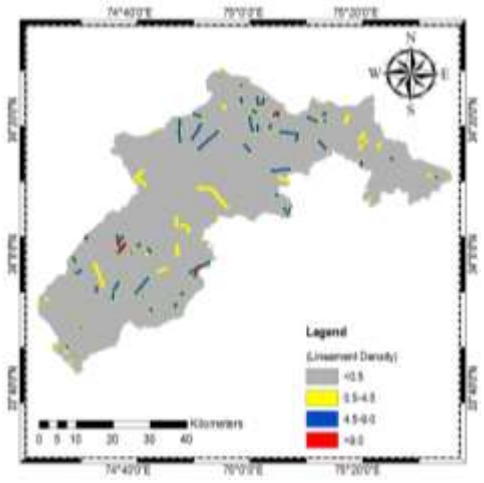

q. **Lineament Density Map (km/km^2)**

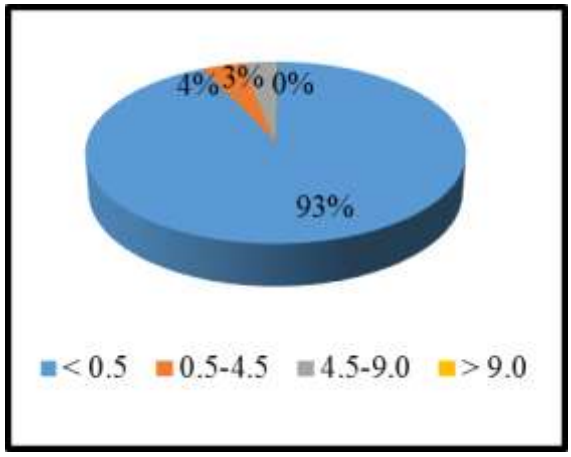

r. **Areal distribution of Lineament density (%)**

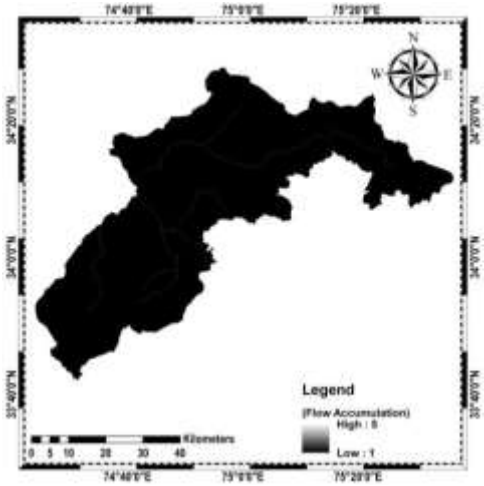

s. **Flow accumulation map**

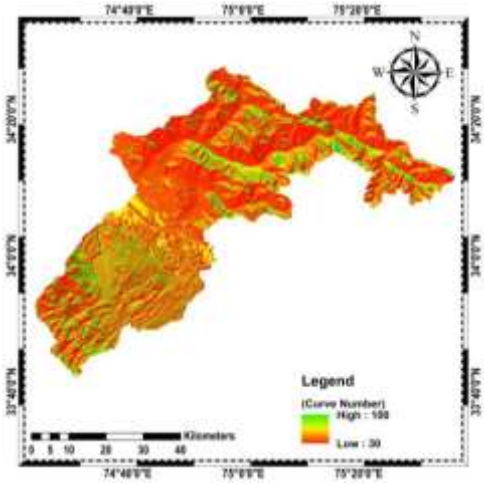

t. **Curve number map**

Fig. 3.4: Various thematic maps generated using different datasets for Central Kashmir

data sets were generated to serve the purpose. To identify land cover change detection, remote sensing data, satellite imagery, and image processing techniques were done within two dates of April 2000 and April 2017 using LISS III 23.5 meters resolution imageries. Arc GIS 10.4.1 software was used to identify the changes. Seven land use/Land cover classes were identified using Supervised Classification. A broad outline of the various methodological steps is provided in figure 3.5, for which a brief description is produced as follows.

The Central Kashmir Valley's boundaries were determined using ASTER DEM, which comprises three districts and four watersheds. The details of the datasets used were downloaded from the various websites given in table 3.6. In order to generate the LU/LC map using satellite images, a LU/LC classification technique has been used. The appropriate number of LU/LC classes depends on the requirements of a specific project for a specific application (Saha *et al*., 2005). Seven major LU/LC classes were chosen for mapping the entire study area viz; waterbodies/wetlands, glacier/snow, forests, agriculture, horticulture/plantation, wasteland/barren, and built-up/utility. Following the development of the classification scheme, one of the most extensively used image classification techniques, supervised classification, was used to map all of the land use/land cover classes to assess the land use pattern and its geographic variation using widely available satellite data. Prior to choosing training samples, the empirical approach of satellite data, Google Earth photographs, and toposheet of the subject region were thoroughly explored. The minimum number of training samples for most of the classes was 100. Before being utilized as input for any applications, the classified images were further checked for accuracy. Individual accuracy evaluation parameters can be used in the study to evaluate the model performance of a specific category or class of interest. The accuracy of this study was assessed using an error matrix.

Table 3.6: Datasets used for the LU/LC map generation

S No.	Data Set	Source
1.	ASTER DEM (30 m)	https://search.earthdata.nasa.gov/search
2.	LISS III (23.5 m)	https://bhuvan.nrsc.gov.in/
3.	SOI (Toposheets) Scale 1:50,000	https://www.surveyofindia.gov.in/

3.8 Identification of recharge zones and rainwater harvesting suitability

Before the weighted overlay analysis, the resulting thematic layers were converted into raster format with a 30 m resolution. Using the spatial analysis tool, a weighted overlay method was used to integrate all the thematic maps and derive the groundwater rechargeable areas and rainfall harvesting suitability levels.

3.8.1 Analytic Hierarchy Process (AHP) for Water Harvesting

To successfully implement potential surface water harvesting and groundwater recharge potential zonation, site selection modelling, suitable criteria, and constraint factors had to be defined. The criteria chosen for determining the rainwater harvesting suitability were LU/LC, slope, soil, flow accumulation, rainfall/precipitation, and curve number, and for groundwater recharge, zonation criteria chosen were LU/LC, slope, soil, altitude, rainfall/precipitation, geology, geomorphology, drainage density, and lineament. The final suitability and recharge zonation maps were obtained by overlaying all these maps using weighted overlay analysis in Arc GIS 10.4.1. The brief methodology adopted for this study is given in figure 3.6. Using a standard scale of values, the weighted overlay analysis standardized the diverse and dissimilar data provided so that it could be easily integrated. It uses two indices: the Standardized Compound Weight Index (CWI) and the Suitability Level Index (SLI) for the Weighted Overlay Process (WOP) (SLI). The Compound Suitability Index (CSI) was used to determine the final score for criterion constraints.

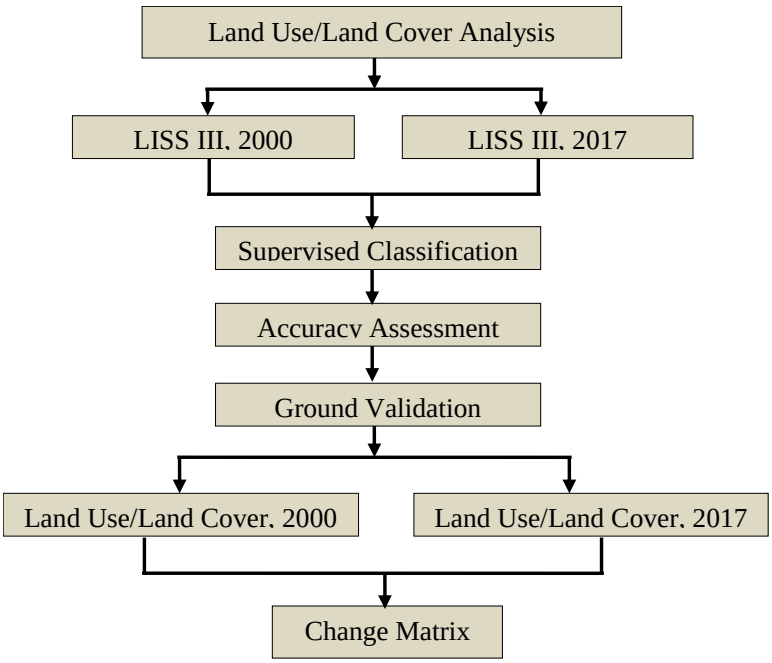

Fig. 3.5: Methodological steps for LU/LC change matrix

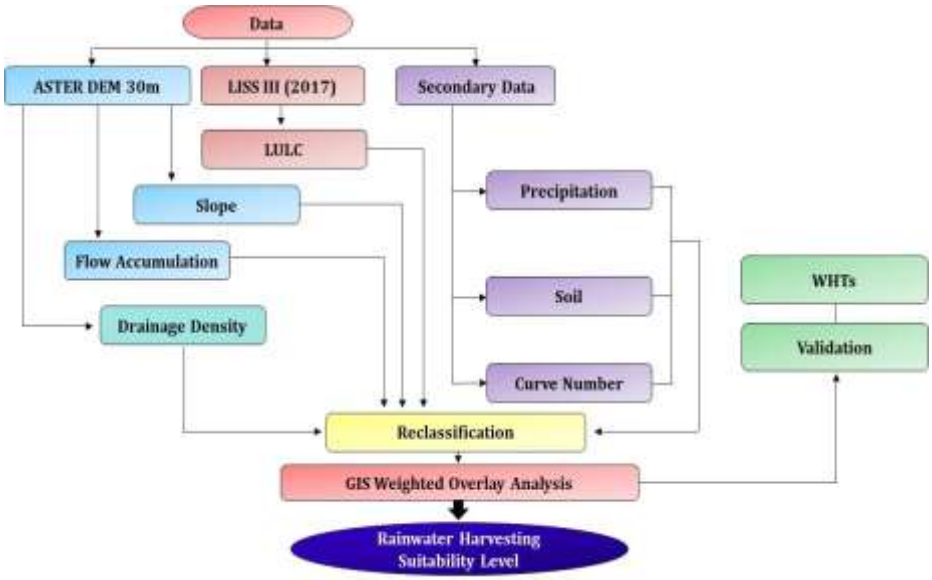

Fig. 3.6: Methodology adopted for the identification of rainwater harvesting suitability zones

3.8.2 Compound Suitability Index (CSI)

The CSI is obtained by combining the CWI and SLI to describe the suitability of a given theme and is given by:

$$CSI = \sum(CWI_{factor} \times SLI_{factor}) \qquad \textbf{(3.5)}$$

Where CSI is Compound Suitability Index for each factor/criterion, CWI factor is the relative importance weight for each factor/criterion, and SLI factor is the Suitability Level Index for each factor/criterion.

For calculating the weights and consistency ratio by the AHP method, the steps followed were: (a) generation of the pair-wise comparison matrix, (b) the criterion weights computation, and (c) the consistency ratio estimation.

Consistency ratio (CR) is one of the processes in the AHP technique that measures the consistency of numerous aspects of the process. Its value should be less than or equal to 0.01(or 10%) for reliable outcomes.

3.8.3 Normalized Pair-Wise Comparison Matrix and Factor Weightings

In pair-wise comparison, the values in each column of the comparison matrix for water harvesting were summed, and after that, every element of the respective column was divided by its column total to acquire the Normalized pair-wise comparison matrix from which the final factor weightings were obtained.

The consistency of the calculated pairwise comparison was then evaluated using consistency ratio (CR) to check if the evaluation between the chosen factors falls within the acceptable limits. The CR should be below 10%. CR was calculated using the following:

$$CR = \frac{CI}{RI} \qquad \textbf{(3.6)}$$

Where CI is the consistency index; RI is the random index, and the consistency index (CI) was calculated by:

$$CI = \frac{\lambda - n}{n-1} \qquad \textbf{(3.7)}$$

Where λ = consistency vector; n = number of factor (criteria) under consideration. The consistency vector was determined by:

$$\lambda = \frac{\text{Weighted sum vector}}{\text{Factor's weight}} \qquad \textbf{(3.8)}$$

The consistency ratio calculated for the analysis was 0.05 (or 5%), which was within the suitable range. A similar methodology was used for the groundwater zonation map using nine parameters in AHP (Fig. 3.7).

The weighted linear combination (WLC) and the Boolean technique are the primary techniques employed in the GIS environment to map potential sites (Al-Adamat *et al.*, 2010). The WLC method offers better site selection because of its flexibility in selecting optimal sites than the Boolean method, which renders constricted site selection owing to OR or AND operation (Malczewski, 2004). In our study, we exploited the Weighted Overlap Tool in ArcGIS 10.4.1, which is based on the linear combination technique. In WLC, equal or unequal weights are assigned to different thematic layers, and sub-categories or each thematic layer are rated (ranked) at varying scales. The weights obtained from the AHP technique are multiplied with ranks given to each sub-category, which are further linearly summed, resulting in the final potential map.

3.9 Geophysical exploration for lithological investigation and groundwater validation

The primary aim of electrical resistivity surveys is to demarcate the low resistivity zones and high resistivity zones in the area under consideration. In order to cover all three districts, 03 electrical soundings were carried out in a grid pattern covering the entire study area. All three soundings were near the observation springs and wells. Vertical electrical soundings (VES) were conducted using a Schlumberger electrode array with a maximum half-current electrode spacing of 200 m (AB/2). To acquire sounding data, a predetermined set

of current electrode separations with computed geometric factors was utilized. An AIMIL-make signal stacking-based signal enhancement resistivity meter is the instrument for collecting data. All the locations of VES points were recorded with the help of the Global Positioning System (Garmin make GPS). When the apparent resistivity is multiplied by the geometric factor, the instrument directly delivers the resistance value for each current electrode spacing. The data is utilized to create resistivity maps at AB/2 separation, which shows the variation in resistivity values within the region in terms of high and low resistivity zones. The interpreted findings indicate the true resistivity and thickness values. The findings may then be used to create a geo-electric section that depicts subsurface formations.

3.9.1 Field Procedure for Vertical Electrical Sounding

The measuring instrument (resistivity meter) is placed at an observation station suitable for spreading the cable in either direction (Plate 3). Non-polarizing electrodes are placed at predetermined distances on each side of the designated center near the measuring equipment to measure potential differences. Connect the closest pair of potential electrodes to the appropriate terminals on the device using a PVC-covered cable. A 90V power supply unit also powers the instruments. On each side of the center, current electrodes are pushed 10 to 15 cm into the ground. PVC wire connects these current electrodes to the instruments. When the equipment is switched on, the meter shows some self-potential, which is compensated by bringing the value to zero by operation compensator controls provided in the equipment. The current is sent into the earth through the current electrode pair. The working steps followed during the groundwater resistivity investigation are given in figure 3.8, and the working principle of the resistivity meter is shown in figure 3.9.

Plate 3: Field investigation of groundwater resistivity profiling in Central Kashmir

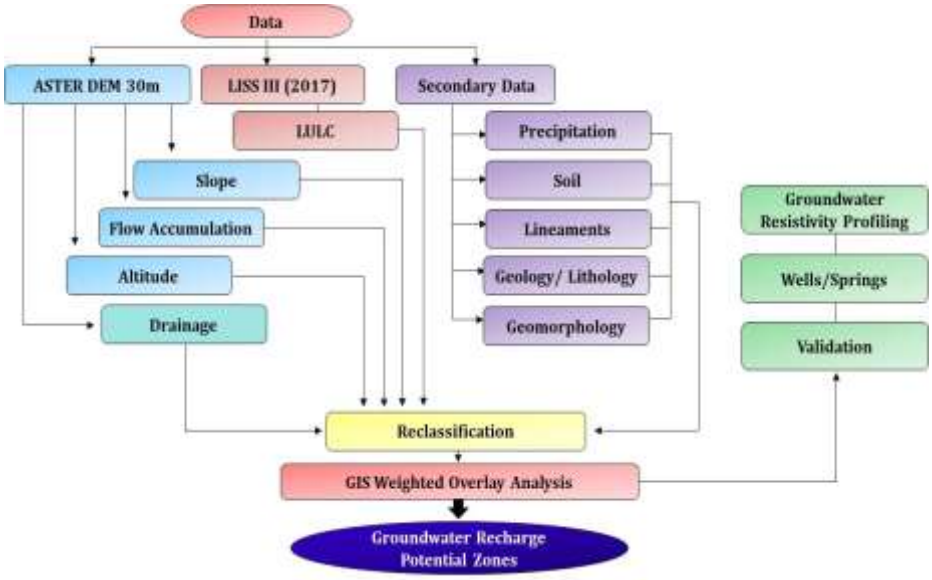

Fig. 3.7: Methodology adopted for the identification of groundwater recharge potential zones

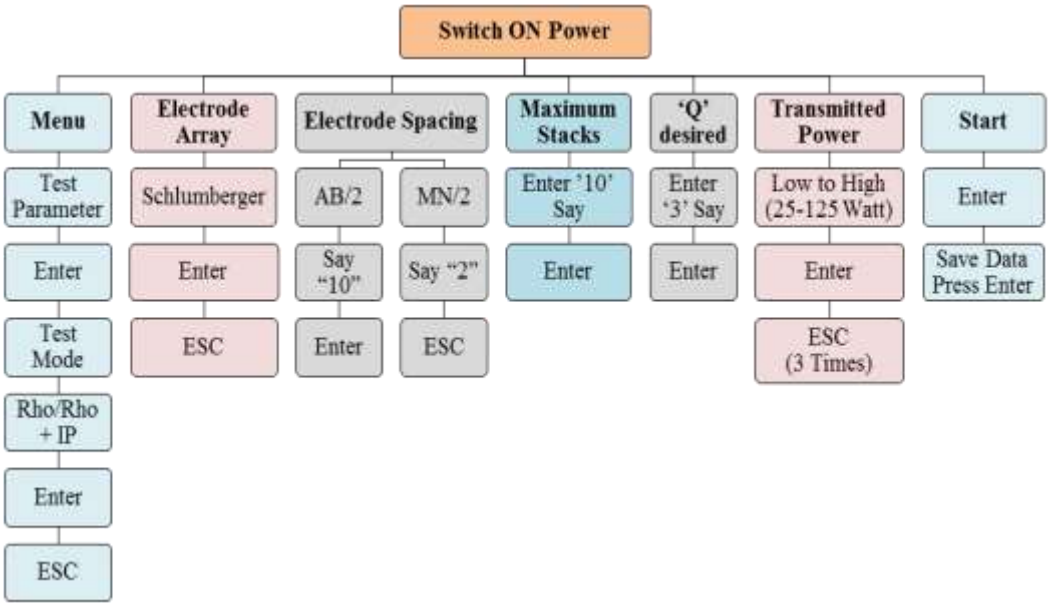

Fig. 3.8: Working steps followed during geophysical groundwater resistivity investigation

3.9.2 Vertical Electrical Soundings

Geophysical surveys form a relatively quick, economical, and non-destructive way to gain subsurface information about the earth. In environmental, hydrogeological, and engineering applications, the electrical resistivity approach has emerged as a viable tool among the many geophysical methods (Vandam and Meulankamp, 1967; Loke and Barker, 1996). 1D sounding with the typical four-probe resistivity meter was used to determine the aquifer geometry in the research region. Using the curve-matching approach, we were able to determine the resistivity and thickness of the layer and, as a result, the depth sections of the profile. The resistivity values of the weathered and fractured zones are used to interpret them. Partial curve matching extracted the initial model parameters from VES data collected during field experiments. The preliminary interpretation of the VES curves was carried out by the curve matching technique (Orellena and Moony 1966) and INTERPEX 1D software (Babachev, 2003) (Plate 4). The methodological steps followed for interpreting the resistivity data are given in figure 3.10. Targeting the geological result is the specific feature distinguishing Interpex from other popular automatic inversion programs. The resistivity field data can only be understood if the apparent resistivity is taken into account. Resistivity master curves for Schlumberger array setup have made it easier to comprehend the sounding field data in terms of both quality and quantity. Curve matching was effectively employed until a linear digital filter revolutionized resistivity master curve computation. Interpretation and inversion techniques were popularised by computer-aided interpretation and inversion methods. The initial phase in the computer-aided interpretation process is still the curves matching approach, which offers the layer value from the computer-aided analysis. In resistivity-sounding data interpretation, the geological formation is believed to be level or near horizontal ground with two, three, or more resistivity and thickness layers.

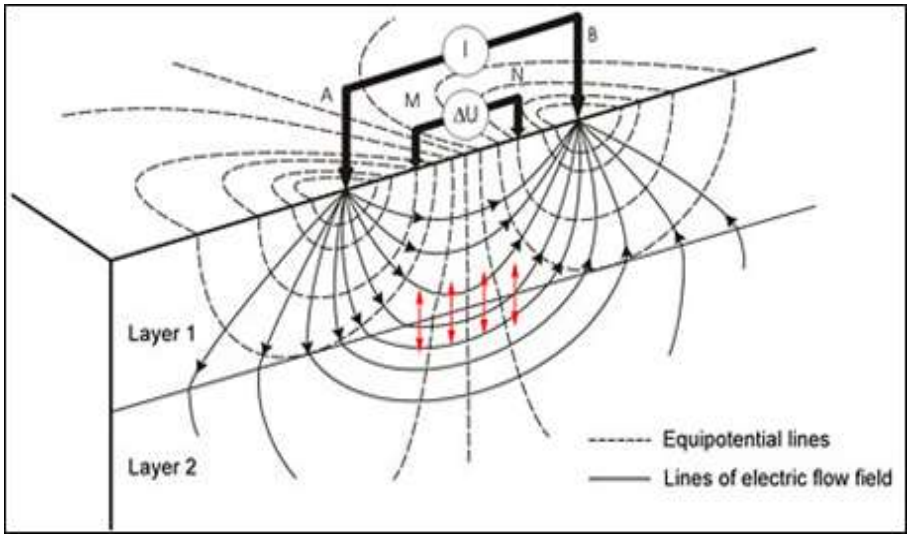

Fig. 3.9: Working principle of the groundwater resistivity meter

Fig. 3.10: Methodological steps followed during interpretation of resistivity data

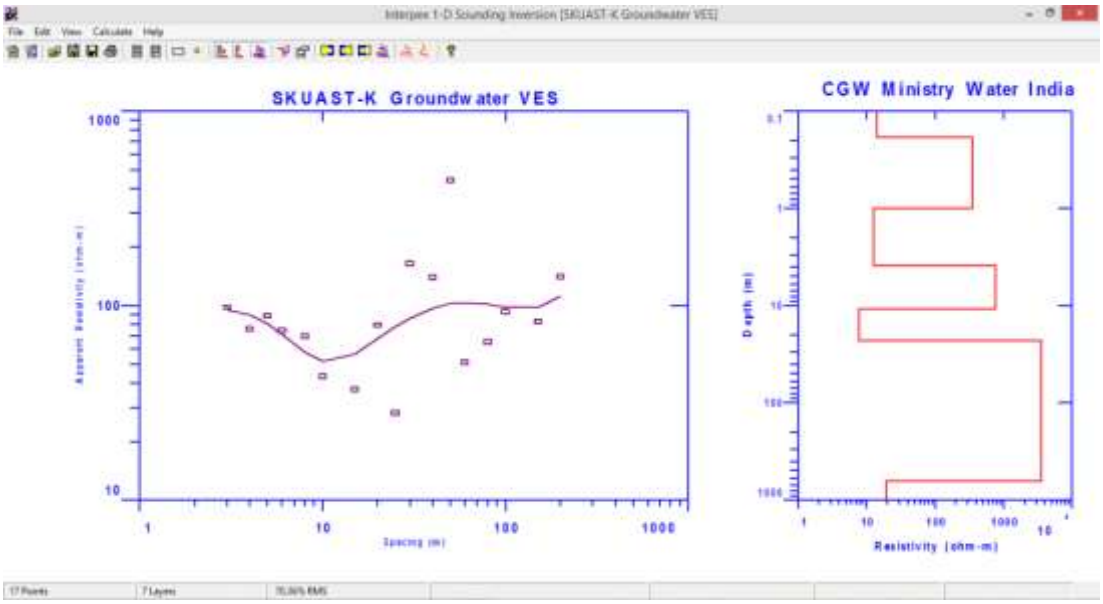

Plate 4: Interpretation of groundwater resistivity data using INTERPEX 1D software

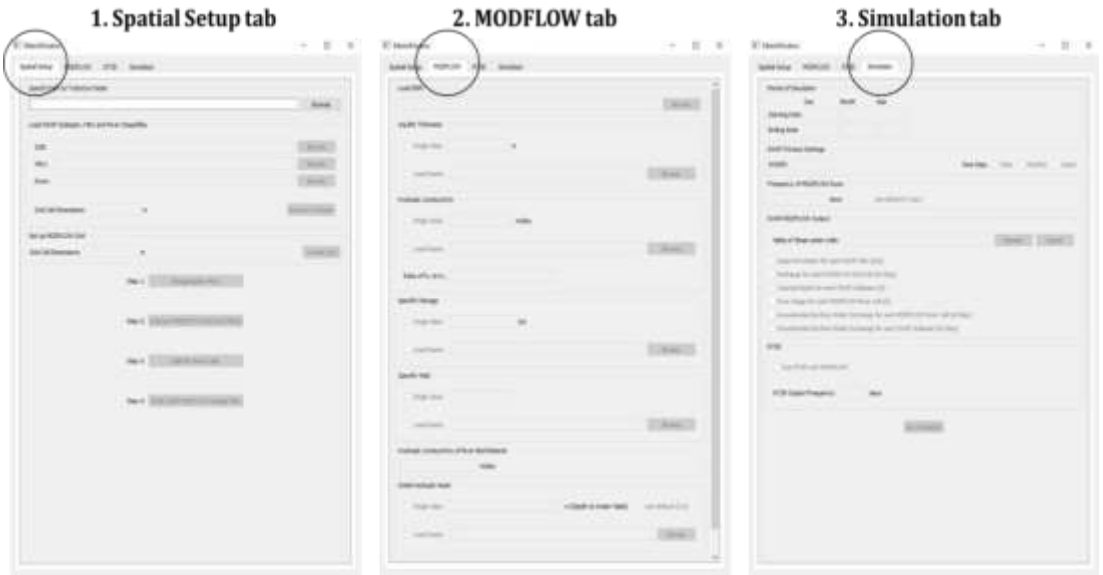

Plate 5: SWAT-MODFLOW interface for creating a fully linked surface and groundwater model

3.10 Modelling of catchments (surface, groundwater modeling, and coupling of models developed)

3.10.1 Description of Hydrological SWAT Model

The SWAT model is a long-term, continuous simulation watershed model. On a daily time scale, it predicts the influence of management on water, sediment, and agricultural chemical production. Watersheds may be divided into smaller sub-watersheds, which allows the model to simulate a high degree of geographic information while using little computation. Crop/vegetation growth and nutrient cycle are all considered in SWAT simulations. Watersheds may be modelled with fewer monitoring data and evaluated using other inputs such as climate, land-use practices, land cover and water flow, nitrogen cycling, and other outputs. Weather, hydrology, soil temperature, plant growth, nutrients, pesticides, and land management are important model components. Several model components have already been tested and shown to work in a range of watershed environments.

Sub-watersheds and Hydrologic Response Units (HRUs) are created within a watershed using SWAT, each having comparable land use, management, and soil characteristics. In a simulated SWAT operation, the positions of the HRUs cannot be determined. Multiple strata exist in the soil profile. Infiltration, evaporation, plant absorption, lateral flow, and percolation are all ways that water moves through the soil. Each HRU in a sub-watershed contributes to the outflow via channels, ponds, and/or reservoirs with its own load of flow, sediment, nutrients, and pesticides. SWAT simulates the hydrological cycle using Equation 3.9 (Ghoraba, 2015). Arnold *et al.,* (1998, 2000, 2005) describe the model and its components in detail.

$$SW_t = SW_0 + ?_{i=1}^{t}\left(R_{day} - Q_{surf} - E_a - w_{seep} - Q_{gw}\right) \quad \textbf{(3.9)}$$

where t is time (days), SW_o and SW_t are the initial and final soil water content, R_{day}, Q_{surf} , E_a, w_{seep} and Q_{gw} are the quantities of rainfall, surface runoff, total evapotranspiration, amount of water entering the vadose zone from soil profile and return flow respectively in i^{th} day. All parameters have units in mm.

The SCS-CN curve number approach is used to estimate streamflow for selected catchments:

$$Q = \frac{(P-0.2S)^2}{P+0.8S)} \quad \textbf{(3.10)}$$

where Q is the cumulative surface runoff, mm; P is the cumulative rainfall, mm; S is the retention parameter, mm. QSWAT is an extension of QGIS, which provides a graphical interface that is simple to use for a SWAT model. QSWAT is used in this study for modelling the streamflow of the four catchments of Central Kashmir. The detailed procedure for streamflow simulation is shown in Fig. 3.11.

3.10.1.1 Data description and model setup

SWAT requires meteorological, hydrologic, and physical factors for hydrological projects. This study employed monthly and daily data from 1 January 1989 to 31 December 2019 over the simulation period (including warming up, calibration, and validation). 1989-90 was the warming-up phase, 1991-2000 was the calibration period, and 2001-2019 was the validation period. Figure 3.12 shows the geographical dispersion of this work's data. The SWAT project and its statistics are briefly described.

SWAT needs a contour and slope digital elevation model, climate, soil properties, and land cover. Add water infrastructure and land management methods. First, the watershed, sub-basins, and reaches are delineated. Physically-based SWAT extracts topography, contour, and slope from a digital elevation model. After adding DEM, the model utilizes contours and watershed slopes to

predict flow direction and accumulation. Once flow direction and accumulation are specified, the model constructs a stream network where each reach drains a sub-basin into the main reach. Each reach has an ending. The modeller selects a node corresponding to the outlet where discharge measurements are collected. This outflow establishes the basin's lowest limit, dependent on its location and the stream network.

Land use, soil type and slope data are needed to establish HRUs. HRUs were developed using unique combinations of land use, soil type, and slope after those classifications were specified. Depending on the land use, soil type, and slope at each grid, the HRUs divide the watershed into multiple homogenous units. Each subbasin has its hydrologic response unit. The HRUs for each sub-basin must be determined using land use and soil information. It has been imported into the model with consideration for the land use and soil map. Soil look-up tables are used to identify the kind of soil that should be simulated for each land use category, which is then linked to the SWAT database and reclassified.

According to infiltration rate and other features, the soil map reclassified the information into nine soil categories that are used as inputs to SWAT model inputs. Maps of land use, soil, and slope were layered on top of one other. The threshold percentage technique was utilized to eliminate minor land use, soil, and slope, with a 5% land use threshold and a 10% soil and slope threshold. The model created a report detailing the locations of the various HRUs in the various sub-basins where they were located.

The last step before running the simulation was to create the input tables, which included information on the weather. The weather data comprises precipitation, maximum and lowest temperature, humidity, solar radiation, wind speed, and other relevant information.

The features of surface runoff were determined by defining watershed parameters. Successfully rewritten and stored in the model geodatabase. The model was then run to simulate surface runoff after this step. The framework of the streamflow simulation using the SWAT model is described in figure 3.11.

3.10.1.2 SWAT model inputs

Additionally, SWAT needs daily/sub-daily time steps of meteorological data and the topography, soil, and LULC information. SWAT's primary input data are DEM, LULC, soil characteristics, and daily meteorological information (precipitation, maximum and minimum air temperature, relative humidity, wind speed, and solar radiation).

3.10.1.3 Digital Elevation Model (DEM)

All the topographic parameters of the catchment and sub-catchment up to the HRUs level are generated from the digital elevation model. Area, slope, slope length, channel length, channel slope, channel breadth, and channel depth are only some of the characteristics considered. ASTER (Advanced Spaceborne Thermal Emission and Reflection Radiometer) DEM with a 30-meter spatial resolution was acquired from the USGS website and utilized as an input dataset for demarcation and model implementation in this study.

3.10.1.4 Land use/land cover map

LULC details are essential in hydrologic models like SWAT to create HRUs. The LULC map for this investigation was created using LISS III 2017 imagery (Fig. 3.4(o,p)). It was modified and ground-truthed to match SWAT plant databases. Linking the land use map to the SWAT database requires a comma-delimited file (.csv) look-up table with 4-letter SWAT codes for LULC categories.

3.10.1.5 Soil type and characteristics

Catchment hydrology is also heavily influenced by soil characteristics. Based on the National Bureau of Soil Survey and Land-use Planning (NBSS&LUP), Nagpur, this study defined the distinct soil classes. A total of fourteen soil types were found in the research area. Then, based on Fey's criteria, the soil forms were categorized into nine soil types and mapped for the area (Fey, 2010). A map of the catchment's many principal soil types is shown in figure 3.4. (m,n). This was done by creating a comma-delimited (.csv) look-up table that specified the SWAT code for distinct soil map categories.

3.10.1.6 Weather database

Precipitation, temperature, relative humidity, solar energy, and wind speed are all required variables in the SWAT model. An additional weather generation function in the SWAT programme helps us fill in data gaps in simulated periods. With this tool, we can also generate long-term daily precipitation rates, maximum and lowest temperatures, relative humidity, solar energy, and wind speed. Indian Meteorological Department (IMD) Srinagar, J&K, and Agricultural Meteorological Field Unit (AMFU), SKUAST-Kashmir, J&K, provided the long-term data details.

The observed and simulated climate data were put in separate text files in the prescribed format for input in the SWAT model. Look-up tables were prepared for linking the weather database of the precipitation (mm), $T_{max,}$ and T_{min} (^{o}C) with the SWAT model.

3.10.1.7 Other data for model calibration and validation

One dataset of daily discharge data was collected for calibration and validation purposes for this study. The daily discharge data were available for the four Jhelum tributaries (Dudhgnaga Stream, Sunkhnag Stream, Harwan Steam,

and Sindh Stream) from 1991 to 2019 and were used for the study. As a result, daily discharge data for Central Kashmir were obtained from the Department of Irrigation and Flood Control, Srinagar, J&K (Jal Shakti Department).

3.10.2 Calibration validation and sensitivity analysis

A hydrologic model's effectiveness depends greatly on its calibration and sensitivity analysis (Abbaspour, 2015; Kouchi *et al.,* 2017). It is only with observed data that the calibration and validation procedures may be used effectively. Discharge data, in particular, is crucial in this process.

Model uncertainties might be from driving factors (e.g., climatic data), the conceptual model itself, observed data, or uncertainty during parametrization. Using Latin Hypercube Sampling, SWAT-probability CUP's distribution for propagating model uncertainty to parameters and outputs is 95%. 95% probability distributions are computed at the 2.5% and 97.5% levels of an output variable's cumulative distribution (95PPU). SWAT-CUP uses two indicators to assess uncertainty. These are the P-factor, the percentage of observed data enveloped by the model (the 95PPU), and the R-factor, the 95PPU envelope thickness. The methodology followed for the calibration and validation of the streamflow simulation using SWATCUP is described in figure 3.12.

SUFI2 offers several model performance indicator options. The method uses the Nash-Sutcliffe coefficient (NS) for this study's calibration and validation. R^2, percent bias, and the root mean squared error ratio to observed data standard deviation (RSR) were also evaluated. Performance indices were calculated using equations 3.11-3.14.

$$\mathrm{NSE} = 1 - \frac{\sum_i (Q_m - Q_s)_i^2}{\sum_i (Q_{m,i} - \bar{Q}_m)^2} \qquad \textbf{(3.11)}$$

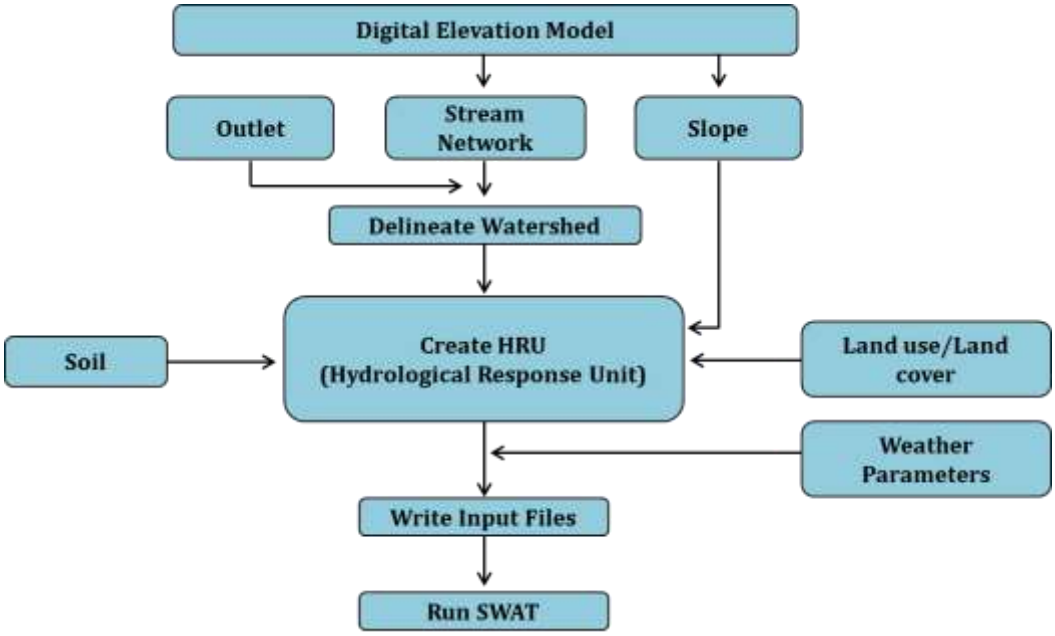

Fig. 3.11: Framework for streamflow simulation using the QSWAT model

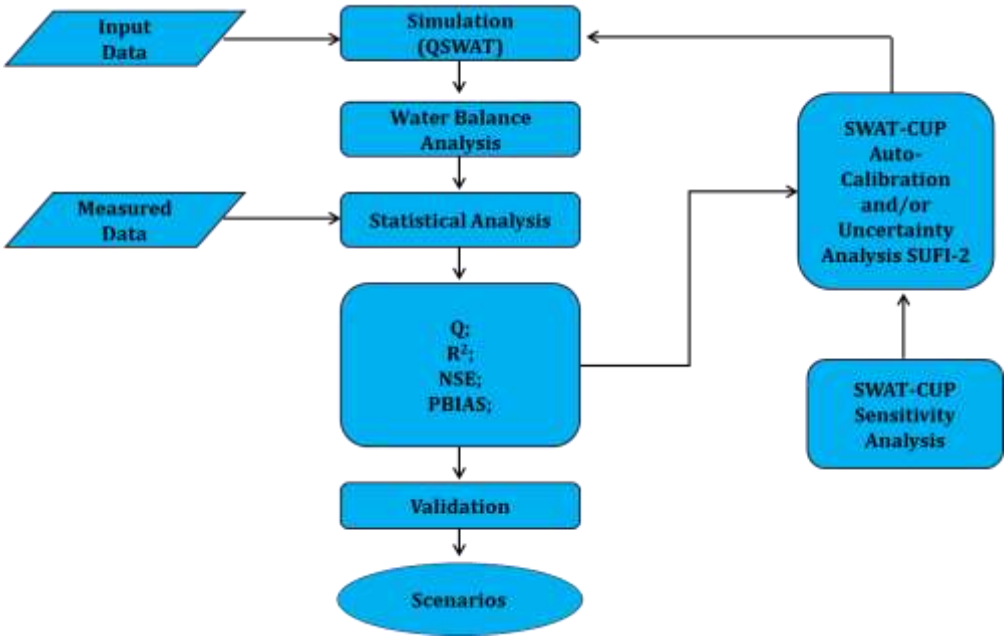

Fig. 3.12: Framework for SWAT model calibration and validation

$$R^2 = \frac{[\sum_i (Q_{m,i} - \bar{Q}_m)(Q_{s,i} - \bar{Q}_s)]^2}{\sum_i (Q_{m,i} - \bar{Q}_m)^2 \sum_i (Q_{s,i} - \bar{Q}_s)^2} \quad \textbf{(3.12)}$$

$$PBIAS = 100 \frac{?_{i=1}^{n} (Q_m - Q_s)_i}{?_{i=1}^{n} Q_{m,i}} \quad \textbf{(3.13)}$$

$$RSR = \frac{\sqrt{\sum_{i=1}^{n} (Q_m - Q_s)_i^2}}{\sqrt{\sum_{i=1}^{n} (Q_{m,i} - \bar{Q}_m)^2}} \quad \textbf{(3.14)}$$

Where NS represents the Nash-Sutcliffe coefficient, R^2 represents the coefficient of determination, PBIAS represents the percent bias, RSR represents the ratio of the root mean square error to the standard deviation of measured data, Q represents a variable (e.g., discharge), m and s represent measured and simulated variables, and i represents the i^{th} observed or modelled data.

Global Sensitivity Analysis is used to ascertain the degree of importance assigned to each calibration procedure's input parameters. Multiple regression analysis on the parameters obtained by the Latin hypercube and the objective function allows one to determine how sensitive the parameters are. The p-value and t-statistic were utilized as statistical indicators of significance. The t-statistic is the ratio between the parameter coefficient and the standard error. The regression coefficient is evaluated on this scale. Because of this, a parameter is considered sensitive when the coefficient is larger than the standard error. For a given parameter, a higher p-value indicates less sensitivity, as determined by the t-statistic, while a lower p-value indicates more sensitivity, as determined by the t-distribution student's table (Abbaspouri, 2015).

For a period of 10 years (1991–2000), the SWAT model is calibrated. A 19-year validation period (2001–2019) for all four Central Kashmir catchments follows the model calibration. During the validation phase, the model is simulated using the parameters that were optimized during calibration.

3.10.3 Overview of SWATMOD-Prep

SWATMOD-Prep is a graphical user interface for creating a fully linked SWAT-MODFLOW model from an existing SWAT (version 2012) model generated using the QSWAT interface. The programme is only available for Windows, and the difference grid for a MODFLOW model is linked with the HRUs and subbasins of the SWAT model through geoprocessing algorithms. The requirements for this model are SWAT model version 2012 and existing SWAT projects with zero thresholds HRUs.

3.10.3.1 SWAT-MODFLOW layout of interface used

SWATMOD-Prep consists of 3 tabs: The spatial Setup tab is where the SWAT model is loaded, the grid cell size is specified, and linking operations are carried out, the MODFLOW tab is where the data needed to build the MODFLOW model is loaded, and the Simulation tab is where the timing information, output options, and simulation run are configured (Plate 5).

Spatial Setup: The interface provides the basic linkage between the existing SWAT model and a new MODFLOW model. The following steps highlighted for this setup are:

1. Specify Path to TxtInOut Folder (Already simulated SWAT model)
2. Load SWAT DEM, Sub-basin, HRU, and River Shapefiles
3. Convert to Raster
4. Set up MODFLOW Grid
5. Disaggregate HRUs

6. Intersect MODFLOW Grid and DHRUs
7. Identify river cells
8. Write SWAT-MODFLOW linkage files

MODFLOW tab: The MODFLOW tab and the related loaded data will generate a single-layer MODFLOW model for the watershed study. Aquifer parameters, streambed conductivity, and beginning values of groundwater hydraulic heads are all required to build a MODFLOW model. Each grid cell in the MODFLOW input files requires a value for each parameter. Most parameters in the interface can be specified as a single value that is then duplicated to each grid cell or as spatially distributed values. All spatial input to the SWATMODFLOW interface must be in the GeoTIFF format (*.tif). To convert the spatial information from shapefiles or other raster formats to the GeoTIFF format, any GIS software can be used. The following steps highlighted for this setup are given below

1. Load DEM
2. Aquifer Thickness
3. Hydraulic Conductivity
4. The ratio of horizontal K to vertical K
5. Specific Storage
6. Specific yield
7. Hydraulic conductivity of river bed material
8. Initial hydraulic head
9. Write MODFLOW input files

Simulation tab: Once all information needed has been provided, the 'Run Simulation' button becomes active, and the user can start the SWAT-MODFLOW simulation. The following steps highlighted below are to be performed for the simulation of SWAT-MODFLOW.

1. Period of Simulation
2. SWAT Printout Settings
3. Frequency of MODFLOW Runs

4. SWAT-MODFLOW Output
5. Run Simulation

3.10.3.2 Output files to analyze model results

The SWAT-MODFLOW simulation output will generate several primary output files and some extra files. These are in addition to the standard SWAT output files that are used to show water budgets, discharge, head, and other data.

3.10.4 Groundwater Modeling System (MODFLOW model) description and simulation

Groundwater Modeling Simulation 10.3 Software was used to create a steady-state groundwater flow model. Identifying the governing equation, selecting a grid design, and estimating model parameters were some of the major steps in developing the model.

3.10.4.1 MODFLOW Simulation

It is possible for the aquifer layers to be confined, unconfined, or a combination of both in a MODFLOW-2000-simulated irregularly-shaped flow system. External stressors, such as flow to wells, areal recharge, evapotranspiration, and flow-through streambeds, may be used to simulate flow in the system. An anisotropic (grid-aligned) anisotropy in any layer's hydraulic conductivities or transmissivities is conceivable, and heterogeneous storage coefficients. Simulated head and flux boundaries enable water to flow through the model outer boundary at the rate of a head difference between a "source" of water located outside the modelled region and a boundary block situated inside it. The framework of the groundwater modeling simulation using GMS software is given in figure 3.13.

Using equation 3.15, MODFLOW combines Darcy's Law with the concept of mass conservation to obtain the governing three-dimensional flow equation (McDonald and Harbaugh, 1988; Harbaugh *et al.*, 2000).

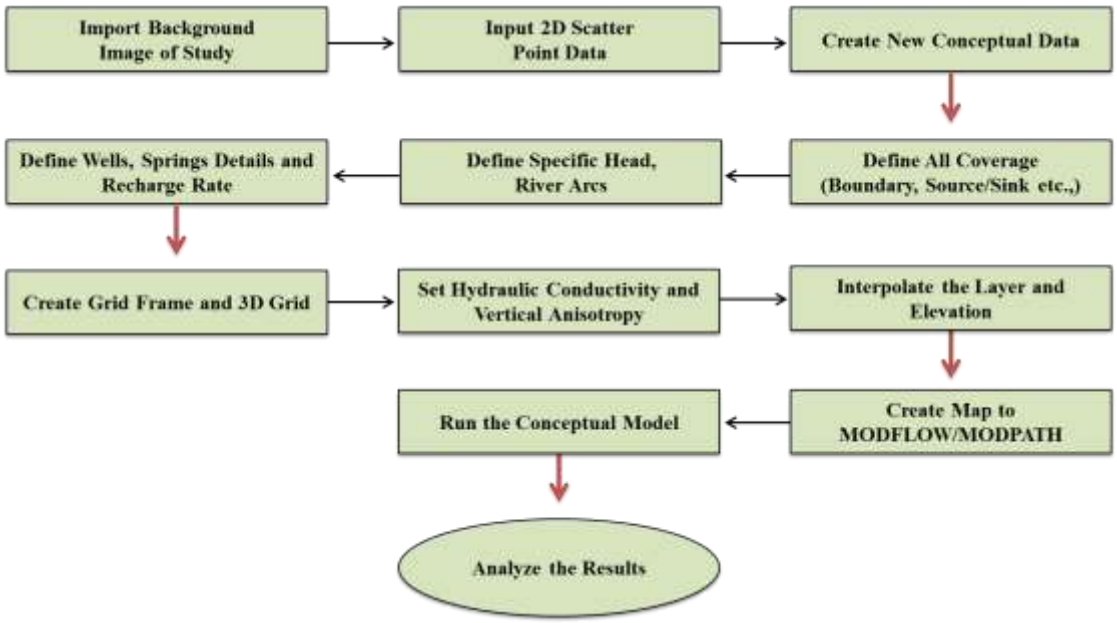

Fig. 3.13: Framework of the groundwater modeling simulation using GMS software

$$\frac{\partial}{\partial x}\left(K_{xx}\frac{\partial h}{\partial x}\right)+\frac{\partial}{\partial y}\left(K_{yy}\frac{\partial h}{\partial y}\right)+\frac{\partial}{\partial z}\left(K_{zz}\frac{\partial h}{\partial z}\right)+W=S_s\frac{\partial h}{\partial t} \qquad \textbf{(3.15)}$$

Where, K_{xx}, $K_{yy,}$ and K_{zz} = hydraulic conductivity along the x, y, and z coordinate axes, m/day; h = hydraulic head, m; W = volumetric flux per unit volume and represents sources and/or sinks of water, m^3/day; S_s = specific storage of the porous material m^{-1}; and t = time, day.

An averaged version of equation 3.15 is solved using MODFLOW. The finite-difference approximation is used to solve the groundwater flow problem. Medium properties are considered to be homogeneous in all blocks of the flow region. To build the blocks, you need to create a grid of lines that are all perpendicular to each other. The thickness of the model layers may be varied. Each block or cell has its own flow equation. The resulting matrix problem may be solved using one of several solvers; the user can choose the most appropriate solver depending on the situation. Inflow and outflow rates, as well as cumulative volume balances, are calculated at each time step.

3.10.4.2 Discretization of the model

The conceptual module of the Groundwater modelling system software was used to discretize the study region into 91 rows and 123 columns. The layer has a total of 11193 cells, with a surface area of 542*542 m^2.

An unconfined aquifer was modelled in the hydrogeological setting of the study region (14-15 m thickness). The hydrogeologic framework was used to determine the thickness of the layer at various locations. The aquifer and gauge data were used to import the surface elevation, the bottom elevation of the top layer, and the bottom elevation of the aquifer layer into the GMS (MODFLOW model). The model period's average spring discharge and well observation data were also included.

3.10.4.3 Estimation of model parameters

GMS software needs aquifer characteristics, sources, sinks, groundwater recharge, etc. Hydraulic conductivity (K), specific storage (Ss), evapotranspiration (ET), and groundwater recharge as model inputs.

3.10.4.3.1 Aquifer parameters

The top layer and unconfined aquifer hydraulic conductivity (K) values were obtained from existing data and field experiments utilizing a groundwater resistivity meter and glueph permeameter. Table 3.7 lists the hydraulic conductivity of several lithological layers.

Table 3.7: Material type and hydraulic conductivity (K) values used for different lithological units

S No.	Material Type	K (m/day)
1	Clay	0.05
2	Clay silty	0.1
3	Clay silty with sand	1
4	Clay with interbed of sand	5
5	Clay with Gravel	10
6	Sand	100
7	Sand Fine	30
8	Sand Medium	50
9	Sand	100
10	Sand With Silt	30
11	Sand coarse with gravel	150

12	Mixed sand and silt	100
13	Silt	1
14	Gravel	200

(Khan *et al.*, 2003)

3.10.4.3.2 Evapotranspiration package

The MODFLOW Evapotranspiration Package simulates transpiration, direct evaporation, and seepage at the ground surface. Evaporation rate and extinction depth are needed.

Evapotranspiration package:

- ET only at the top layer
- Max ET rate = 0.0025 m/day (reference ET)

3.10.4.3.3 Stream package

In order to model the impact of a surface water body on groundwater flow, the steam boundary condition is used. Hydraulic gradients between surface water bodies and the groundwater system determine whether or not they contribute water to the groundwater system or serve as groundwater discharge zones. MODFLOW Stream Package uses a seepage layer to separate the surface water from the groundwater system to model the interaction between the two. For each grid cell with a stream boundary, the Stream Package input file needs data on stream stage elevation, streambed bottom elevation, and conductance. For a given length of reach (L), width (W), thickness (M), and vertical hydraulic conductivity (K) of the streambed material, one may derive conductance C. The formula for this calculation is as follows (WHI, 2005):

$$C = \frac{K \times L \times W}{M} \qquad \textbf{3.16)}$$

Where,

C = Conductance (m^2/day)

K = defined in the hydraulic conductivity section,

L = 542 m,

W = 20-30 m and

M = 1-2 m

- Nallah/stream bed elevation = 3 m
- Nallah/stream stage = 1.5 m

3.10.4.3.4 Well package

The injection and pumping wells in the well package are intended to simulate the aquifer's inflow and outflow. Pumping rates are negative for extraction (pumping) wells and positive for injection (recharge) wells. Wells in the MODFLOW pumping system is simulated using the well package. The study region includes 208 geotagged and operational wells. The groundwater flow model used Central Groundwater Board well output data as sinks.

- The yield of the wells ranges from 0.57 to 95 m^3/day
- Average discharge = 13 m^3/day

3.10.4.3.5 Recharge package

MODFLOW's Recharge Package is often used to simulate groundwater recharge from the surface. Precipitation percolating into the groundwater system is the most common method of recharge. Other recharge sources, such as artificial recharge or canal seepages, may also occur. For each grid cell in the horizontal plane, a two-dimensional array of recharge values is required, and a two-dimensional array of the layer numbers where the recharge will be applied. The Chaturvedi equation approach is used to calculate recharge from precipitation (Chaturvedi, 1973).

$$R = 2.0*(P - 15)^{0.4} \quad \textbf{(3.16)}$$

Where,

- R = net recharge due to precipitation during the year (inch);
- P = annual precipitation (inch).

MODFLOW recharge package simulates the areal groundwater recharge. The model used equation 3.16 recharge estimate. Recharge was estimated empirically due to a lack of field data. Table 3.8 shows recharge values for various time slices. Predicted precipitation was utilized for RCP 4.5 and 8.5 rechargings.

Table 3.8: Predicted average annual precipitation and computed recharge for the different scenarios for Central Kashmir

Time period	**Baseline (1985-2019)**	**Future Scenario (2021-2095)**	
		RCP 4.5	**RCP 8.5**
Precipitation (mm)	779.29	914.51	1009.19
Recharge (m/day)	0.000418	0.000464	0.000496

3.10.5 Data output

The model output structure is intended to govern printed information regarding the amount, type, and frequency. This investigation evaluated the hydraulic head and budget terms as the default outputs.

3.11 Measuring the impact of changing environment and suggesting the best measures for springshed management.

Future changes will alter regional hydrologic cycles, affecting the quantity and quality of regional water resources (Gleick, 1989). As a result, the effect of changing environmental conditions has been assessed for Central Kashmir under RCP 4.5 and 8.5 scenarios by modelling regionally varying water balance components by linking the outputs of RCMs, surface, and groundwater models. The geographical distribution of groundwater drafts and pumping rates were mapped into the GIS environment and used to input the surface and groundwater model (hydrological models). The model was used to produce the hydraulic heads and flow budget for the present and future climate scenarios. These data from multiple models over different periods were finally utilized to assess environmental change's influence on springshed hydrology.

Chapter-4

EXPERIMENTAL FINDINGS

This chapter deals with the research findings of various methods adopted for analysis mentioned in chapter 3 to assess hydrogeological characteristics and springshed modelling to determine the environmental change impact assessment in Central Kashmir. Analyzing the results obtained in the field investigation and modelling is essential to derive a conclusive strategy for managing the water resources, especially springs and groundwater bodies in the study area.

The results of the study are presented in the chronological order to comprehend the broader aspect of the research activities with the following major headings:

4.1 Bias computation and correction of modelled climate data

4.2 Future Climate Scenarios under RCP 4.5 and 8.5 scenarios for AMFU Shalimar

4.3 Future Climate Scenarios under RCP 4.5 and 8.5 scenarios for IMD Srinagar station

4.4 Land use and land cover (LU/LC) change detection in the Central Kashmir

4.5 Delineation of groundwater recharge potential zones of the Central Kashmir

4.6 Identification of rainwater harvesting suitability level of Central Kashmir

4.7 Vertical Electrical Sounding (VES) analysis of the subsurface layers of the Central Kashmir

4.8 Parameter sensitivity analysis, calibration, and validation of the model

4.9 Streamflow of various catchments of Central Kashmir under different RCP scenarios

4.10 Groundwater head and water-table depth of the various catchments of Central Kashmir under different RCP scenarios

4.11 Simulation of groundwater model and groundwater behavior for Central Kashmir

4.12 Spring discharge behavior during the reporting period

4.13 Effect of changing environmental conditions on springshed hydrology

4.1 Bias computation and correction of modelled climate data

4.1.1 Maximum and minimum temperature data correction

Monthly averages of the observed and Hadley Center Global Environment Model 2 - Earth System (GCM-HAD GEM2 ES) calculated maximum temperature (T_{max}) and minimum temperature (T_{min}) for the site during a 10-year period (2010-2019) revealed that the modelled temperature approximated the observed seasonal cycle. However, the predicted T_{max} values were greater than those observed in May, June, August, September, October, and December, and lower in January for both Central Kashmir stations. Modelled T_{min} followed a similar pattern to T_{max}, although the modelled values were greater for May, June, July, August, September, October, and December and lower for November (Fig. 4.1(a,b)) for the IMD Srinagar and AMFU Shalimar stations. The statistical parameters of the annual mean (μ) and standard deviation (σ) of T_{max} for AMFU Shalimar under the RCP 4.5 scenario showed that the μ and σ of modelled T_{max} were 3 and 20% more than that of the observed, respectively, while the μ and σ of modelled T_{min} were 33 and 31% more than that of the observed T_{min} data. Under RCP 8.5 Scenario the μ and σ for modelled T_{max} were 4 and 22% more as compared to observed T_{max}. While in the case of modelled $T_{min,}$ μ and σ were more by 38 and 33% than observed $T_{min,}$ respectively (Table 4.5(a,b)). Comparing modeled variable of the RCP 4.5 scenario with the IMD Srinagar station observed variables, the μ of the modelled T_{max} was 3% more than that of the observed while as σ of modelled T_{max} was 20% more than that of observed T_{max} data. In $T_{min,}$ both μ and σ of modelled were 33% more than observed (Table 4.10(a,b)).

Fig. 4.1(a): Biases in average modelled data of T_{max}

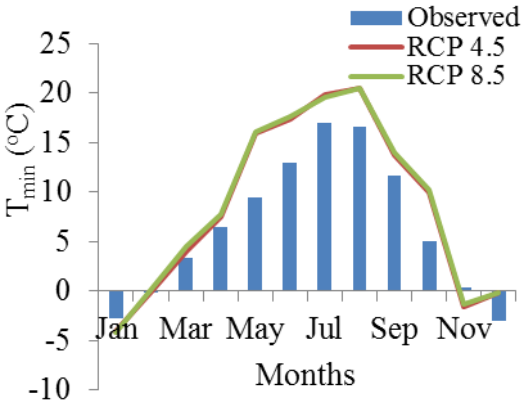

Fig. 4.1(b): Biases in average modelled data of T_{min}

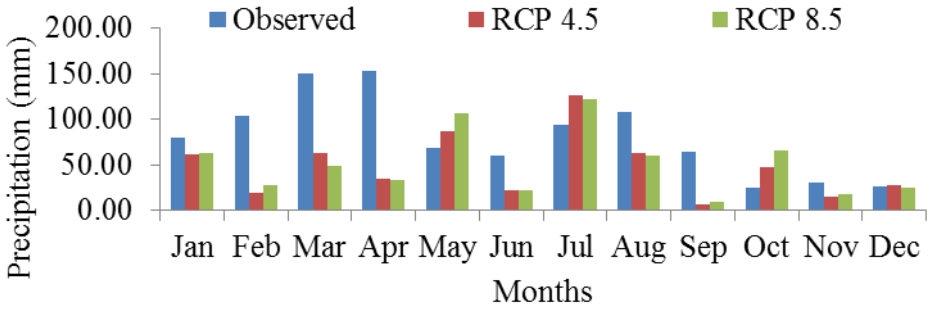

Fig. 4.1(c): Biases in average modelled data of Precipitation

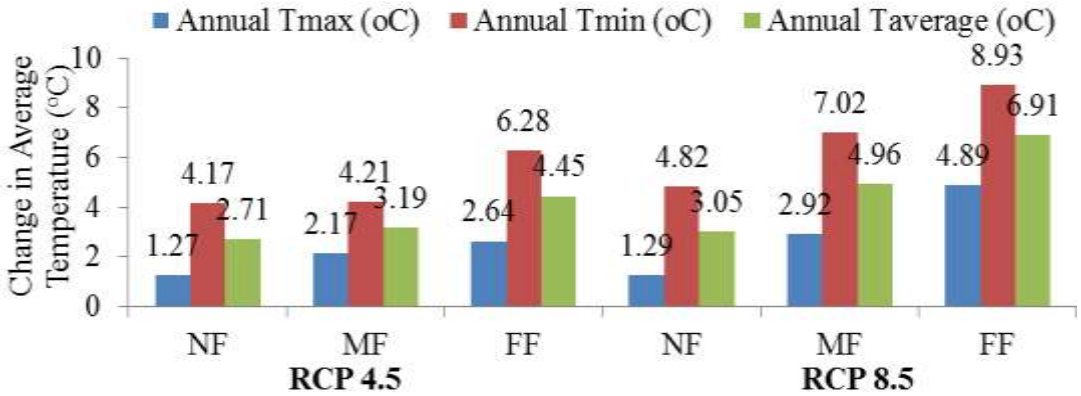

Fig. 4.2: Change in average temperature from baseline in different time slices for AMFU Shalimar

4.1.2 Precipitation data correction

In precipitation, the modelled precipitation was less during January, February, March, April, June, August, September, and November for both the stations considered for the study. The model predicted higher precipitation than observed in the remaining months of the year (Fig. 4.1(c)). The analysis of the statistical parameters under RCP 4.5 scenario revealed that in the case of precipitation, μ of the modelled precipitation (RCP 4.5) was 32% less than that of the observed, and σ for the same was 30% less for the Shalimar station. Under the RCP 8.5 scenario, μ and σ were 30 and 29% less than observed precipitation (Table 4.5(a,b)). The μ and σ of the modeled RCP 4.5 precipitation for the IMD Srinagar station were 22 and 31% less than the observed precipitation. In the RCP 8.5 scenario case, the μ and σ of modelled precipitation were less than observed by 21 and 30%.

4.1.3 Correction functions derived using modified difference approach method

Correction functions for T_{max} and T_{min} under RCP 4.5 and 8.5 for both the stations considered using a modified difference approach were developed using equations 3.1 & 3.2 for each calendar month (Table 4.1, 4.2, 4.6 & 4.7). For both T_{max} and T_{min} these correction functions were used to the modelled data to get it closer to the observed data. The calculated statistical parameters of T_{max} and T_{min} for both stations showed that discrepancies in monthly mean values were comparable in corrected modelled and observed T_{max} and T_{min}. Still, differences in standard deviation and variation values were higher in corrected and observed T_{max} and T_{min} than in modelled and observed data after correction (Table 4.5 & 4.10). Correction functions for precipitation based on the modified difference approach are presented in Tables 4.1, 4.2, 4.6 & 4.7 for both stations of Central Kashmir considered for the study. Statistical parameters demonstrated that model-corrected precipitation differed from observed precipitation, making it unreliable. Model corrected and observed precipitation had higher mean (μ), standard

deviation, and variance than modelled and observed (Table 4.5 & 4.10).

4.1.4 Correction functions derived using the linear scaling method

Under RCP 4.5 and 8.5, correction functions for T_{max} and T_{min} using the linear scaling method for AMFU and IMD station were developed based on equations 3.3 and 3.4 for each calendar month (Table 4.3, 4.4, 4.8 & 4.9). Temperature correction functions were used for both T_{max} and T_{min} to match the observed and model-corrected temperatures. Table 4.5 for AMFU Shalimar and Table 4.10 for IMD Srinagar show the calculated statistical parameters of T_{max} and T_{min}. At a monthly time scale, the discrepancies in mean values were comparable in model corrected and observed T_{max} and T_{min} for both the stations. The corrected and observed T_{max} and T_{min} data had fewer mean, standard deviation, and variance discrepancies than the modelled and observed data. Model corrected cumulative precipitation data and observed precipitation differed less when linear scaling correction functions for precipitation were applied. Model corrected and observed precipitation had smaller variation in mean (μ), standard deviation (σ) and variance (σ^2) than modelled and observed precipitation (Table 4.5 & 4.10).

4.1.5 Best estimate

T_{max}, T_{min}, and precipitation were all corrected using different methods at monthly time scales, and tables 4.5 and 4.10 show that the root mean squared error (RMSE) for both T_{max} and T_{min} was the lowest in both RCPs and for both stations under consideration when using a monthly correction function of linear scaling.

On a monthly time scale, the RMSE for the modelled T_{max} was 5.11%, which was increased to 6.49 % by the modified difference approach but decreased to 5.34% by the linear scaling method for the IMD Srinagar station. For AMFU Shalimar station, the RMSE for the modelled T_{max} was 5.86%, which was increased to 6.41% by the modified difference approach but decreased to 5.31% by the linear scaling method for IMD Srinagar station.

RMSE for modelled T_{min} was 5.37 %, which was modified to 6.17 % using the modified difference approach on a monthly time scale, and 4.59 % using the linear scaling method for the IMD Srinagar station. For the AMFU Shalimar station, the RMSE was increased to 6.08% by the modified difference approach but decreased to 4.57% by the linear scaling method (Tables 4.5 and 4.10).

The modelled cumulative precipitation for the IMD station had a RMSE of 9.13 %. It was enhanced to 10.93 % using the modified difference approach but was dropped to 9.64% using the linear scaling method (Table 4.10). RMSE for AMFU Shalimar was modified to 10.73 and 9.53 from 9.54 after applying the modified difference approach and the linear scaling method, respectively (Table 4.5).

Analyzing the results, the linear scaling method accomplished better than the modified difference approach. Further analysis was done using the model corrected data using the linear scaling method, and corrected scenarios were divided into three-time slices to predict the climate change extent while comparing with the baseline.

The three-time slices are the near future (NF) climate change projection (2021–2045), mid future (MF) projection (2046–2070), and far future (FF) projection (2071–2095).

Table 4.1: Correction functions using modified difference approach for modelled monthly average temperature and precipitation for AFMU SKUAST-Kashmir under RCP 4.5

Month	T_{max} (^{o}C)	T_{min} (^{o}C)	Precipitation (mm)
January	T_{cor}=8.34+0.821*(T_{mod}-14.45)	T_{cor}=-2.71+0.757*(T_{mod}+1.39)	P_{cor}=(P_{mod}-0.88)*(1.425)
February	T_{cor}=10.23+0.829*(T_{mod}-11.08)	T_{cor}=-0.066+0.759*(T_{mod}+0.142)	P_{cor}=(P_{mod}+0.26)*(1.456)
March	T_{cor}=16.01+0.826*(T_{mod}-18.17)	T_{cor}=3.34+0.760*(T_{mod}-2.7)	P_{cor}=(P_{mod}+2.59)*(1.448)
April	T_{cor}=19.39+0.828*(T_{mod}-18.9)	T_{cor}=6.45+0.761*(T_{mod}-5.41)	P_{cor}=(P_{mod}+1.26)*(1.467)
May	T_{cor}=24.43+0.827*(T_{mod}-20.44)	Tcor=9.43+0.759*(T_{mod}-2.85)	P_{cor}=(P_{mod}-2.13)*(1.429)
June	T_{cor}=28.11+0.829*(T_{mod}-25.4)	T_{cor}=13.02+0.761*(T_{mod}-8.63)	P_{cor}=(P_{mod}+0.60)*(1.424)
July	T_{cor}=29.98+0.832*(T_{mod}-29.43)	T_{cor}=16.97+0.766*(T_{mod}-14.11)	P_{cor}=(P_{mod}-1.43)*(1.422)
August	T_{cor}=29.43+0.832*(T_{mod}-26.43)	T_{cor}=16.55+0.765*(T_{mod}-12.64)	P_{cor}=(P_{mod}+1.58)*(1.436)
September	T_{cor}=27.27+0.834*(T_{mod}-25.89)	T_{cor}=11.67+0.763*(T_{mod}-9.65)	P_{cor}=(P_{mod}+1.71)*(1.432)
October	T_{cor}=22.87+0.833*(T_{mod}-19.79)	T_{cor}=5.06+0.762*(T_{mod}-0.16)	P_{cor}=(P_{mod}-0.52)*(1.427)
November	T_{cor}=15.17+0.833*(T_{mod}-15.18)	T_{cor}=0.4+0.759*(T_{mod}-2.44)	P_{cor}=(P_{mod}+0.64)*(1.446)
December	T_{cor}=9.89+0.839*(T_{mod}-7.58)	T_{cor}=-3.04+0.767*(T_{mod}+5.87)	P_{cor}=(P_{mod}+0.43)*(1.446)

Table 4.2: Correction functions using modified difference approach for modelled monthly average temperature and precipitation for AFMU SKUAST-Kashmir under RCP 8.5

Month	T_{max} (^oC)	T_{min} (^oC)	Precipitation (mm)
January	$T_{cor}=8.34+0.833*(T_{mod}-14.08)$	$T_{cor}=-2.71+0.760*(T_{mod}+1.19)$	$P_{cor}=(P_{mod}+0.01)*(1.591)$
February	$T_{cor}=10.23+0.841*(T_{mod}-10.45)$	$T_{cor}=-0.066+0.763*(T_{mod}+0.342)$	$P_{cor}=(P_{mod}+0.48)*(1.612)$
March	$T_{cor}=16.01+0.838*(T_{mod}-17.84)$	$T_{cor}=3.34+0.764*(T_{mod}-2.21)$	$P_{cor}=(P_{mod}+2.65)*(1.591)$
April	$T_{cor}=19.39+0.840*(T_{mod}-18.71)$	$T_{cor}=6.45+0.764*(T_{mod}-5.17)$	$P_{cor}=(P_{mod}+1.12)*(1.612)$
May	$T_{cor}=24.43+0.839*(T_{mod}-20.55)$	$T_{cor}=9.43+0.763*(T_{mod}-2.74)$	$P_{cor}=(P_{mod}-2.13)*(1.594)$
June	$T_{cor}=28.11+0.842*(T_{mod}-25.68)$	$T_{cor}=13.02+0.764*(T_{mod}-8.42)$	$P_{cor}=(P_{mod}+0.25)*(1.593)$
July	$T_{cor}=29.98+0.844*(T_{mod}-29.40)$	$T_{cor}=16.97+0.770*(T_{mod}-14.41)$	$P_{cor}=(P_{mod}-0.73)*(1.594)$
August	$T_{cor}=29.43+0.844*(T_{mod}-26.40)$	$T_{cor}=16.55+0.769*(T_{mod}-12.67)$	$P_{cor}=(P_{mod}+1.46)*(1.604)$
September	$T_{cor}=27.27+0.846*(T_{mod}-25.59)$	$T_{cor}=11.67+0.766*(T_{mod}-9.37)$	$P_{cor}=(P_{mod}+1.65)*(1.599)$
October	$T_{cor}=22.87+0.844*(T_{mod}-19.10)$	$T_{cor}=5.06+0.765*(T_{mod}+0.11)$	$P_{cor}=(P_{mod}-0.08)*(1.599)$
November	$T_{cor}=15.17+0.845*(T_{mod}-14.95)$	$T_{cor}=0.4+0.763*(T_{mod}-2.14)$	$P_{cor}=(P_{mod}+0.65)*(1.621)$
December	$T_{cor}=9.89+0.851*(T_{mod}-7.17)$	$T_{cor}=-3.04+0.771*(T_{mod}+5.87)$	$P_{cor}=(P_{mod}+0.49)*(1.621)$

Table 4.3: Corrections using linear scaling for modelled monthly average temperature and precipitation for AFMU SKUAST-Kashmir under RCP 4.5

Month	T_{max} (^oC)	T_{min} (^oC)	Precipitation (mm)
January	6.11	1.32	0.75
February	0.85	-0.076	17.57
March	2.16	-0.64	2.15
April	-0.49	-1.04	10.48
May	-3.99	-6.58	0.51
June	-2.71	-4.39	1.43
July	-0.55	-2.86	0.68
August	-3.00	-3.91	1.83
September	-1.38	-2.02	4.82
October	-3.08	-4.90	0.61
November	0.01	2.04	2.84
December	-2.31	-2.83	2.06

Table 4.4: Corrections using linear scaling for modelled monthly average temperature and precipitation for AFMU SKUAST-Kashmir under RCP 8.5

Month	T_{max} (^oC)	T_{min} (^oC)	Precipitation (mm)
January	5.74	1.52	1.00
February	0.22	-0.276	62.68
March	1.83	-1.13	2.21
April	-0.68	-1.28	8.21
May	-3.88	-6.69	0.51
June	-2.43	-4.6	1.14
July	-0.58	-2.56	0.81
August	-3.03	-3.88	1.72
September	-1.68	-2.3	4.19
October	-3.77	-5.17	0.91

November	-0.22	1.74	2.89
December	-2.72	-2.83	2.36

Table 4.5(a): Statistical parameters of the average annual AFMU SKUAST observed, modelled and model corrected T_{max}, T_{min}, and precipitation by modified difference and linear scaling method under RCP 4.5 Scenario.

Parameter	**Observed**	**Modelled**	**Modified difference approach**	**Linear scaling method**
T_{max} (^{o}C)				
Mean	20.09	20.79	21.34	20.11
Standard deviation	8.73	10.51	11.59	8.83
Variance	76.15	110.45	134.37	77.99
RMSE	-	5.86	6.41	5.31
NRMSE	-	0.30	0.33	0.27
T_{min} (^{o}C)				
Mean	6.42	8.58	9.80	6.47
Standard deviation	7.29	9.58	10.09	8.13
Variance	53.21	91.75	101.87	66.06
RMSE	-	5.67	6.08	4.57
NRMSE	-	0.44	0.47	0.35
Precipitation (mm)				
Mean	2.63	1.78	3.03	2.01
Standard deviation	8.39	5.83	8.25	7.24
Variance	70.39	34.03	68.13	52.37
RMSE	-	9.54	10.75	9.53
NRMSE	-	0.15	0.17	0.15

Table 4.5(b): Statistical parameters of the average annual AFMU SKUAST observed, modelled and model corrected T_{max}, T_{min}, and precipitation by modified difference and linear scaling method under RCP 8.5 Scenario.

Parameter	Observed	Modelled	Modified difference approach	Linear scaling method
T_{max} (^{o}C)				
Mean	20.09	20.96	21.39	20.13
Standard deviation	8.73	10.62	11.63	8.85
Variance	76.15	112.78	135.26	78.32
RMSE	-	5.96	6.46	5.34
NRMSE	-	0.32	0.35	0.28
T_{min} (^{o}C)				
Mean	6.42	8.90	9.84	6.49
Standard deviation	7.29	9.65	10.14	8.15
Variance	53.21	93.12	102.81	66.42
RMSE	-	5.71	6.11	4.59
NRMSE	-	0.45	0.49	0.36
Precipitation (mm)				
Mean	2.63	1.83	3.06	2.03
Standard deviation	8.39	5.94	8.31	7.28
Variance	70.39	35.29	69.06	52.99
RMSE	-	9.61	10.81	9.57
NRMSE	-	0.16	0.19	0.16

Table 4.6: Correction functions derived using modified difference approach for modelled monthly average temperature and precipitation for IMD Srinagar Station under RCP 4.5

Month	T_{max} (^{o}C)	T_{min} (^{o}C)	Precipitation (mm)
Jan	T_{cor}=8.18+0.797*(T_{mod}-13.59)	T_{cor}=-2.35+0.827*(T_{mod}+1.56)	P_{cor}=(P_{mod}-0.10)*(0.94)
Feb	T_{cor}=10.91+0.803*(T_{mod}-12.24)	T_{cor}=0.8+0.827*(T_{mod}-1.58)	P_{cor}=(P_{mod}+1.74)*(2.30)
Mar	T_{cor}=16.16+0.801*(T_{mod}-17.63)	T_{cor}=4.83+0.829*(T_{mod}-5.26)	P_{cor}=(P_{mod}+2.33)*(2.51)
Apr	T_{cor}=20.11+0.803*(T_{mod}-20.39)	T_{cor}=8.56+0.828*(T_{mod}-9.42)	P_{cor}=(P_{mod}+2.85)*(3.41)
May	T_{cor}=24.81+0.802*(T_{mod}-21.01)	T_{cor}=11.52+0.826*(T_{mod}-6.69)	P_{cor}=(P_{mod}-1.31)*(0.61)
Jun	T_{cor}=28.25+0.804*(T_{mod}-25.68)	T_{cor}=15.27+0.827*(T_{mod}-12.97)	P_{cor}=(P_{mod}+0.78)*(2.06)
Jul	T_{cor}=29.9+0.806*(T_{mod}-29.07)	T_{cor}=18.65+0.831*(T_{mod}-17.59)	P_{cor}=(P_{mod}-2.23)*(0.48)
Aug	T_{cor}=29.61+0.805*(T_{mod}-25.59)	T_{cor}=18.16+0.830*(T_{mod}-15.37)	P_{cor}=(P_{mod}-0.07)*(0.97)
Sep	T_{cor}=27.26+0.808*(T_{mod}-25.31)	T_{cor}=13.38+0.829*(T_{mod}-12.57)	P_{cor}=(P_{mod}+1.55)*(7.07)
Oct	T_{cor}=23.24+0.807*(T_{mod}-20.40)	T_{cor}=7.16+0.828*(T_{mod}-3.44)	P_{cor}=(P_{mod}-0.79)*(0.48)
Nov	T_{cor}=15.84+0.807*(T_{mod}-16.49)	T_{cor}=1.74+0.825*(T_{mod}-3.96)	P_{cor}=(P_{mod}+0.26)*(1.47)
Dec	T_{cor}=10.51+0.813*(T_{mod}-8.96)	T_{cor}=-2.2+0.834*(T_{mod}+4.53)	P_{cor}=(P_{mod}-0.17)*(0.79)

Table 4.7: Correction functions derived using modified difference approach for modelled monthly average temperature and precipitation for IMD Srinagar Station under RCP 8.5

Month	T_{max} (^oC)	T_{min} (^oC)	Precipitation (mm)
Jan	$T_{cor}=8.18+0.805*(T_{mod}-13.96)$	$T_{cor}=-2.35+0.831*(T_{mod}+1.04)$	$P_{cor}=(P_{mod}-0.18)*(0.90)$
Feb	$T_{cor}=10.91+0.812*(T_{mod}-11.92)$	$T_{cor}=0.8+0.833*(T_{mod}-0.99)$	$P_{cor}=(P_{mod}+2.06)*(3.04)$
Mar	$T_{cor}=16.16+0.809*(T_{mod}17.57)$	$T_{cor}=4.83+0.835*(T_{mod}-4.83)$	$P_{cor}=(P_{mod}+1.33)*(1.52)$
Apr	$T_{cor}=20.11+0.811*(T_{mod}-19.81)$	$T_{cor}=8.56+0.833*(T_{mod}-9.18)$	$P_{cor}=(P_{mod}+3.80)*(17.13)$
May	$T_{cor}=24.81+0.810*(T_{mod}-20.86)$	$T_{cor}=11.52+0.831*(T_{mod}-6.52)$	$P_{cor}=(P_{mod}-1.59)*(0.56)$
Jun	$T_{cor}=28.25+0.813*(T_{mod}-25.82)$	$T_{cor}=15.27+0.833*(T_{mod}-12.93)$	$P_{cor}=(P_{mod}+0.69)*(1.85)$
Jul	$T_{cor}=29.9+0.815*(T_{mod}-29.05)$	$T_{cor}=18.65+0.836*(T_{mod}-17.66)$	$P_{cor}=(P_{mod}-2.08)*(0.49)$
Aug	$T_{cor}=29.61+0.815*(T_{mod}-25.99)$	$T_{cor}=18.16+0.835*(T_{mod}-15.44)$	$P_{cor}=(P_{mod}+0.00)*(1)$
Sep	$T_{cor}=27.26+0.817*(T_{mod}-25.78)$	$T_{cor}=13.38+0.835*(T_{mod}-12.73)$	$P_{cor}=(P_{mod}+1.56)*(7.30)$
Oct	$T_{cor}=23.24+0.816*(T_{mod}-20.82)$	$T_{cor}=7.16+0.833*(T_{mod}-3.56)$	$P_{cor}=(P_{mod}-1.50)*(0.32)$
Nov	$T_{cor}=15.84+0.816*(T_{mod}-16.82)$	$T_{cor}=1.74+0.830*(T_{mod}-4.15)$	$P_{cor}=(P_{mod}+0.20)*(1.33)$
Dec	$T_{cor}=10.51+0.822*(T_{mod}-8.78)$	$T_{cor}=-2.2+0.839*(T_{mod}+4.57)$	$P_{cor}=(P_{mod}-0.01)*(0.98)$

Table 4.8: Corrections derived using linear scaling for modelled monthly average temperature and precipitation for IMD Srinagar Station under RCP 4.5

Month	T_{max} (^oC)	T_{min} (^oC)	Precipitation (mm)
Jan	5.41	0.79	0.94
Feb	1.33	0.78	2.30
Mar	1.47	0.43	2.51
Apr	0.28	0.86	3.41
May	-3.8	-4.83	0.61
Jun	-2.57	-2.3	2.06
Jul	-0.83	-1.06	0.48
Aug	-4.02	-2.79	0.97
Sep	-1.95	-0.81	7.07
Oct	-2.84	-3.72	0.48
Nov	0.65	2.22	1.47
Dec	-1.55	-2.33	0.79

Table 4.9: Corrections derived using linear scaling for modelled monthly average temperature and precipitation for IMD Srinagar Station under RCP 8.5

Month	T_{max} (^oC)	T_{min} (^oC)	Precipitation (mm)
Jan	5.78	1.31	0.90
Feb	1.01	0.19	3.04
Mar	1.41	0	1.52
Apr	-0.3	0.62	17.13
May	-3.95	-5	0.56
Jun	-2.43	-2.34	1.85
Jul	-0.85	-0.99	0.49
Aug	-3.62	-2.72	1.00
Sep	-1.48	-0.65	7.30

Oct	-2.42	-3.6	0.32
Nov	0.98	2.41	1.33
Dec	-1.73	-2.37	0.98

Table 4.10(a): Statistical parameters of the average annual IMD Srinagar Station observed, modelled and model corrected T_{max}, T_{min}, and precipitation by modified difference and linear scaling method under RCP 4.5 Scenario

Parameter	**Observed**	**Modelled**	**Modified difference approach**	**Linear scaling method**
T_{max} (^{o}C)				
Mean	20.21	20.93	21.87	20.25
Standard deviation	8.89	10.67	11.71	8.89
Variance	79.03	113.84	137.45	78.23
RMSE	-	5.11	6.49	5.34
T_{min} (^{o}C)				
Mean	6.63	8.73	9.98	6.71
Standard deviation	7.41	9.74	10.21	8.19
Variance	54.91	94.86	104.38	66.49
RMSE	-	5.37	6.17	4.59
Precipitation (mm)				
Mean	2.17	1.69	3.12	2.01
Standard deviation	8.57	5.94	8.32	7.32
Variance	73.52	36.03	68.13	52.91
RMSE	-	9.13	10.93	9.64

Table 4.10(b): Statistical parameters of the average annual IMD Srinagar Station observed, modelled and model corrected T_{max}, $T_{min,}$ and precipitation by modified difference and linear scaling method under RCP 8.5 Scenario

Parameter	Observed	Modelled	Modified difference approach	Linear scaling method
T_{max} (^{o}C)				
Mean	20.21	21.15	21.91	20.27
Standard deviation	8.89	10.93	11.78	8.93
Variance	79.03	119.46	138.77	79.48
RMSE	-	5.34	6.53	5.36
T_{min} (^{o}C)				
Mean	6.63	9.05	10.01	6.73
Standard deviation	7.41	9.89	10.29	8.24
Variance	54.91	97.81	105.88	67.89
RMSE	-	5.51	6.25	4.62
Precipitation (mm)				
Mean	2.17	1.71	3.17	2.04
Standard deviation	8.57	5.96	8.39	7.36
Variance	73.52	35.16	70.39	54.17
RMSE	-	9.19	10.99	9.67

Table 4.11: Average annual based climate predictions for AFMU SKUAST Station using LS corrected modeled data

	Observed/ Baseline (1985-2019)	4.5			8.5		
		NF (2021-2045)	MF (2046-2070)	FF (2071-2095)	NF (2021-2045)	MF (2046-2070)	FF (2071-2095)
Annual T_{max} (^{o}C)	19.66	20.93	21.83	22.3	20.95	22.58	24.55
Annual T_{min} (^{o}C)	6.81	10.98	11.02	13.09	11.63	13.83	15.74
Annual $T_{average}$ (^{o}C)	13.24	15.95	16.43	17.69	16.29	18.2	20.15
Average Annual Precipitation (mm)	824.52	1141.6	1060.5	1055.9	1214.5	1172.4	1165.1

Table 4.12: Average annual based climate predictions for IMD Srinagar Station using LS corrected modeled data

	Observed/ Baseline (1989-2019)	4.5			8.5		
		NF (2021-2045)	MF (2046-2070)	FF (2071-2095)	NF (2021-2045)	MF (2046-2070)	FF (2071-2095)
Annual T_{max} (^{o}C)	20.39	21.07	22.37	22.35	21.36	22.99	24.96
Annual T_{min} (^{o}C)	7.96	10.88	11.75	12.16	11.09	12.78	14.83
Annual $T_{average}$ (^{o}C)	14.17	15.96	17.06	17.26	16.23	17.88	19.89
Average Annual Precipitation (mm)	734.06	709.5	763.31	756.24	724.11	828.98	950.04

4.2 Future Climate Scenarios under RCP 4.5 and 8.5 scenarios for AMFU Shalimar

4.2.1 Climate change scenarios analysis in the near future (NF) under RCP 4.5 and 8.5

Analysis under RCP 4.5 & 8.5 scenario from table 4.11 average annual T_{max} and T_{min} showed an increasing trend in the near future (NF) under both the scenarios. The T_{max} and T_{min} were found to increase at the rate of 6.26% and 46.88%, and 6.35% and 52.28% under the RCP 4.5 & 8.5 scenarios, respectively. The average annual precipitation was found to have an increasing trend for the same period under both scenarios at the rate of 32.25% and 38.25%, respectively (Fig. 4.2, 4.3(a,b), and 4.4).

4.2.2 Climate change scenarios analysis in the mid future (MF) under RCP 4.5 and 8.5

Average annual T_{max} and T_{min} showed an increasing trend in the mid-future (MF) under both scenarios. T_{max} and T_{min} were found to increase at the rate of 10.46% and 13.83% and 47.22% and 68.03% for the RCP 4.5 and 8.5 scenarios, relative to the baseline. For both scenarios, the average annual precipitation indicated an increasing trend over the mid-future (MF) at a rate of 25.03% and 34.84%, respectively (Fig. 4.2, 4.3(a,b) and 4.4) (Table 4.11).

4.2.3 Climate change scenarios analysis in the far future (FF) under RCP 4.5 and 8.5

Average annual T_{max} and T_{min} showed an increasing trend in the far future (FF) while comparing with the baseline under both scenarios. T_{max} and T_{min} were also found to increase at the rate of 12.58% and 22.12%, and 63.11% and 79.20%, for RCP 4.5 and 8.5 scenarios from baseline, respectively. The average annual precipitation showed an increasing trend for the far future (FF) under both scenarios at the rate of 24.61% and 34.24%, respectively (Fig. 4.2, 4.3(a,b), and 4.4) (Table 4.11).

4.3 Future Climate Scenarios under RCP 4.5 and 8.5 scenarios for IMD Srinagar station

4.3.1 Climate change scenarios analysis in the near future (NF) under RCP 4.5 and 8.5

Analysis under RCP 4.5 & 8.5 scenario from table 4.12 average annual T_{max} and T_{min} showed an increasing trend in the near future (NF) under both the scenarios. The T_{max} and T_{min} were found to increase at the rate of 3.33% and 36.68%, and 4.76% and 39.32% under the RCP 4.5 & 8.5 scenarios, respectively. The average annual precipitation was found to have a decreasing trend for the same period under both scenarios at -3.35% and -1.35%, respectively (Fig. 4.5, 4.6(a,b), and 4.7).

4.3.2 Climate change scenarios analysis in mid future (MF) under RCP 4.5 and 8.5

Average annual T_{max} and T_{min} showed an increasing trend in the mid-future (MF) under both scenarios. T_{max} and T_{min} were also found at an increasing rate of 9.71% and 12.75%, and 41.61% and 60.56%, for RCP 4.5 and 8.5 scenarios from baseline, respectively. For both scenarios, the average annual precipitation indicated an increasing trend over the mid-future (MF) at a rate of 3.98% and 12.93%, respectively (Fig. 4.5, 4.6(a,b), and 4.7) (Table 4.12).

4.3.3 Climate change scenarios analysis in far future (FF) under RCP 4.5 and 8.5

Average annual T_{max} and T_{min} showed an increasing trend in the far future (FF) while comparing with baseline under both the scenarios. T_{max} and T_{min} also found to be increased at the rate of 9.61% and 22.41%, and 52.76% and 86.31%, for RCP 4.5 and 8.5 scenarios from baseline, respectively. The average annual precipitation showed an increasing trend for the far future (FF) under both scenarios at the rate of 3.02% and 29.42%, respectively (Fig. 4.5, 4.6(a,b), and 4.7) (Table 4.12).

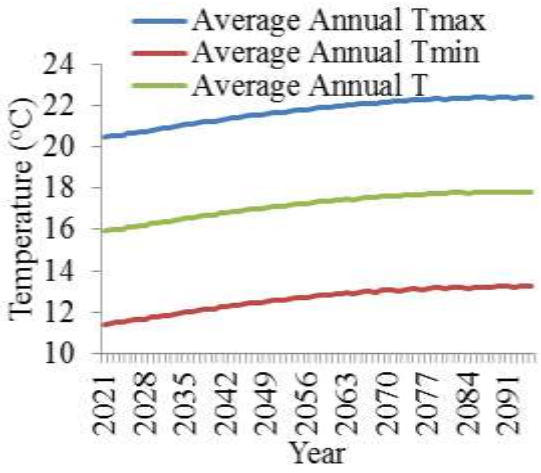

Fig. 4.3(a): Average temperature trend during future under RCP 4.5 scenario for AMFU Shalimar

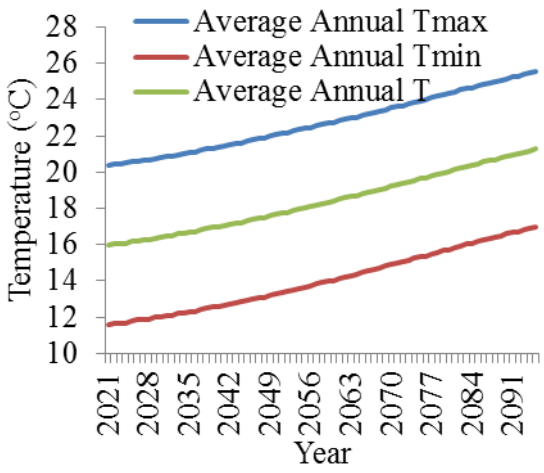

Fig. 4.3(b): Average temperature trend during future under RCP 8.5 scenario for AMFU Shalimar

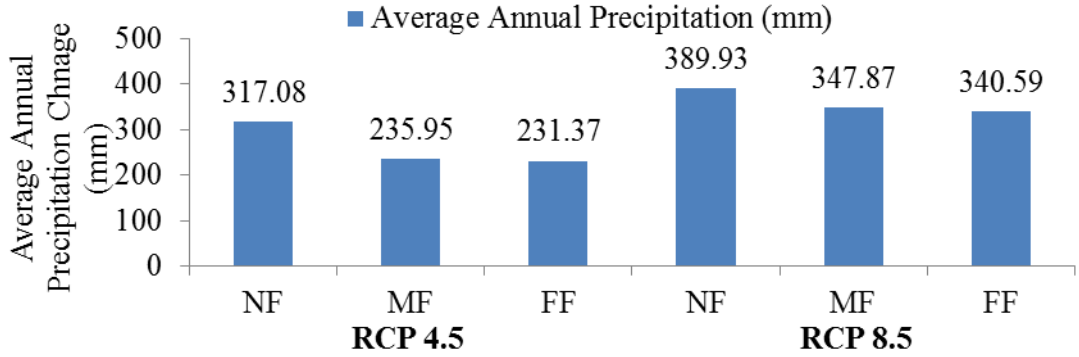

Fig. 4.4: Change in average annual precipitation from baseline in different time slices for AMFU Shalimar

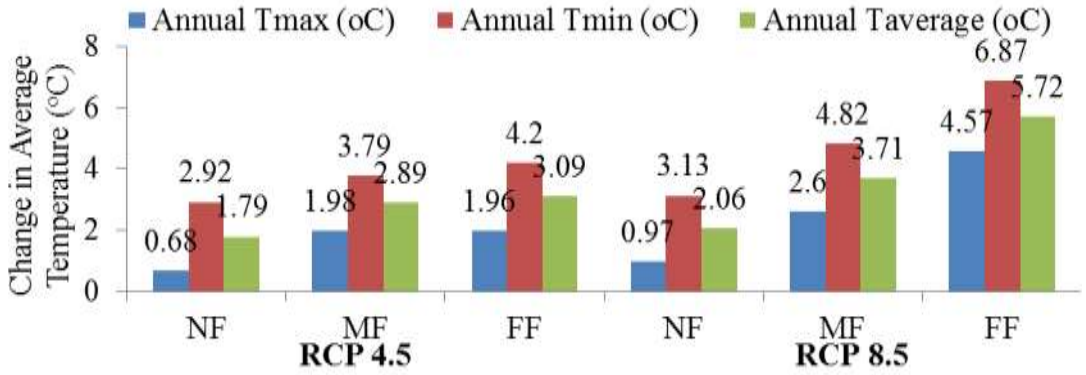

Fig. 4.5: Change in average temperature in different time slices in future for IMD Srinagar

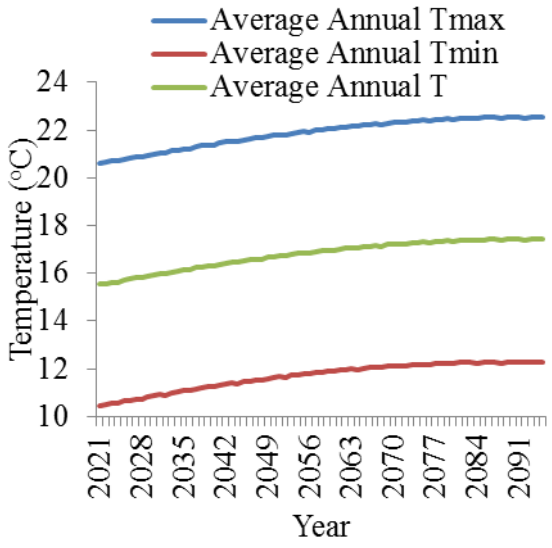

Fig. 4.6(a): Average temperature trend during future under RCP 4.5 scenario for IMD Srinagar

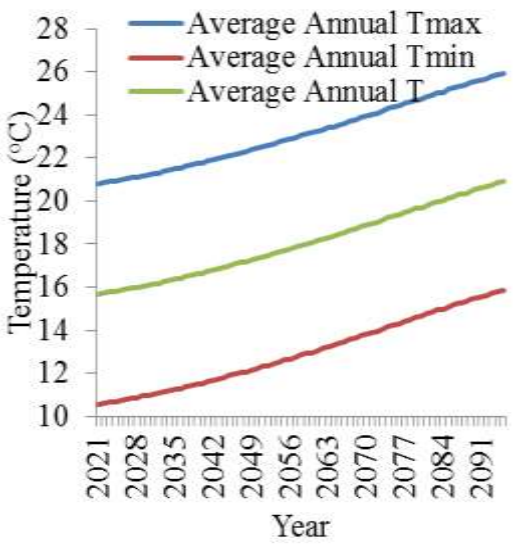

Fig. 4.6(b): Average temperature trend during future under RCP 8.5 scenario for IMD Srinagar

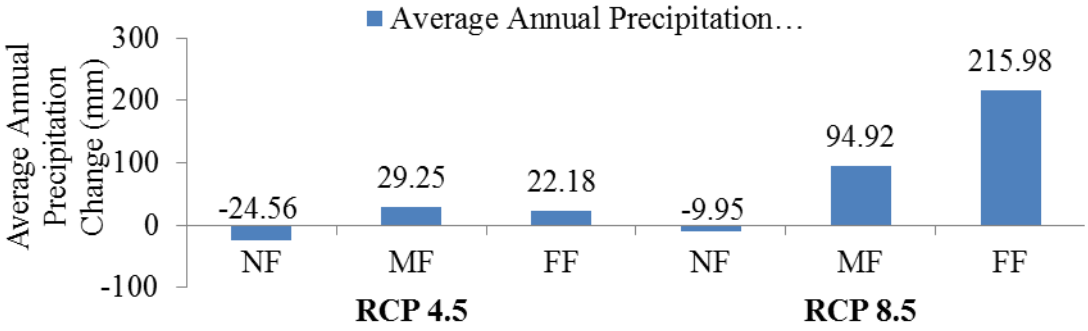

Fig. 4.7: Change in average annual precipitation from baseline in different time slices for IMD Srinagar

4.4 Land use and land cover (LU/LC) change detection in the Central Kashmir

4.4.1 Land Use/Land Cover Analysis - 2000

The LU/LC analysis of the research region was conducted over two time periods, spanning roughly 17 years, between 2000 and 2017. These time frames were selected based on the temporal representation of the coverage and the availability of pertinent remote sensing information. It was found that the research region in 2000 had seven distinct LU/LC classifications (Fig. 4.8(a)). Forest was the dominant land cover category in the study area, with 1339.20 km^2, constituting more than 40 % of the total Central Kashmir Himalayan area. The area under Snow/Glacier was 784.83 km^2 (23.85 %), while Agriculture accounts for 515.72 km^2 (15.67 %). Horticulture covered 293.81 km^2 (8.93 %), and Wasteland/Barren is spread over an area of 215.31 km^2 (6.54 %) of the total area (Table 4.13 and Fig. 4.8(b)). The area under Waterbody/Wetland/Water and Built-Up/Utility constituted 2.40 % and 1.90 %, respectively, of the total area of Central Kashmir Himalayas (Fig. 4.8(a,b)) (Table 4.13). A kappa value of 0.721 and an overall classification accuracy of 82.3% were achieved in the study. Therefore, this classified image is recommended for further investigation because of the significant kappa coefficient value.

4.4.2 Land Use/Land Cover Analysis - 2017

The LU/LC classification of the study area for the year 2017 revealed Seven LU/LC classes (Fig. 4.9(a)) again. Forest remained the dominant land cover type again, covering an area of 1099.02 km^2 (33.40 %). Snow/Glaciers occupied about 799.98 km^2 (24.31 %). Horticulture constituted 463.19 km^2 (14.08 %) while Agriculture covered an area of 357.15 km^2 (10.85 %), followed by Wasteland/Barren as 331.48 km^2 (10.07 %). However, Built-Up covered an area of 170.01 km^2 (5.17 %), while Waterbody/Wetland was 69.66 km^2 (2.12 %) of the total area of the Kashmir Himalayas (Fig. 4.9(a,b)) (Table 4.13). Overall

classification accuracy of 84.7 % and a kappa coefficient of 0.742 were observed for the classified image. The kappa coefficient is substantial, indicating that the categorized imagery is appropriate for further analysis.

4.4.3 Change Detection Analysis of Land Use/Land Cover for Central Kashmir Himalayas

Post-classification LU/LC change is shown for two time periods, 2000 and 2017 (Table 4.13). The investigation revealed that there had been a significant shift in many LU/LC categories. From 2000 to 2017, the area under Horticulture/Plantation, Built-up/Utility, and Wasteland/Barren has steadily expanded, while the area under Forest and Agriculture has steadily decreased. The analysis of table 4.13 has revealed that the area under Forest has decreased from 1339.20 km^2 in 2000 to 1099.02 km^2 in 2017, thus registering a decline rate of 7.30 % (Fig. 4.10). The agriculture class has also shown a decreasing trend from 2000 to 2017. The area has decreased from 515.72 km^2 to 357.15 km^2, with an area loss of 158.58 km^2 (4.82 %) (Table 4.13). While Built-Up category has shown an increasing trend from 2000 to 2017 and has increased from 118.98 km^2 to 186.73 km^2 (table 4.13) thus showing an increase of 67.75 km2 registering a growth rate of 3.26 % (Fig. 4.10). Horticulture has also registered a positive increase from 2000 to 2017. The area has increased from 293.81 to 463.19 km^2 (table 4.13), showing an increase of 169.39 km^2 (5.15 %). The area under water bodies in 2000 was 79.00 km^2 and got reduced to 69.66 km^2 in 2017 with a decrease of 9.34 km^2 (-0.28 %) (Fig. 4.10, Table 4.13). Glaciers have also shown a decreasing trend from 2000 to 2017. The area in 2000 was 784.83 km^2, while it got reduced to 799.98 km^2 in 2017 with a decrease of 118.48 km^2 (-0.89 %) (Fig. 4.10, Table 4.13).

4.4.4 Conversion of Land Use/Land Cover for Central Kashmir Himalayas

The analysis of the study has revealed that different LU/LC classes have shown conversion into different LU/LC categories. Agriculture showed

conversion into three LU/LC categories: Barren, Built-up, and Horticulture. The barren category got changed into four LU/LC classes Agriculture, Built-up, Horticulture, and Forest. The land cover category of the forest showed the conversion into three LU/LC categories, viz. Agriculture, Barren, and Horticulture, while the Built-up category led to no conversion. Horticulture showed the conversion into three Barren, Forest, and Built-up categories. Water bodies/wetlands got changed into Built-up, Agriculture, and Horticulture, while the Glacier/Snow showed the conversion into two categories of Barren and Forest (Fig. 4.11).

Table 4.13: Land Use/Land Cover statistics from 2000 to 2017

LU/LC	2000		2017		Relative Change	
	km^2	%	km^2	%	km^2	%
Waterbody/Wetland	79.00	2.40	69.66	2.12	9.34	-0.28
Snow/Glacier	784.83	23.85	799.98	24.31	-15.15	0.46
Built Up/Utility	62.64	1.90	170.01	5.17	-107.38	3.26
Forest	1339.20	40.70	1099.02	33.40	240.18	-7.30
Horticulture/Plantation	293.81	8.93	463.19	14.08	-169.39	5.15
Agriculture	515.72	15.67	357.15	10.85	158.58	-4.82
Wasteland/Barren	215.31	6.54	331.48	10.07	-116.17	3.53

4.5 Delineation of groundwater recharge potential zones of the Central Kashmir

As a result of a weighted overlay analysis on a number of thematic layers (slope, geological formation, precipitation, drainage density and land cover, lineament density in soil, geomorphology, and altitude), potential recharge zones were identified (Fig. 4.12). Each class has been given the appropriate weightage based on a knowledge-based ranking system from 1 to 9. (9 was assigned to the class having the highest order, and one was assigned to the class having the lowest order). In integrated analysis, determining the proper weight for each class is

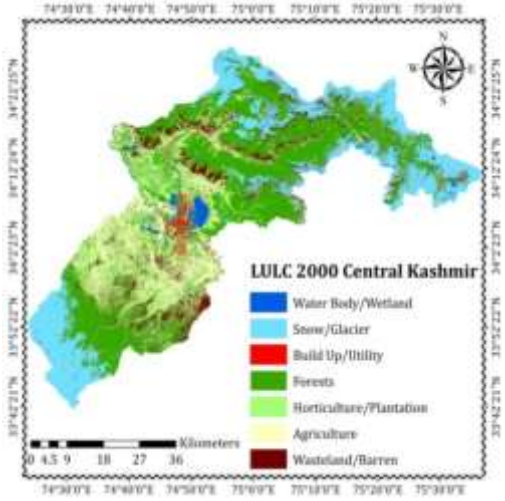

Fig. 4.8(a): LU/LC of Central Kashmir generated from LISS III 2000.

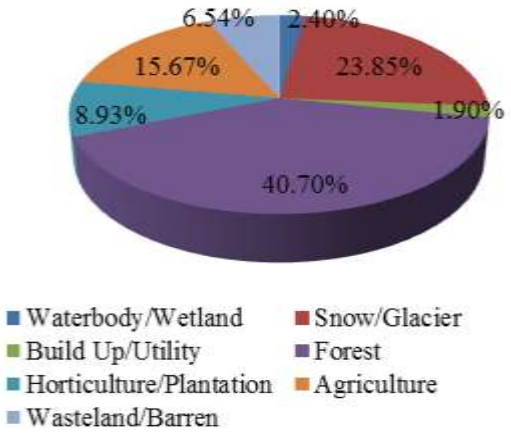

Fig. 4.8(b): Percentage area of LU/LC categories, 2000

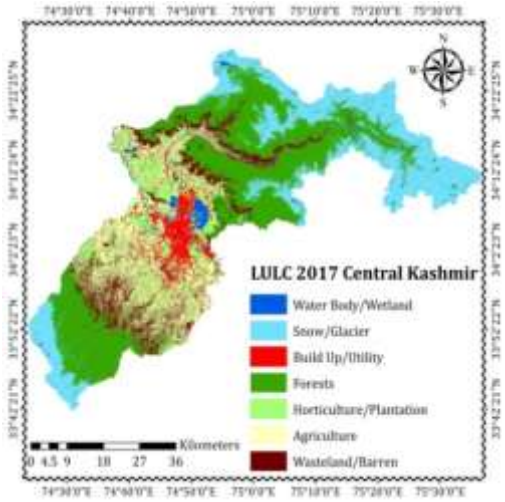

Fig. 4.9(a): LU/LC of Central Kashmir generated from LISS III 2017

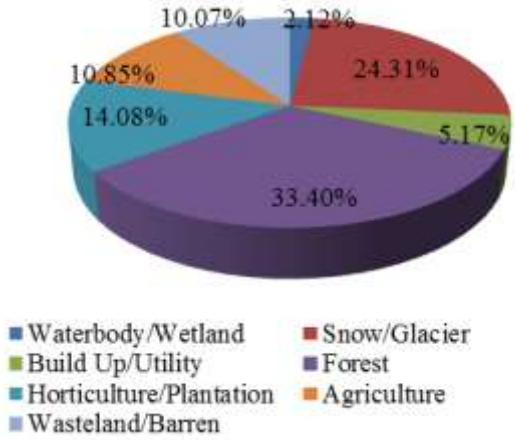

Fig. 4.9(b): Percentage area of LU/LC categories, 2017

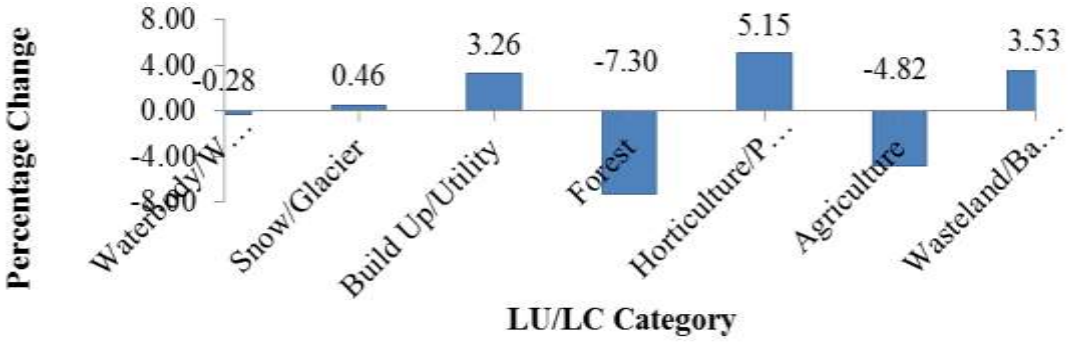

Fig. 4.10: Percentage change of LU/LC categories, 2000 & 2017

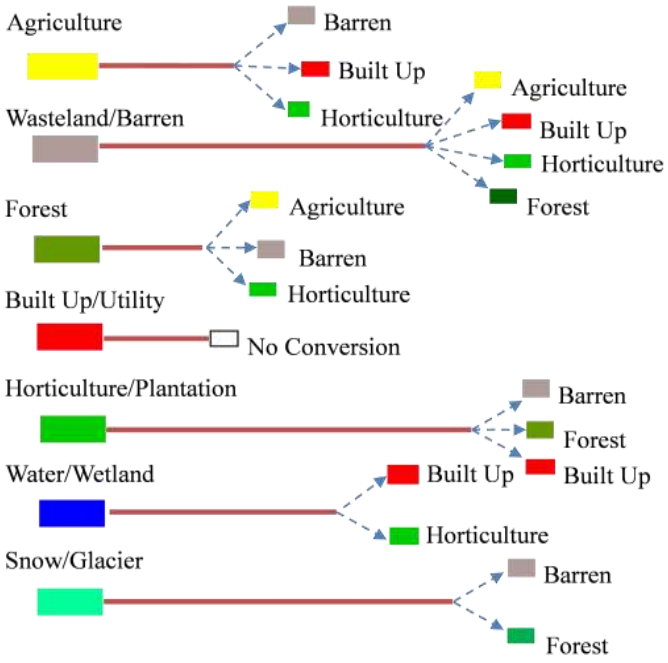

Fig. 4.11: Analysis of conversion of different LU/LC categories of Central Kashmir

crucial since the result is totally dependent on the appropriate weight (Nag and Ghosh 2013).

The groundwater recharge prospects map was categorized into five zones: very high, high, medium, low, and very low. Very low potential areas cover 553.51 km^2 (16.80%), low potential areas cover 999.79 km^2 (30.34%), medium potential areas cover 699.08 km^2 (21.22%), high potential areas cover 710.26 km^2 (21.56%), and very high potential areas cover 332.36 (10.09%) and are presented in Table 4.14. The groundwater recharge potential map and springs in Central Kashmir are shown in Figures 4.12(a,b), respectively.

Table 4.14: Groundwater recharge potential zones and categorization

Groundwater Recharge Zones	**Area (km^2)**	**Area (%)**
Very Low	553.51	16.80
Low	999.79	30.34
Medium	699.08	21.22
High	710.26	21.56
Very High	332.36	10.09

4.6 Identification of rainwater harvesting suitability level of Central Kashmir

The integration of thematic maps resulted in producing the study area's water harvesting suitability level (WHSL) map, as shown in figure 4.14(a). The suitability level map was divided into four zones: very high, high, medium, and low. The map depicts clear zones that meet all the set criteria of suitability. As described in table 4.15, the medium harvesting suitability level dominated the study area, followed by high, low, and very high harvesting suitability levels. A brief description of each zone is given under:

Very High WHSL: This zone covers an area of 422.06 km^2 (12.81%). The high WHSL constitutes a steep slope (>40%), high flow accumulation values,

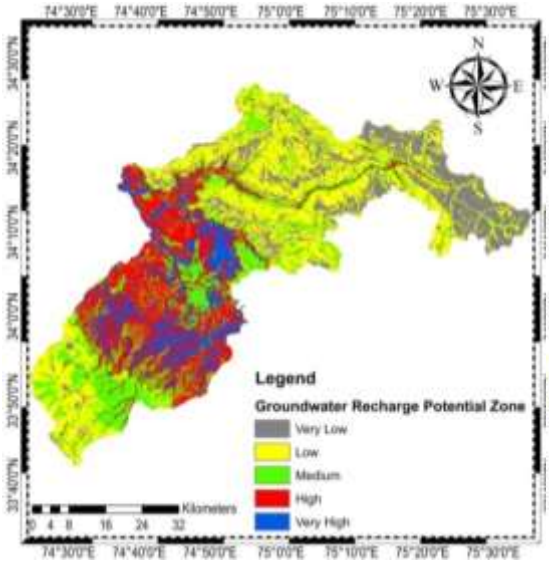

Fig. 4.12(a): Groundwater recharge potential zones of Central Kashmir

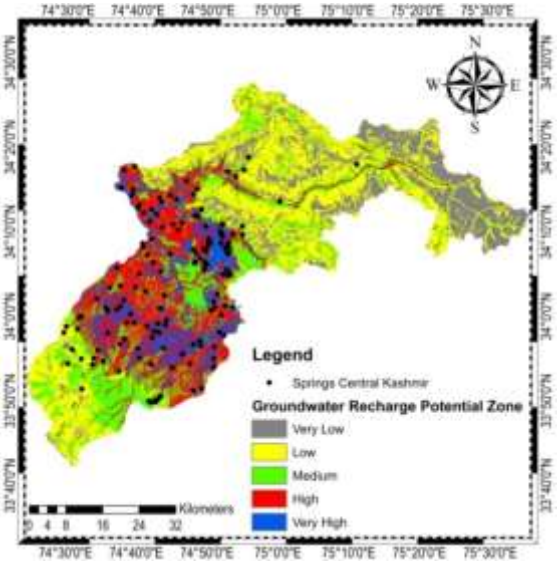

Fig. 4.12(b): Groundwater recharge potential zones and springs geotagged in Central Kashmir

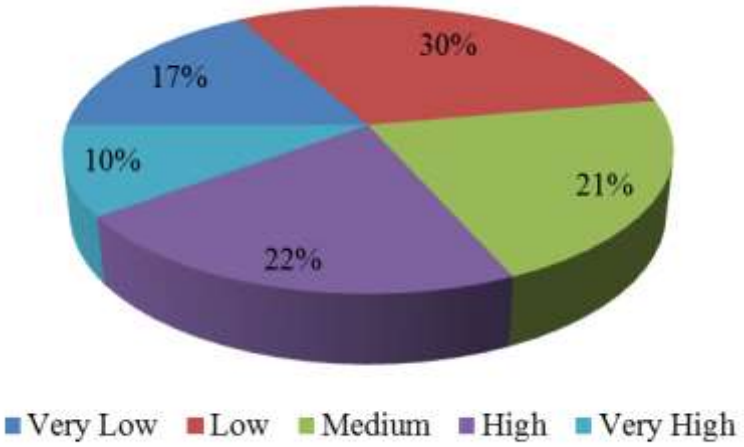

Fig. 4.13: Percentage area of groundwater recharge potential zones in Central Kashmir

slope, and barren land. These factors were considered the critical parameters for very high WHSL as they facilitate high runoff generation.

High WHSL: This zone covers an area of 1070.98 km^2 (32.50%). The high WHSL constitutes mainly of the slope class (>20%), medium flow accumulation values, slope, and barren land. These factors were considered the key parameters for high WHSL as they facilitate medium to high runoff generation.

Medium WHSL: This zone covers an area of 1165.67 km^2 (35.38%) of the total area. This zone was characterized by slope classes of (5-10%) and (10-20%), agriculture & horticulture fields, and sandy soils. Taking all these parameters into consideration, the WHSL was found to be moderate in this zone

Low WHSL: This zone covered an area of 636.29 km^2 (19.31%) of Central Kashmir and was characterized by nearly level to the very gentle slope (<5%), low flow accumulation, built-up units, high content sandy soils, which constitute for low WHSL.

The springs in Central Kashmir with overlapping rainwater harvesting suitability level is shown in figure 4.14(b). The resulting map clearly indicates that about 40% of geotagged springs fall in the medium to very high suitability level. The harvesting of rainwater is easy in these zones for the recharging of the regional aquifers.

Table 4.15: Rainwater harvesting suitability level and categorization of groups in Central Kashmir

Rainwater Harvesting Suitability	**Area (km^2)**	**Area (%)**
Low	636.29	19.31
Medium	1165.67	35.38
High	1070.98	32.50
Very High	422.06	12.81

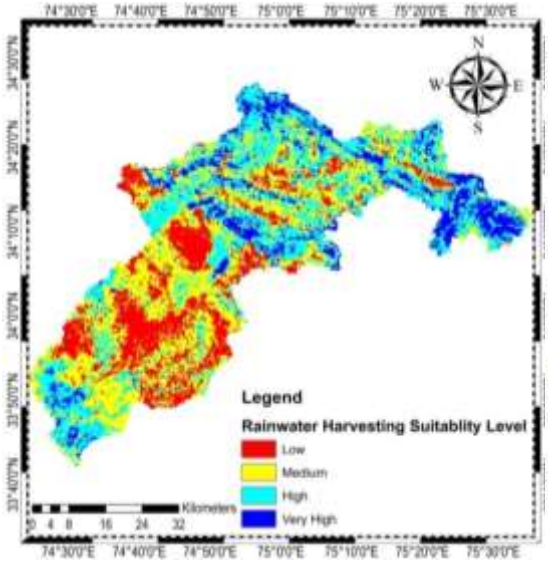

Fig 4.14(a): Water harvesting suitability level map of Central Kashmir

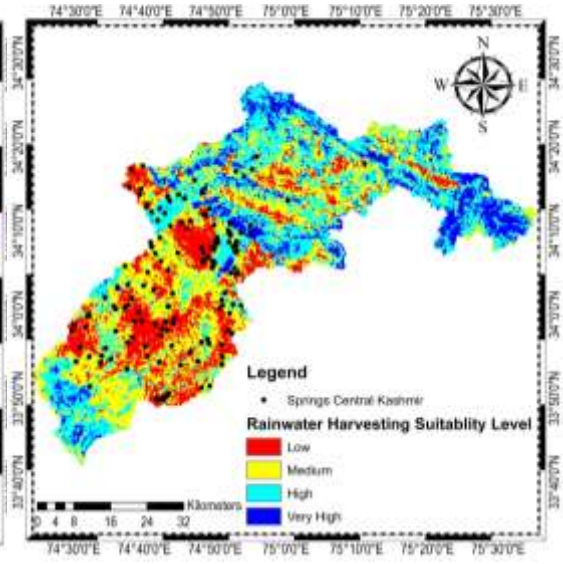

Fig. 4.14(b): Water harvesting suitability level map and springs geotagged in Central Kashmir

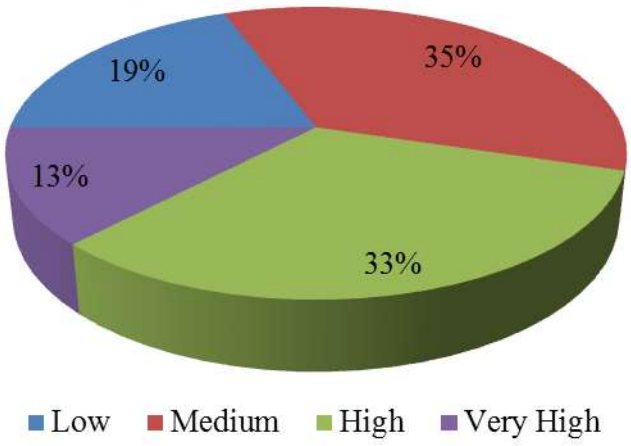

Fig. 4.15: Percentage area of rainwater harvesting suitability level in Central Kashmir

4.7 Vertical Electrical Sounding (VES) analysis of the subsurface layers of the Central Kashmir

Vertical Electrical Sounding (VES) model resistivity values and their corresponding thickness and depth for SKUAST Kashmir, Shalimar campus is shown in table 4.16. The top layer of soil cover shows a low resistivity value of 15.4 Ω/m with a thickness of 0.2 m. The Medium to Course Sand with Gravel layer has a resistivity value of 347.1 Ω/m and a thickness of 0.8 m. The third layer corresponds to Clay with Course Material with a resistivity of 13.2 Ω/m and a thickness of 2.9 m. The fourth layer has a resistivity of 762.8 Ω/m and a thickness of 6.9 m, and the layer material is Medium to Course Sand with Granular Material. The Sandy Clay (Fine to Medium Sand) layer has a resistivity value of 8.2 Ω/m with a thickness of 12.9 m. The sixth layer has Sandy Clay with Extra Course Material with a resistivity value of 3487.7 Ω/m and a thickness of 618.6 m. Layer 5 with Sandy Clay (Fine to Medium Sand) material of 12.9 m thickness and depth at 10.9 - 23.7 mbgl has good groundwater availability, which is well validated with available well log data and groundwater depth data of the location. The majority of the groundwater-bearing zones in the study area may be found between the clay and the sandy clay layer, which is the fifth layer. The porosity and permeability of the aquifer contents are responsible for this. Given its high porosity, clay can hold up to half its weight in water. The microscopically tiny space between clay particles with a huge surface area favours sluggish movement and water retention. When it comes to aquifers, clays aren't as excellent as sandy clays with lesser porosity, which have more interconnected pores which allow for more water to flow freely (Singhal & Gupta, 2010). The weathered basement is the main aquifer (water-bearing unit) in the study region because of the excellent porosity and permeability properties of the material.

VES model resistivity values their corresponding thickness and depth for SKUAST Kashmir, Shuhama campus is shown in table 4.17. The topsoil layer shows a low resistivity value of 20.4 Ω/m with a thickness of 0.6 m. The Sandy Medium to Coarse Panjal Trap and Quartzite layer has a resistivity value of 55.4 Ω/m and a thickness of 2.4 m. The third layer corresponds to Clay, with a coarse material layer with a resistivity of 41.9 Ω/m and a thickness of 11.1 m. The fourth layer has a material of Clay with Fine to Medium Sand with a resistivity value of 10.7 Ω/m and a thickness of 11.3 m. The Medium to Course Sand with a Granular Material layer has a resistivity value of 434.9 Ω/m with a thickness of 25.0 m. The fourth layer corresponds to the layer with good groundwater availability validated with groundwater depth and well log available data.

VES model results of resistivity values and their corresponding thickness and depth for KVK, Budgam are shown in table 4.18. The topsoil layer shows a low resistivity value of 31.0 Ω/m with a thickness of 1.7 m. The second layer of clay with semi-plasticity with a few coarse granular materials has a resistivity value of 405.0 Ω/m and a thickness of 1.5 m. The third layer corresponds to the Silty Clay layer with resistivity value and thickness of 6.0 Ω/m and 2.3 m, respectively. The fourth layer has a resistivity value of 22.4 Ω/m and a thickness of 31.2 m with a material of Sandy Clay (Fine to Medium). The Sand Course to Granular with Kankar layer 5 has a resistivity value of 9020.3 Ω/m with a thickness of 489.8 m. The freshwater availability beneath the ground is found to be abundant in layer 4 with sandy clay material, which is well according to the groundwater depth data and well log available data of the site.

The resistivity survey results were analyzed and interpreted to delineate the geoelectric sections of the study area. Five to six different layers were delineated from the resistivity survey at each VES point. The underlying layer shows a sharp increase in resistivity, indicating that it has different geoelectrical properties from the preceding layers and cannot be estimated.

Table 4.16: Summary of VES model resistivity values and their corresponding thickness and depth for SKUAST Kashmir, Shalimar Campus

Layer	Resistivity (Ohm m)	Thickness (m)	Depth (mbgl)	Lithology	Groundwater
1	15.5	0.2	0.2	Soil Cover	
2	347.1	0.8	1	Medium to Course Sand with Gravel	
3	13.2	2.9	3.9	Clay with Course Material	
4	762.8	6.9	10.9	Medium to Course Sand with Granular Material	
5	8.2	12.9	23.7	Sandy Clay (Fine to Medium Sand)	**Fresh Groundwater**
6	3487.7	618.6	642.3	Sandy Clay with Extra Course Material	

Table 4.17: Summary of VES model resistivity values and their corresponding thickness and depth for SKUAST Kashmir, Shuhama Campus

Layer	Resistivity (Ohm m)	Thickness (m)	Depth (mbgl)	Lithology	Groundwater
1	20.4	0.6	0.6	Soil Cover	
2	55.4	2.4	3.0	Sand Medium to Coarse Panjal Trap and Quartzite	
3	41.9	11.1	14.1	Silty Clay with Gravel	
4	10.7	11.3	25.4	Clay with Fine to Medium Sand	**Fresh Groundwater**

5	434.9	25.0	50.4	Medium to Course Sand with Granular Material	

Table 4.18: Summary of VES model resistivity values and their corresponding thickness and depth for KVK, Budgam

Layer	Resistivity (Ohm m)	Thickness (m)	Depth (mbgl)	Lithology	Groundwater
1	31	1.7	1.7	Soil Cover	
2	405	1.5	3.2	Clay with semi plasticity with few course granular material	
3	6	2.3	5.5	Silty Clay	
4	22.4	31.2	36.7	Sandy Clay (Fine to Medium)	**Fresh Groundwater**
5	9020.3	489.8	526.5	Sand Course to Granular with Kankar	

4.8 Parameter sensitivity analysis, calibration, and validation of the model

After including the input data, the first two years (1989–1990) were used as a warm-up phase, and the SWAT model was run for ten years (1991–2000) with the default settings to simulate streamflow in the four catchments. It is important to calibrate the model since the simulated streamflow for the four catchments prior to calibration does not exhibit adequate results. For the streamflow simulation sensitivity analysis, 12 hydrological parameters were investigated before the model was calibrated. It was determined to calibrate and optimize the values of the parameters that were found as sensitive. SUFI 2 global sensitivity analysis was used in SWAT CUP to perform parameter sensitivity analyses over a period of 10 years, which included the time required for

calibration. Snowmelt dominates the streamflow due to the catchment's high elevation of 5380m and location. Consequently, the snow parameters, temperature, precipitation lapse rates, curve numbers, and 100 iterations for each input parameter change were optimized.

The SWAT model is calibrated for ten years (1991–2000). After calibration, the model is validated for 19 years (2001–2019) for all four catchments. The optimized parameters generated during calibration are utilized to simulate the model for the validation period. Table 4.19 shows the statistical evaluation coefficients of the observed and simulated streamflow for calibration and validation. For calibration, the coefficient of determination R^2 is 0.97 for the Dal catchment, 0.56 for the Sindh catchment, 0.63 for the Dudhganga catchment, and 0.61 for the Sukhnag Catchment. The Nash Sutcliffe efficiency NSE values obtained were 0.96 for the Dal catchment, 0.66 for the Sindh catchment, 0.61 for the Dudhganga Catchment, and 0.59 for the Sukhnag catchment. The coefficient of determination R^2 for validation is 0.97 for the dal catchment, 0.58 for the Sindh catchment, 0.64 for the Dudhganga catchment, and 0.61 for the Sukhnag catchment. The Nash Sutcliffe efficiency NSE values obtained were 0.94, 0.64, 0.60, and 58 for the Dal, Sindh, Dudhganga, and Sukhnag Catchments. The other evaluation coefficients for the calibration and validation of the model are given in table 4.19. The hydrographs of the observed and simulated streamflow for calibration and validation for the catchments of Central Kashmir are shown in Fig. 4.16(a,b), Fig. 4.17(a,b), Fig. 4.18(a,b), Fig. 4.19(a,b).

Table 4.19: Summary of evaluation coefficients for calibration and validation

Category	**Variable**	**Dal**	**Sindh**	**Dudhganga**	**Sukhnag**
Calibration	p-factor	0.66	0.57	0.51	0.53
	r-factor	0.47	0.43	0.25	0.18
	R^2	0.97	0.56	0.63	0.61
	NS	0.96	0.66	0.61	0.59

	PBIAS	41.7	51.4	55.0	54.3
	MNS	0.77	0.52	0.39	0.37
	Mean_sim(Mean_obs)	5.37(5.53)	26.50(45.25)	2.94(3.92)	4.11(5.44)
	StdDev_sim(SD_obs)	4.70(5.27)	18.16(37.87)	2.47(5.18)	4.57(8.59)
Validation	p-factor	0.68	0.58	0.54	0.56
	r-factor	0.45	0.44	0.24	0.19
	R^2	0.97	0.58	0.64	0.61
	NS	0.94	0.64	0.60	0.58
	PBIAS	42.7	52.1	57.0	54.6
	MNS	0.78	0.53	0.39	0.38
	Mean_sim(Mean_obs)	5.61(5.45)	27.70(44.87)	2.99(3.89)	4.09(5.39)
	StdDev_sim(SD_obs)	4.67(5.18)	19.16 (36.65)	2.65 (5.11)	4.55(8.18)

4.9 Streamflow of various catchments of Central Kashmir under different RCP scenarios

After calibration and validation, the developed model was further used for streamflow generation under different emission scenarios of RCP 4.5 and 8.5 for the Dal catchment. The discharge under RCP 4.5 from the beginning of the near future to the mid future will increase, and by the end of the century or far future discharge will decrease (Fig. 4.20(a)). The results are well according to the scenario assumption since RCP 4.5 is considered a controlled scenario. The average discharge generated under the scenario considered is at par with the observed average discharge of the baseline period (1991-2019). RCP 8.5 scenario simulation results for the Dal catchment showed an increase in the discharge throughout the future and less increase at the end of the century (Fig. 4.20(b)). The average predicted discharge under RCP 8.5 scenarios is three times more than

the average discharge generated under RCP 4.5. The details of the observed and predicted discharge under various scenarios are given in table 4.20.

Similarly, the calibrated and validated models of the various catchments in Central Kashmir were used for streamflow generation under the different scenarios considered. The average predicted streamflow results of the Sindh catchment showed similar trends as observed for the Dal catchment ((Fig. 4.21(a,b)). The average discharge would decrease by 5.93 cumec under the RCP 4.5 compared with the baseline. The average discharge would increase under the RCP 8.5 scenario by 2.52 cumec with respect to baseline observed average discharge. The average observed and predicted discharge is given in table 4.20.

Predicted discharge for the Dudhganga catchment would increase in the near future and decrease in the mid future until the end of the century under the RCP 4.5. The vice versa results have been observed under the RCP 8.5, where the discharge would show a similar trend in the near and mid future as shown in the baseline period (Fig. 4.22(a,b)). The discharge would increase considerably in the far future with respect to the baseline and other time slices under the scenario. The average discharge would decrease by 0.8 cumec and increase by 1.28 cumec under RCP 4.5 and 8.5 scenarios with respect to baseline time average discharge. The percentage change and other details are given in table 4.20.

A similar kind of trend was observed for the Sukhnag catchment under both the scenarios considered for the study as observed for the Dudhganga catchment (Fig. 4.23(a,b)). The average predicted discharge would decrease by 0.9 cumec under the RCP 4.5 scenario and increase by 0.82 cumec under the RCP 8.5 scenario. The details of the observed and predicted discharge are given in table 4.20.

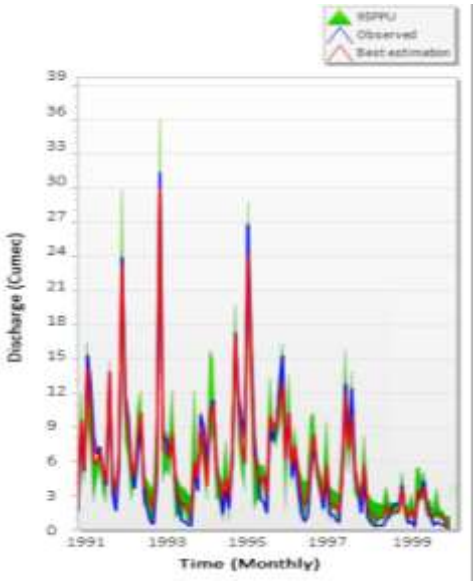

Fig. 4.16(a): Observed and Simulated hydrographs for calibration of Dal catchment

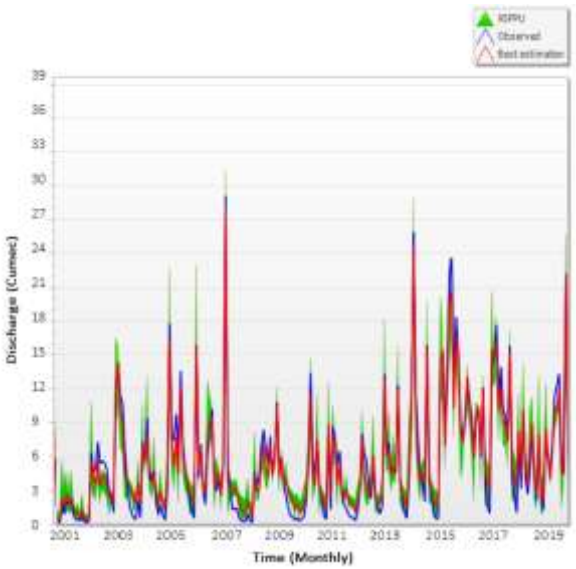

Fig. 4.16(b): Observed and Simulated hydrographs for validation of Dal catchment

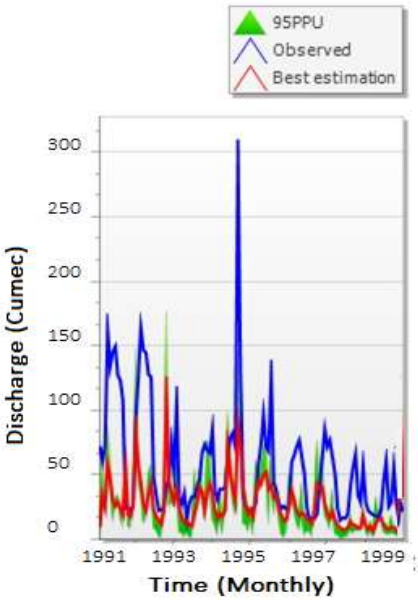

Fig. 4.17(a): Observed and Simulated hydrographs for calibration of Sindh catchment.

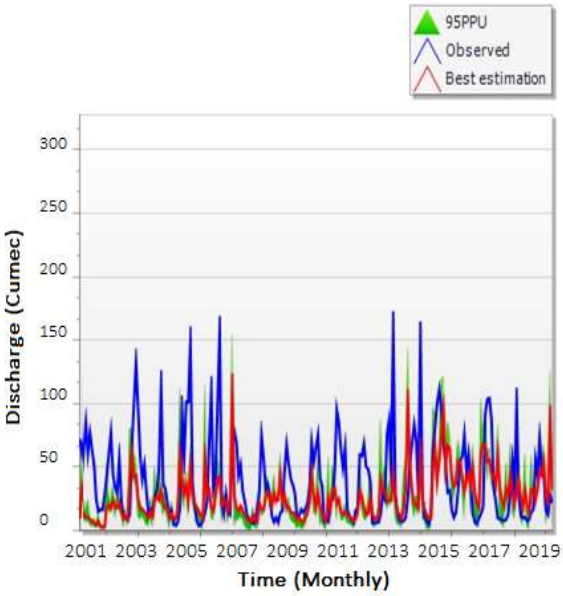

Fig. 4.17(b): Observed and Simulated hydrographs for validation of Sindh catchment

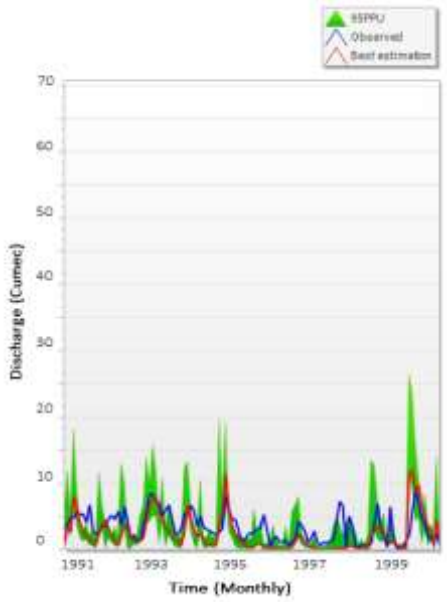

Fig. 4.18(a): Observed and Simulated hydrographs for calibration of Dudhganga catchment.

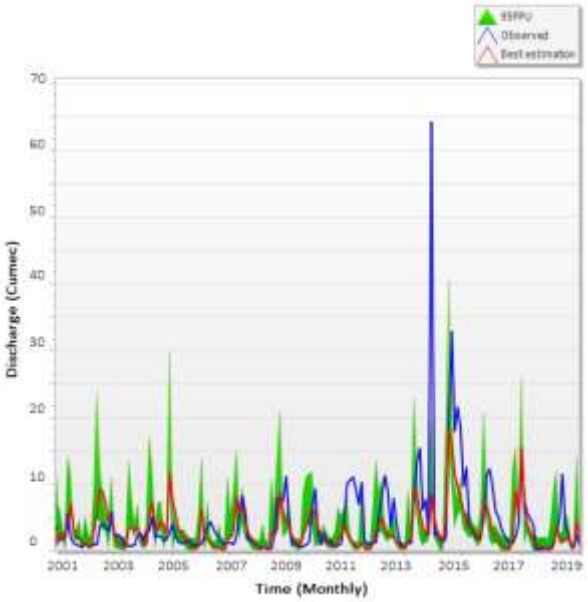

Fig. 4.18(b): Observed and Simulated hydrographs for validation of Dudhganga catchment

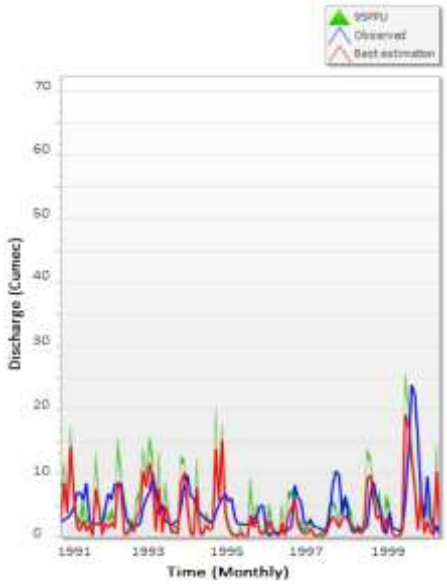

Fig. 4.19(a): Observed and Simulated hydrographs for calibration of Sukhnag catchment

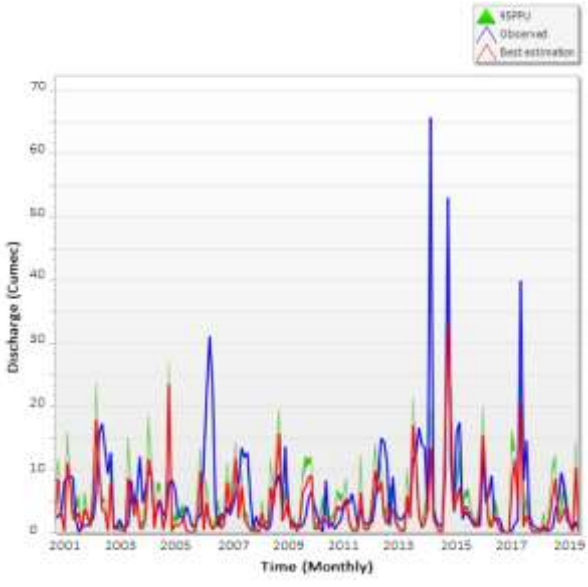

Fig. 4.19(b): Observed and Simulated hydrographs for validation of Sukhnag catchment

Table 4.20: Average Streamflow (Cumec) for the period 2021-2095 during the different scenarios in Central Kashmir

Catchment		Observed	Scenario	
			RCP 4.5	RCP 8.5
Dal	Average discharge (Cumec)	2.31	5.44	14.61
	Change in average discharge (Cumec)		3.13	12.3
	% Change		135.49	532.46
Sindh	Average discharge (Cumec)	45.25	39.32	47.77
	Change in average discharge (Cumec)		−5.93	2.52
	% Change		−13.11	5.57
Dudhganga	Average discharge (Cumec)	3.91	3.11	5.19
	Change in average discharge (Cumec)		−0.8	1.28
	% Change		−20.46	32.73
Sukhnag	Average discharge (Cumec)	5.43	4.53	6.25
	Change in average discharge (Cumec)		−0.9	0.82
	% Change		−17.3499	15.6722

4.10 Groundwater head and water-table depth of the various catchments of Central Kashmir under different RCP scenarios

SWAT model outputs were coupled with MODFLOW using the SWAT-MODFLOW interface, and the linked models were simulated for all the catchments of Central Kashmir. The simulations were done under RCP 4.5 and 8.5 scenarios and for the baseline period for comparison purposes.

The observed maximum groundwater head at the higher reaches of the Dal catchment is found to be 4296 m (amsl) which is going to decline in the future by

13 m from 4296 m to 4283 m under the RCP 4.5 scenario and 16 m from 4296 m to 4280 m under RCP 8.5 scenario. Similarly, the groundwater head of the lower parts of the catchment, mainly in the valley region, will decline by 1 m from 1574 m to 1573 m under both the scenarios of RCP 4.5 & 8.5 (Fig. 4.24-4.26(a,b)) (Table 4.21).

Similarly, the groundwater head in the Sindh catchment would decline compared to the observed head in the baseline period. The head would fall from 5362 m to 5348 and 5341 m during RCP 4.5 and 8.5 scenarios, respectively, in the higher reaches of the catchment. The fall would be 14 and 21 m under the RCP 4.5 and 8.5 scenarios, respectively, in higher reaches of the catchment. In the lower parts of the Valley, the head would fall by 1 m from 1574 m (amsl) to 1573 during both scenarios when compared with the observed head (Fig. 4.27-4.29(a,b)) (Table 4.21).

The groundwater head in the Dudhganga catchment would fall in the future, considering the RCP scenario. The head would fall by 13 to 16 m in the higher reaches of the catchment from 4624 to 4611 m and 4608 m during RCP 4.5 and 8.4 scenarios, respectively. The lower parts of the valley would also show the same trend, although the fall of the head would be only 1 m from 1581 m to 1580 m under both scenarios (Fig. 4.30-4.32(a,b)) (Table 4.21).

Sukhnag catchment shows similar kinds of results in groundwater head depletion. The head would fall from 4534 m to 4520 and 4515 m during RCP 4.5 and 8.5 scenarios, respectively. The fall would be 14 m under RCP 4.5 and 19 m under RCP 8.5 in the higher reaches of the catchment. The groundwater head in the lower parts of the Sukhnag catchment would decline by 1 m from 1582 m to 1581 m under both the RCP scenarios (Fig. 4.33-4.35(a,b)) (Table 4.21).

Under both scenarios, the water table depth would increase in all the catchments of central Kashmir in the future. The maximum increase in average water table depth (mbgl) would be in the Sindh catchment by 7.5 and 11 m under

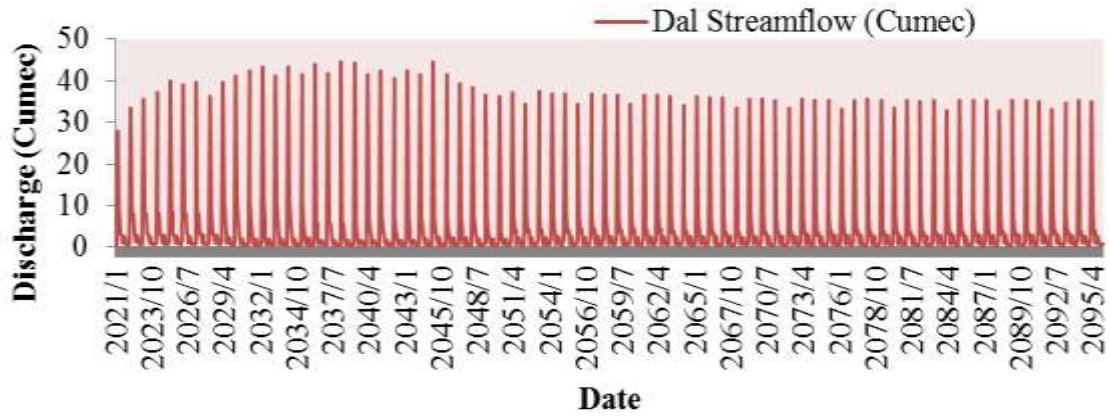

Fig. 4.20(a): Streamflow of the Dal catchment in future under RCP 4.5 scenario

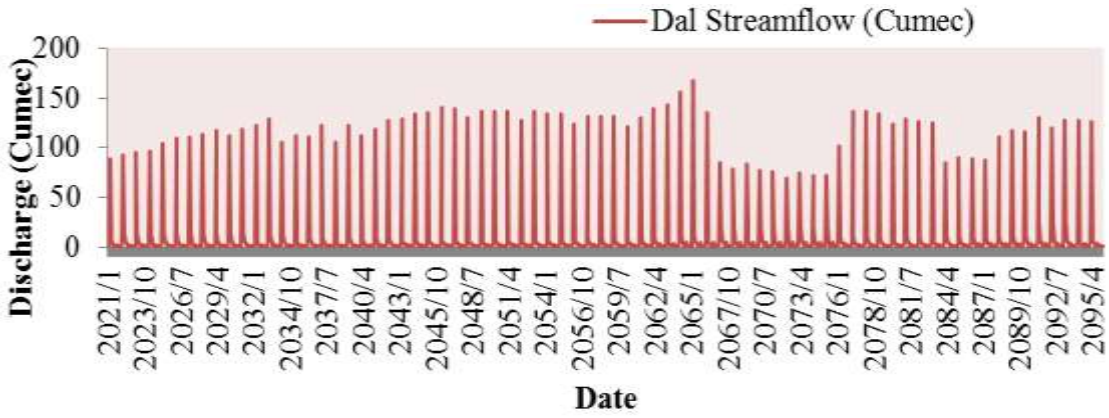

Fig. 4.20(b): Streamflow of the Dal catchment in future under RCP 8.5 scenario

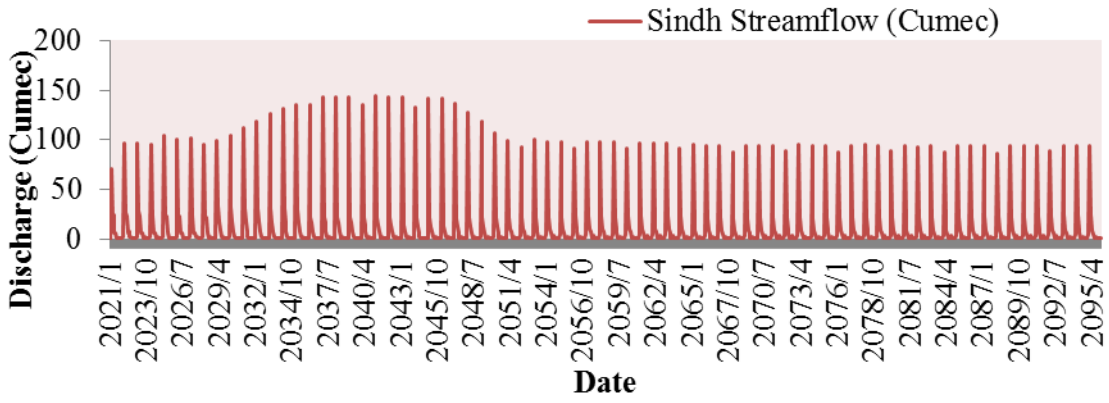

Fig. 4.21(a): Streamflow of the Sindh catchment in future under RCP 4.5

scenario

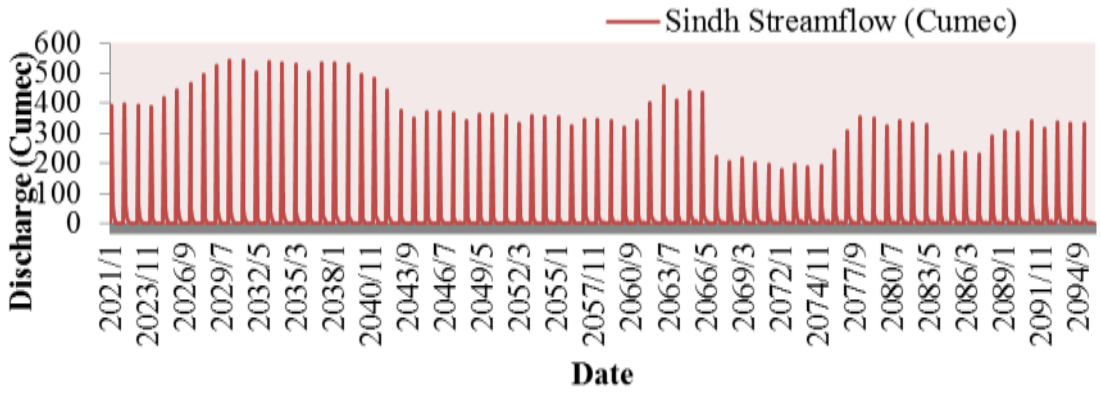

Fig. 4.21(b): Streamflow of the Sindh catchment in future under RCP 8.5 scenario

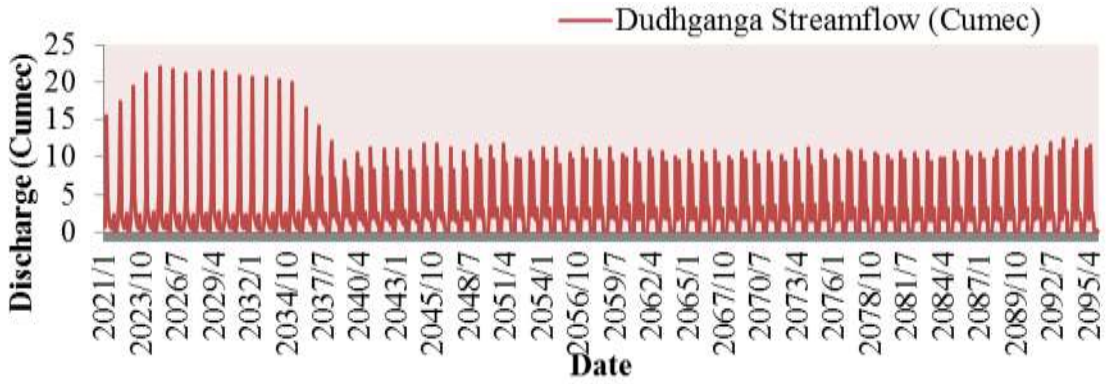

Fig. 4.22(a): Streamflow of the Dudhganga catchment in future under RCP 4.5 scenario

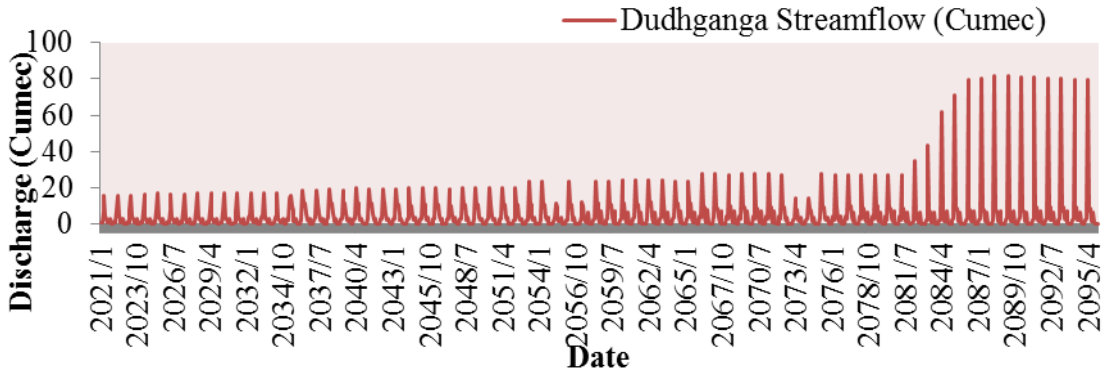

Fig. 4.22(b): Streamflow of the Dudhganga catchment in future under RCP 8.5 scenario

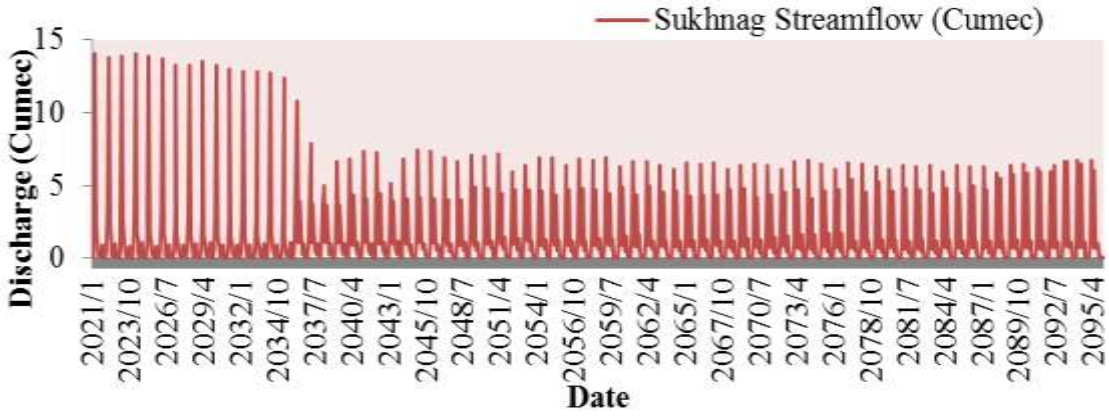

Fig. 4.23(a): Streamflow of the Sukhnag catchment in future under RCP 4.5 scenario

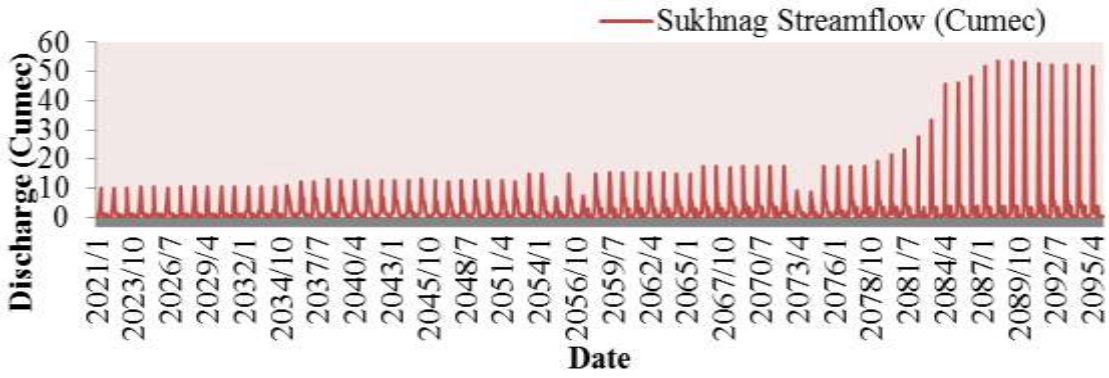

Fig. 4.23(b): Streamflow of the Sukhnag catchment in future under RCP 8.5 scenario

RCP 4.5 and 8.5 scenarios, and the minimum increase would be in the Dal catchment by 7 and 8 m during RCP 4.5 and 8.5 scenarios respectively (Table 4.21).

Table 4.21: Groundwater Head (m) during the different scenarios in Central Kashmir

Catchment		Observed	Scenario	
			RCP 4.5	RCP 8.5
Dal	Maximum Groundwater Head (m) amsl	4296	4283	4280
	Change in Maximum Groundwater Head (m)		−13	−16
	Minimum Groundwater Head (m) amsl	1581	1580	1580
	Change in Minimum Groundwater Head (m)		−1	−1
	Average Change in Groundwater Head (m)		−7	−8
Sindh	Maximum Groundwater Head (m) amsl	5362	5348	5341
	Change in Maximum Groundwater Head (m)		−14	−21
	Minimum Groundwater Head (m) amsl	1574	1573	1573
	Change in Minimum Groundwater Head (m)		−1	−1
	Average Change in Groundwater Head (m)		−7.5	−11
Dudhganga	Maximum Groundwater Head (m) amsl	4624	4611	4608
	Change in Maximum Groundwater Head (m)		−13	−16
	Minimum Groundwater Head (m) amsl	1581	1580	1580
	Change in Minimum Groundwater Head (m)		−1	−1
	Average Change in Groundwater Head (m)		−7	−8.5
Sukh nag	Maximum Groundwater Head (m) amsl	4534	4520	4515
	Change in Maximum		−14	−19

	Groundwater Head (m)			
	Minimum Groundwater Head (m) amsl	1582	1581	1581
	Change in Minimum Groundwater Head (m)		−1	−1
	Average Change in Groundwater Head (m)		−7.5	−10

4.11 Simulation of groundwater model and groundwater behavior for Central Kashmir

Discretization of the groundwater aquifer for the study area is shown in Fig. 4.36(a). Using these future RCPs (4.5 and 8.5), we ran individual simulations to estimate the levels of groundwater heads for each time slice from the baseline scenario.

Groundwater head contour maps and a flow budget are the end results of a MODFLOW (GMS) simulation. Below are contour maps of the simulated groundwater head for each RCP considered. The flow budget shows the sum of all inputs and outputs from the sources and sinks to the groundwater resources.

4.11.1 Groundwater simulation for a present time slice (Baseline)

The simulation for baseline was carried out by giving all the inputs to the model from the aquifer's top and bottom elevation to sources and sinks input data (observed values and computed values). Contour maps of the groundwater head for this time slice show that area in the valley has a water table higher than the areas of the mountain regions (Fig. 4.36(a)). The top layer of the unconfined aquifer groundwater head contour map shows the water table level contour map since the water is under atmospheric pressure. The average water table depth inside the well in the baseline simulation is about 5.1 mbgl.

4.11.2 Groundwater simulation for future under RCP 4.5 scenario (2021-2095)

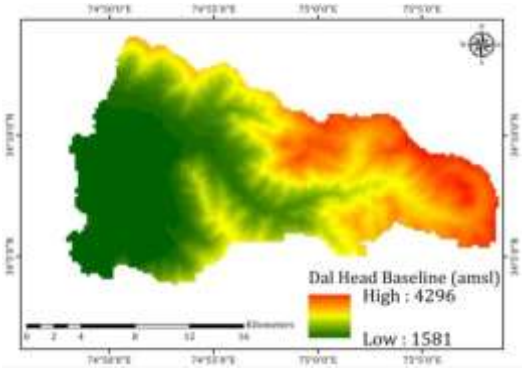

Fig. 4.24(a): Dal catchment groundwater head (m, amsl) during baseline

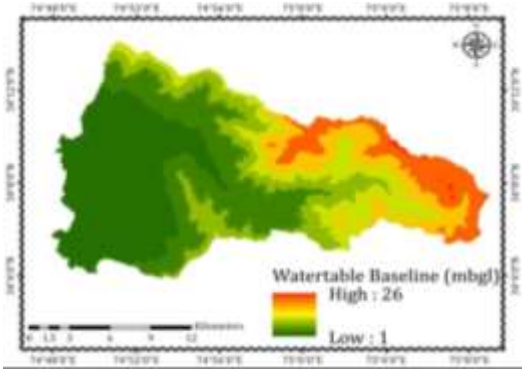

Fig. 4.24(b):Dal catchment watertable depth (mbgl) during baseline

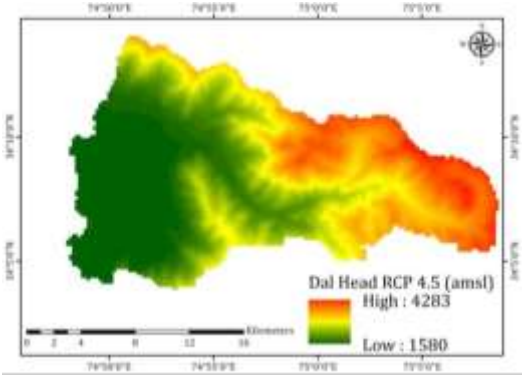

Fig. 4.25(a): Dal catchment groundwater head (m, amsl) during RCP 4.5 scenario

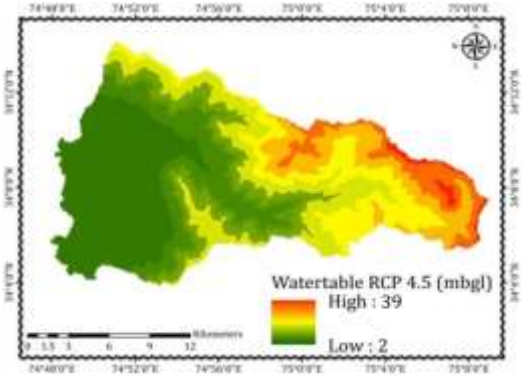

Fig. 4.25(b): Dal catchment watertable depth (mbgl) during RCP 4.5 scenario

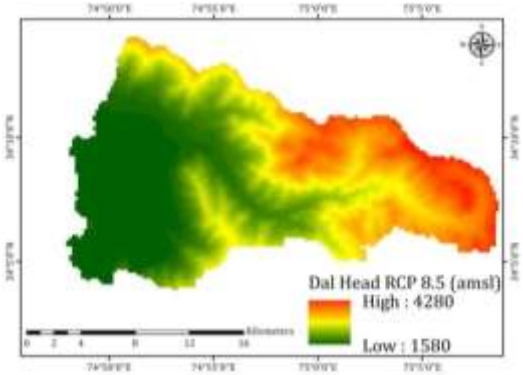

Fig. 4.26(a): Dal catchment groundwater head (m, amsl) during RCP 8.5 scenario

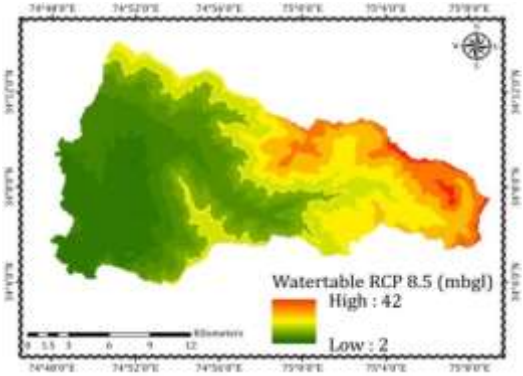

Fig. 4.26(b): Dal catchment watertable depth (mbgl) during RCP 8.5 scenario

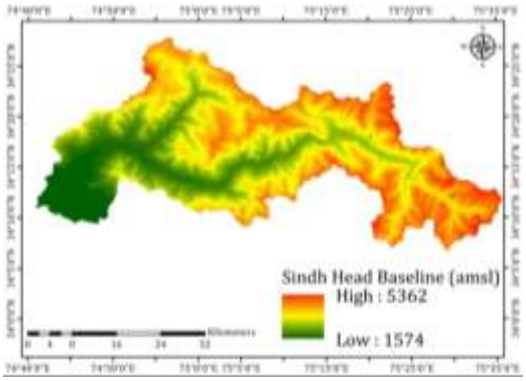

Fig. 4.27(a): Sindh catchment groundwater head (m, amsl) during baseline

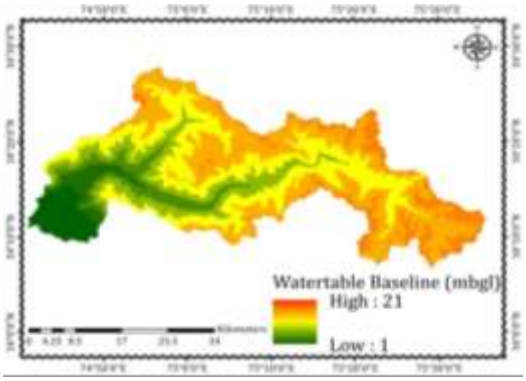

Fig. 4.27(b): Sindh catchment watertable depth (mbgl) during baseline

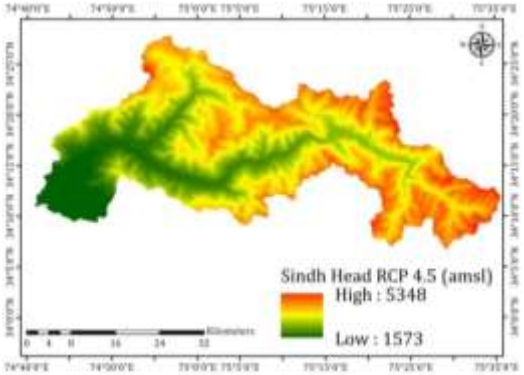

Fig. 4.28(a): Sindh catchment groundwater head (m, amsl) during RCP 4.5 scenario

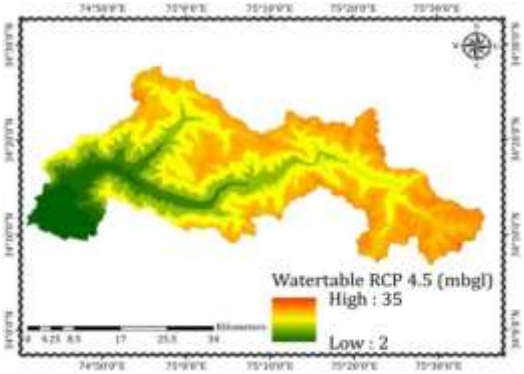

Fig. 4.28(b): Sindh catchment watertable depth (mbgl) during RCP 4.5 scenario

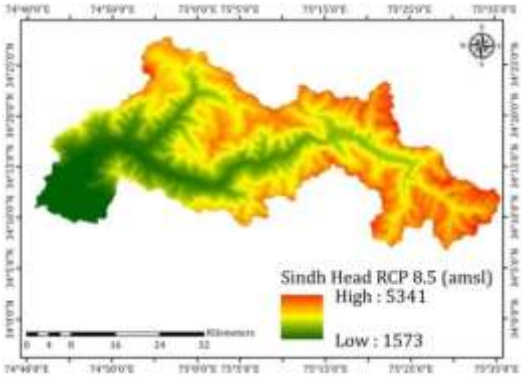

Fig. 4.29(a): Sindh catchment groundwater head (m, amsl) during RCP 8.5 scenario

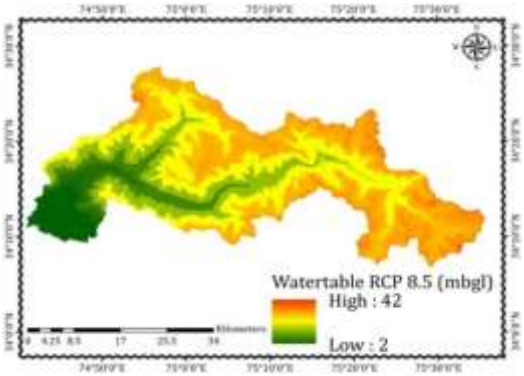

Fig. 4.29(b): Sindh catchment watertable depth (mbgl) during RCP 8.5 scenario

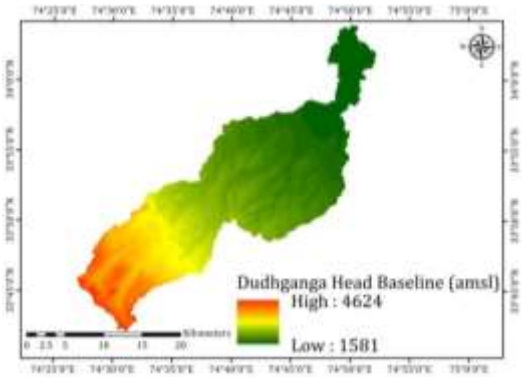

Fig. 4.30(a): Dudhganga catchment groundwater head (m, amsl) during baseline

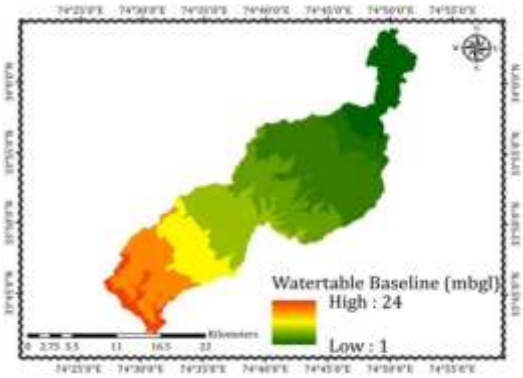

Fig. 4.30(b): Dudhganga catchment watertable depth (mbgl) during baseline

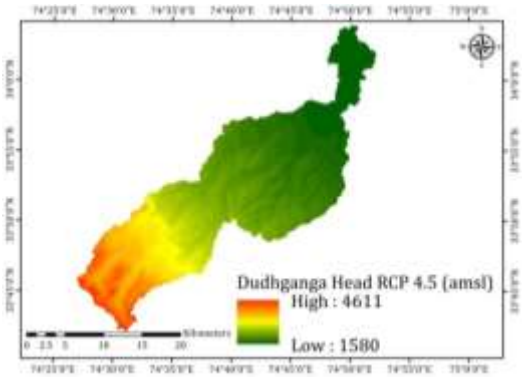

Fig. 4.31(a): Dudhganga catchment groundwater head (m, amsl) during RCP 4.5 scenario

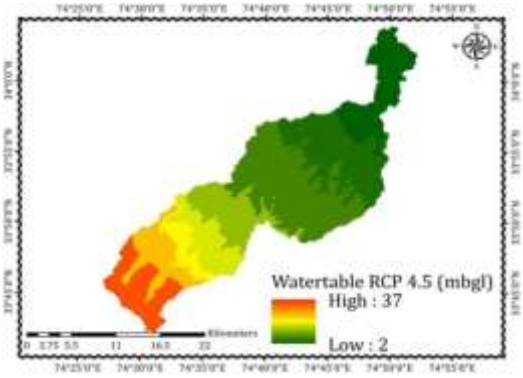

Fig. 4.31(b): Dudhganga catchment watertable depth (mbgl) during RCP 4.5 scenario

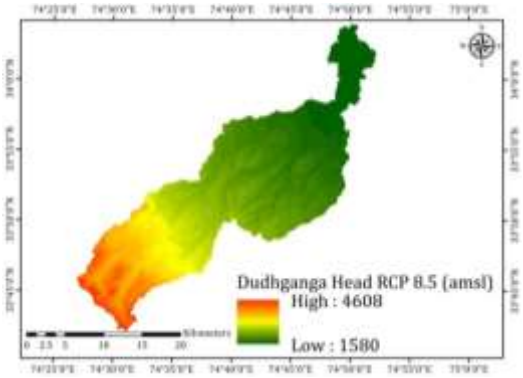

Fig. 4.32(a): Dudhganga catchment groundwater head (m, amsl) during RCP 8.5 scenario

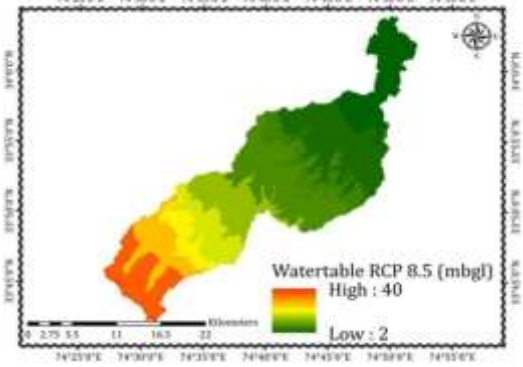

Fig. 4.32(b): Dudhganga catchment watertable depth (mbgl) during RCP 8.5 scenario

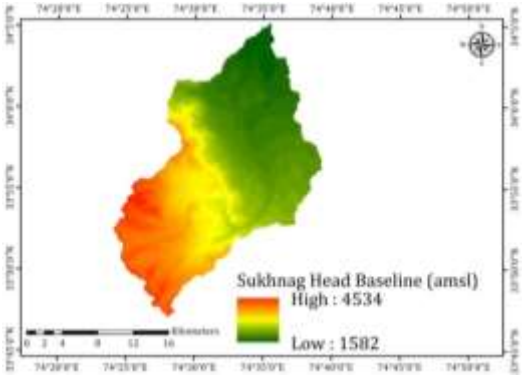

Fig. 4.33(a): Sukhnag catchment groundwater head (m, amsl) during baseline

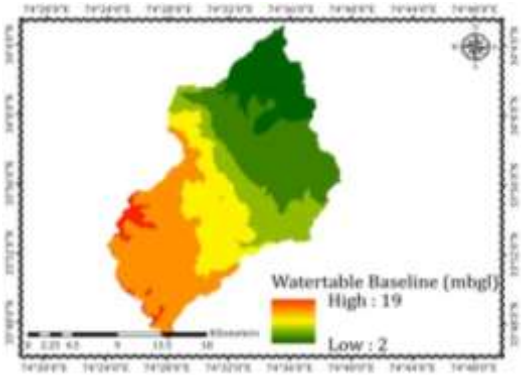

Fig. 4.33(b): Sukhnag catchment watertable depth (mbgl) during baseline

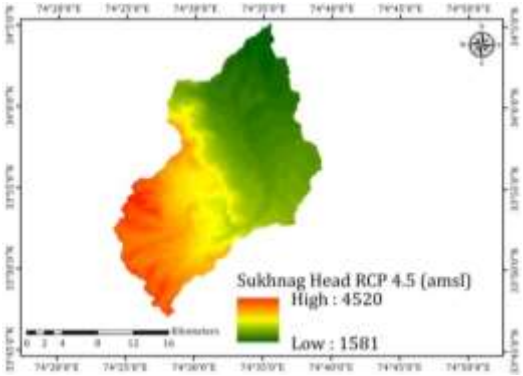

Fig. 4.34(a): Sukhnag catchment groundwater head (m, amsl) during RCP 4.5 scenario

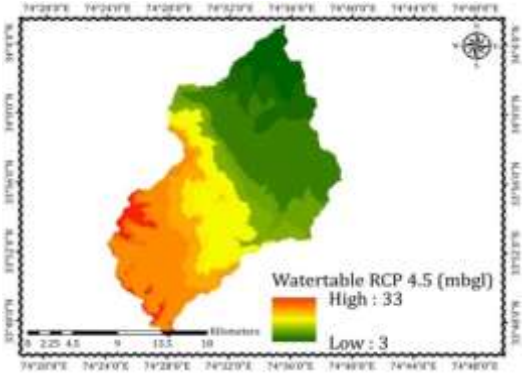

Fig. 4.34(b): Sukhnag catchment watertable depth (mbgl) during RCP 4.5 scenario

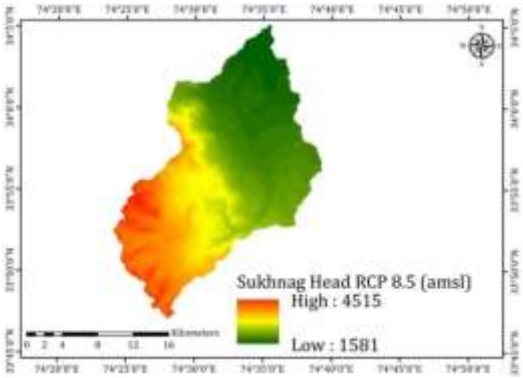

Fig. 4.35(a): Sukhnag catchment groundwater head (m, amsl) during RCP 8.5 scenario

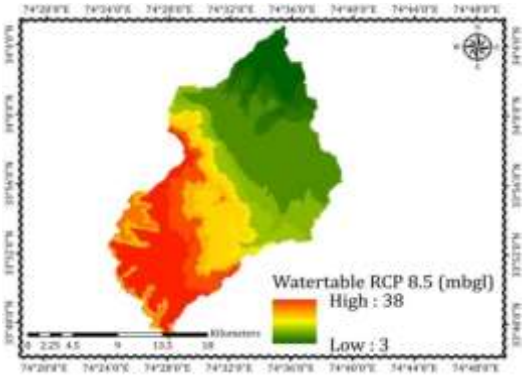

Fig. 4.35(b): Sukhnag catchment watertable depth (mbgl) during RCP 8.5 scenario

Groundwater simulation under RCP 4.5 for Central Kashmir was carried out to keep all the inputs the same except the recharge package. Average recharge was calculated for the future scenario considering RCP 4.5 scenario climate variables (2021-2095). While analyzing the groundwater contour map, it was observed that watertable would fall in the whole of Central Kashmir when compared with the baseline, and the average depth of the water table inside wells would be 5.9 mbgl during RCP 4.5 shown in Fig. 4.36(b).

4.11.3 Groundwater simulation for Central Kashmir under RCP 8.5 (2021-2095)

Groundwater simulation was carried out in the same manner as the simulation for RCP 4.5, keeping all the inputs the same except the recharge package. Average recharge was computed for the RCP 8.5 (2021-2095) based on average precipitation in that time slice. The water table of the unconfined aquifer will further fall in the future under the RCP 8.5 scenario when compared with the Baseline and RCP 4.5 scenario. The average water table level inside wells will be 6.3 mbgl during the RCP 8.5 scenario, as shown in Fig. 4.36(c).

The above data indicate that in simulations for three different time periods, the average annual water table level inside wells would decline by 0.8 mbgl under the RCP 4.5 and 1.2 mbgl under the RCP 8.5 scenario compared to that of the baseline period. The maximum number of wells surveyed and monitored are within the valley part, and the average depth inside the wells was 5.1 mbgl considered the baseline for the study.

4.11.4 Flow budget for Central Kashmir

Hydrological models analyzed the flow budgets under different scenarios. It was observed that recharge would decrease in both the scenarios of RCP 4.5 & 8.5 from all sources and sinks compared with the baseline.

The simulations carried out for different time slices indicated that the total Flow In and total Flow Out during the baseline time slice was computed as 2058635.86 m^3/day and 2058633.55 m^3/day, respectively (Table 4.22), which indicates 2.32 m^3/day is the overall addition of water to the groundwater system from all sources and sinks. Under the RCP 4.5 scenario, total Flow In and Flow Out from all sources and sinks were computed as 2502989.71 m^3/day and 2509989.94 m^3/day, respectively, which indicated -7001.23 m^3/day is the overall extraction from the groundwater system (Table 4.22). Flow budget under the RCP 8.5 scenario concluded that total Flow In and total Flow Out from all sources and sinks were computed as 2883014.95 m^3/day and 2894018.1 m^3/day, respectively, which indicated -11003.15 m^3/day of water is the overall extraction (depletion) from the groundwater system (Table. 4.22).

Table 4.22: Flow budgeting of Central Kashmir under different scenarios

Flow Budget	Baseline scenario	RCP 4.5 scenario	RCP 8.5 scenario
Budget Term	Flow (m^3/day)		
Flow-IN			
River leakage	78311.13	68164.08	58617.21
Recharge	1980324.74	2434825.63	2824397.74
Total IN	2058635.86	2502989.71	2883014.95
Flow-OUT			
Constant Head	210922.79	239942.37	258290.35
Wells	18155.00	18155.00	18155.00
River Leakage	1829555.75	2251893.57	2617572.75
Total OUT	2058633.55	2509989.94	2894018.1
Summary			
IN-OUT	2.32	-7001.23	-11003.15

4.12 Spring Discharge Measurement

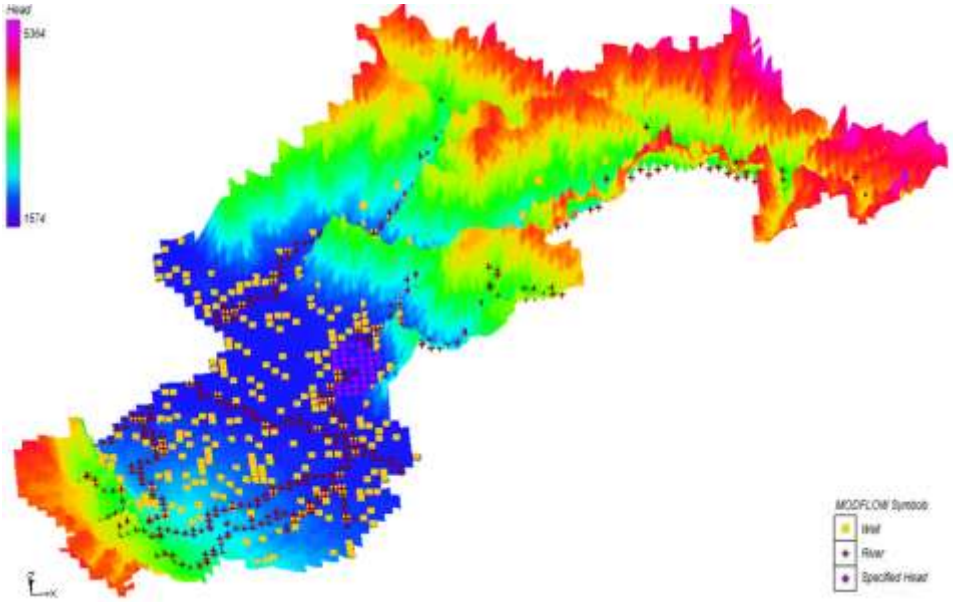

Fig. 4.36(a): Groundwater head (m, amsl)) of Central Kashmir during baseline time period

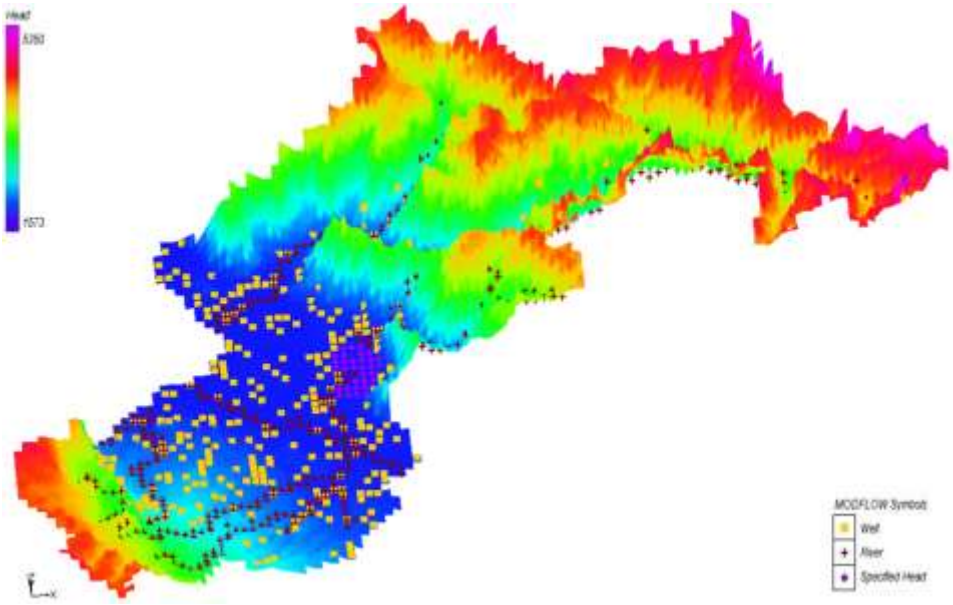

Fig. 4.36(b): Groundwater head (m, amsl) of Central Kashmir during RCP 4.5 scenario

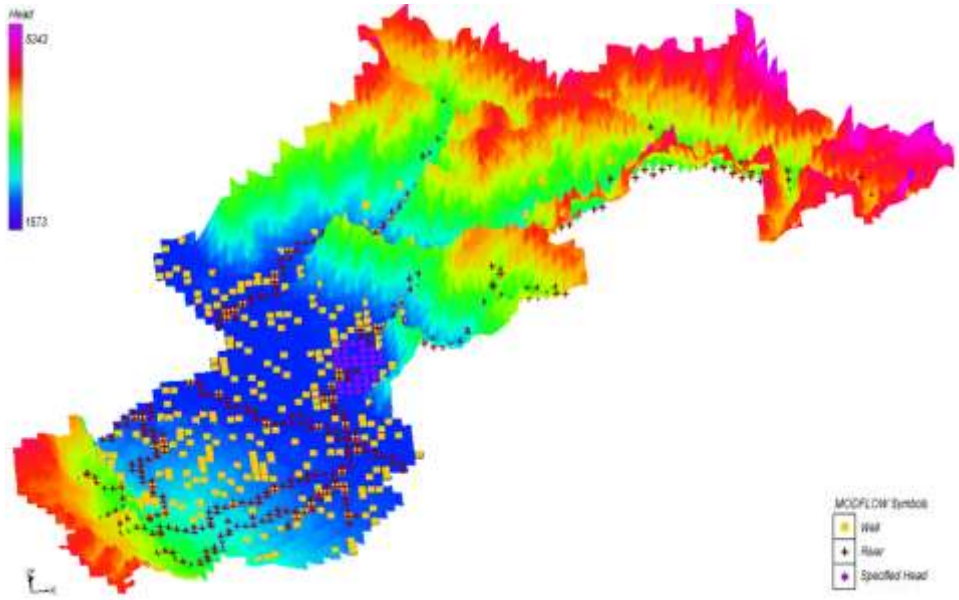

Fig. 4.36(c): Groundwater head (m, amsl) of Central Kashmir during RCP 8.5 scenario

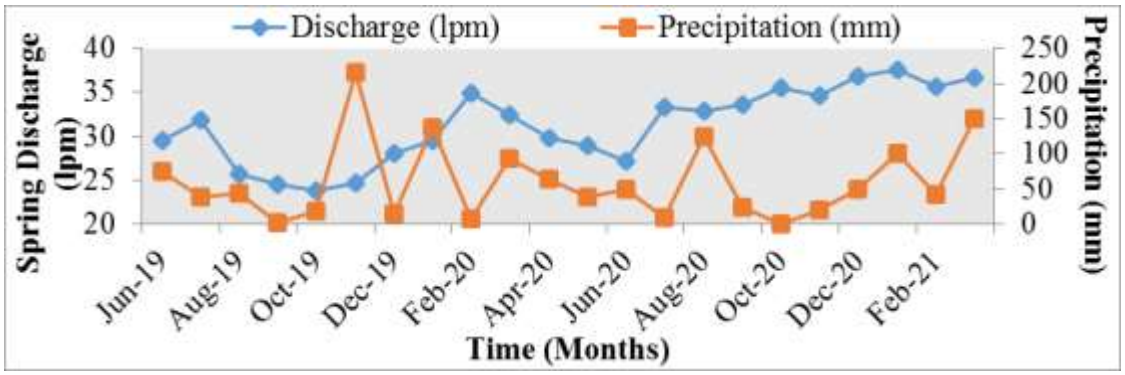

Fig. 4.37(a): Discharge of Budgam-I spring and cumulative precipitation for different months in Budgam town

In the study area, all the springs selected for discharge measurement had a pipe outlet whose discharge was measured using the container and stopwatch. Selected springs in Budgam showed significant seasonal variation in discharge, which ranged from 23.76 lpm (October) to 37.57 lpm (January) in Budgam-I spring and 2.98 lpm (October) to 5.57 lpm (July) in Budgam-II spring. The positive discharge trend has been observed in Budgam-I spring during the reporting period from June 2019-March 2021, which means discharge from the spring increased significantly. This spring being managed by the local committee and less change in LU/LC around the spring periphery, which acts as a recharge area, is the main reason behind the increased spring outflow. No trend has been observed in Budgam-II spring discharge since the periphery area has shown significant LU/LC change in the past decade, and significant transformation has been seen in agriculture and barren land to built-up and settlements. The lag has also been observed in spring discharge. The monthly spring discharge values of Budgam-I and Budgam-II springs from June 2019 to March 2021, and July 2019 to March 2021 are given in table 4.23 and figures 4.37(a) and 4.37(b).

The discharge of the SKUAST spring had considerably decreased during the reporting period, and a significant seasonal variation was also observed. The minimum and maximum discharge measured from the spring were 2.11 lpm during December and 6.43 lpm during May. The LU/LC of the periphery recharge area had been considerably transformed from the agriculture, horticulture, and fallow land to built-up and settlements class. The average measured discharge values during the reporting period (October 2019-March 2021) are given and shown in table 4.24 and figure 4.37(c).

The spring in Khag village also showed a significant seasonal variation, and the discharge varied from 9.64 lpm (September) to 14.65 lpm (March). Overall no trend has been demonstrated during the monitoring period. The spring responds promptly to weather events less lag than other selected springs in Central Kashmir. The LU/LC of the periphery recharge also changed in the past decade,

and a significant transformation was seen in agriculture and barren land to built-up/settlements and horticulture. Although the spring was managed with a propped water harvesting tank, the discharge does not show any trend, although a constant trend was followed due to the region's change in LU/LC. The monthly average discharge values from September 2019 to March 2021 are given in table 4.25 and figure 4.37(d).

One more spring in the Dal catchment in Chatterhama village also showed significant seasonal variation in discharge, and readings were taken every quarter. The spring discharge variation ranged from 31.31 lpm (quarter 4) to 41.94 lpm (quarter 2). The LU/LC periphery, which acts as the recharge area, is also transformed to a large extent. A significant change has been observed in agriculture and barren to built-up/settlement and horticulture. Table 4.26 and figure 4.37(e) show the average discharge values.

Table 4.23: Discharge of springs for different months in Budgam town

	Budgam-I Spring (Shah Nag)		**Budgam-II Spring**	
Month-Year	Discharge (lpm)	Precipitation (mm)	Discharge (lpm)	Precipitation (mm)
Jun-19	29.57	75	NA	NA
Jul-19	31.87	38	5.57	38
Aug-19	25.67	44	4.94	44
Sep-19	24.45	2	3.66	2
Oct-19	23.76	19	2.98	19
Nov-19	24.67	215	3.45	215
Dec-19	27.99	15	3.58	15
Jan-20	29.54	137	4.14	137
Feb-20	34.97	7	4.39	7
Mar-20	32.46	94	4.88	94

Apr-20	29.86	64	4.93	64
May-20	28.85	39	5.33	39
Jun-20	27.15	49	5.15	49
Jul-20	33.32	10	4.95	10
Aug-20	32.86	124	3.74	124
Sep-20	33.58	23	3.27	23
Oct-20	35.53	0	3.89	0
Nov-20	34.59	21	3.79	21
Dec-20	36.75	49	4.15	49
Jan-21	37.57	101	4.20	101
Feb-21	35.67	41	5.33	41
Mar-21	36.65	150	5.45	150

Table 4.24: Discharge of spring for different months in SKUAST Shalimar

Month-Year	Discharge (lpm)	Precipitation (mm)
Oct-19	11.86	31
Nov-19	6.18	232
Dec-19	5.53	17
Jan-20	4.39	31
Feb-20	4.27	0
Mar-20	5.53	139
Apr-20	7.64	146
May-20	6.43	80
Jun-20	5.98	61
Jul-20	5.26	20
Aug-20	4.46	125

Sep-20	3.75	70
Oct-20	2.48	0
Nov-20	2.56	36
Dec-20	2.11	61
Jan-21	3.94	102
Feb-21	4.76	32
Mar-21	4.88	141

Table 4.25: Discharge of spring for different months in Khag village

Month-Year	Discharge (lpm)	Precipitation (mm)
Sep-19	9.96	2
Oct-19	12.99	19
Nov-19	13.53	215
Dec-19	12.64	15
Jan-20	12.95	137
Feb-20	13.99	7
Mar-20	14.65	94
Apr-20	13.76	64
May-20	11.76	39
Jun-20	13.16	49
Jul-20	12.93	10
Aug-20	10.08	124
Sep-20	9.65	23
Oct-20	11.61	0
Nov-20	12.71	21
Dec-20	12.45	49

Jan-21	12.75	101
Feb-21	13.02	41
Mar-21	14.02	150

Table 4.26: Discharge of spring for different months in Chatterhama village

Quarter-Year	Discharge (lpm)	Precipitation (mm)
Jul-Sep (Quar-3) 2019	38.61	84
Oct-Dec (Quar-4) 2019	32.75	249
Jan-Mar (Quar-1) 2020	39.22	238
Apr-Jun (Quar-2) 2020	41.94	152
Jul-Sep (Quar-3) 2020	36.02	157
Oct-Dec (Quar-4) 2020	31.31	70
Jan-Mar (Quar-1) 2021	37.59	292

4.13 Effects of changing environment on springshed hydrology

Environmental changes like climate change and the LULC change are linked with springshed hydrology. The future climate scenarios generated show a significant change in the future, and with the result of this change, the hydrology of the springheds will affect. Similarly, a change in LULC also results in a change in springhseds hydrology. Some of the major findings are discussed in the subsequent part of this section.

The LU/LC change matrix in the last 18 years (2000-2017) significantly changed in Central Kashmir. The maximum negative change was seen in Forest (07.30%), and the maximum positive change was seen in Horticulture/Plantation with 5.15%. This change has resulted in the spring flow behavior in the study region. During the reporting period, a few selected springs where LULC has changed significantly resulted in a drastic reduction in spring discharge. The discharge from the untreated springs decreases continuously because of the rapid

change in LU/LC and the climatic variability. Seasonal variation of spring flow discharge is prevalent in the area, and few of the springs were found dried during the spring survey.

Results showed that the average spring discharge from treated and managed springs was almost constant throughout the recording period. Some of the springs and wells increased the discharge mainly due to the constructed water harvesting and recharging structures and fewer LULC changes in the nearby peripheral areas. Few springs respond to the rainfall in a few hours to days, resulting in a significant increase in spring flow. The reason may be the recharging of the nearby peripheral area due to infiltrated rainfall and then appearing as a baseflow from the spring.

From the results, it has been inferred that the study area is mostly dominated by low GWRP comprising 30% of the total area, followed by high GWRP comprising 22%, medium GWRP comprising 21%, very low GWRP comprising 17%, and very high GWRP comprising of 10% of the total area, respectively. In the case of rainwater harvesting suitability level (WHSL) study area is mainly dominated by medium water harvesting suitability level comprising 31% of the total area, followed by low WHSL comprising 28%, high WHSL comprising 23%, and very high WHSL comprising of 18% of the total area, respectively.

Identification of GWRP & WHSL in the area can efficiently minimize the time, labor, and money, thereby enabling quick decision-making for sustainable water resources management, especially spring rejuvenation, to ensure water security in Central Kashmir.

The findings of the study demonstrate the powerful capabilities of GIS in handling digital data to select the optimum sites for groundwater and rain/snow water harvesting. Such a zonation assumes importance in planning strategies to manage water resources effectively.

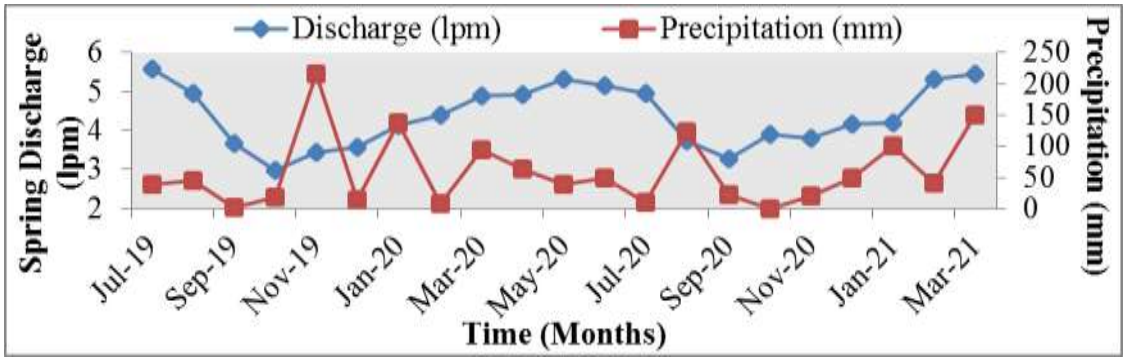

Fig. 4.37(b): Discharge of Budgam-II spring and cumulative precipitation for different months in Budgam town

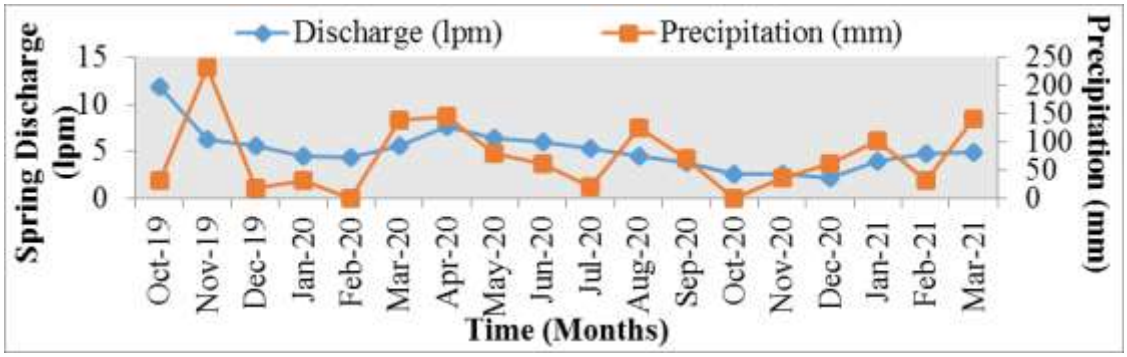

Fig. 4.37(c): Discharge of SKUAST Shalimar spring and cumulative precipitation for different months

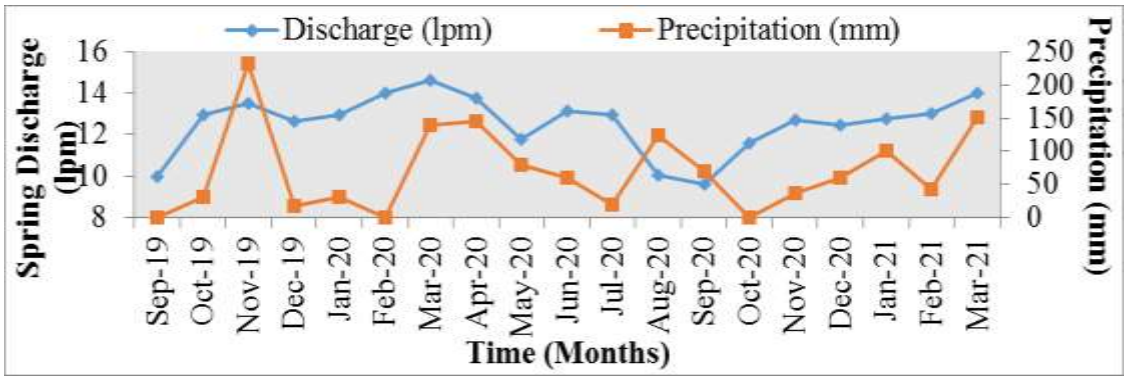

Fig. 4.37(d): Discharge of Khag spring and cumulative precipitation for different months

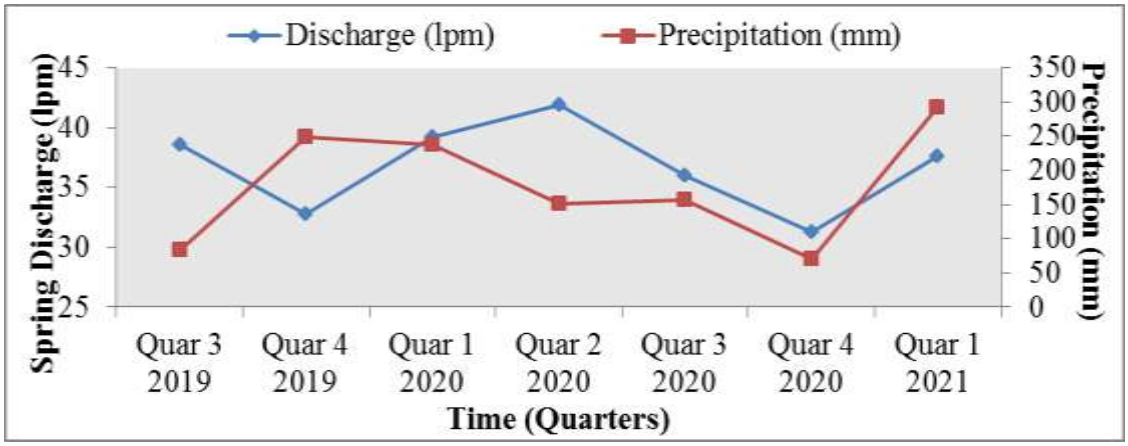

Fig. 4.37(e): Discharge of Chatterhama spring and cumulative precipitation for different months

Chapter-5

DISCUSSION

The dissection of the results gathered, unearthing the reasoning behind and comparative analysis with the literature cited forms an essential part of any research activity. The study provides a generalized framework for assessing the effect of environmental change on springshed hydrology in Central Kashmir Valley. The varying aquifer layer property and climate conditions consisted of linking the outputs of the climate model to the integrated catchment modelling (surface and groundwater modeling) using various softwares like SWAT, SWAT-MODFLOW, GMS, etc.

5.1 Climate change prediction

In many earlier studies (Aggarwal and Mall, 2002; Mall *et al.,* 2006), the future climate was predicted in relation to the modeled climate data of baseline (1961-1990) without considering the observed data. In comparison, the present study considers the observed/station data. The projected time trends for the future showed an increase in T_{max}, $T_{min,}$ and precipitation under the RCP 4.5 and 8.5 scenarios for both stations. The mean temperature would increase in all the three-time slices (NF, MF, and FF) of the future under both the scenarios and for both the stations of AMFU and IMD compared to the baseline period. The precipitation would increase continuously for the AMFU Shalimar under both scenarios. For the IMD Srinagar station, precipitation would decrease in the near future and then increase through MF and EF. These findings are consistent with those by Kumar *et al.,* (2011), who used PRECIS to project warming and an upsurge in rainfall for India by the end of the 21st century under the A1B scenario, and with those by Chaturvedi *et al.,* (2012) who used multi-model outputs for climate projections to show that the states of Rajasthan, Madhya Pradesh, Uttar Pradesh, Uttaranchal, Himachal, Delhi, Punjab, and Haryana are expected to experience high temperatures. According to the PRECIS climate model, the Indo-Gangetic plains

may expect an increase in average temperatures of 0.5 -1 ^{o}C during the MC and 3.5-4.5 ^{o}C by the end of the century, as well as an increase in the frequency of extremely severe temperatures and wet, rainy weather seasons. Crop harvests would be cut short due to the higher temperatures (Jalota *et al.,* 2012; Kaur *et al.,* 2012). The research also found that under SRES A2 and B2 scenarios, average annual temperature and precipitation will rise in all three time slices in the future (Ali *et al.,* 2021).

5.2 Hydrogeological investigation of the study area

In environmental, hydrogeological, and engineering applications, the electrical resistivity approach has emerged as a viable tool among the many geophysical methods (Vandam and Meulankamp, 1967; Loke and Barker, 1996). 1D sounding with the typical four-probe resistivity meter was used to determine the hydrogeological investigation of the region. The preliminary interpretation of the VES curves was carried out by the curve matching technique (Orellena and Moony 1966) and INTERPEX 1D software (Babachev, 2003).

The resistivity survey results were analyzed and interpreted to delineate the geoelectric sections of the study area. Five to six different layers were delineated from the resistivity survey at each VES point. The underlying layer shows a sharp increase in resistivity, indicating that it has different geoelectrical properties from the preceding layers. All the investigated locations were appropriate for the installation of wells and suitable for recharging groundwater systems where spring discharge is decreasing. A similar study was undertaken by (Bhatnagar *et al.,* 2022), who determined that the VES approach is quite significant in the field of groundwater prospecting and engineering studies in the Rajouri district of J&K. Based on the criteria, nine VES sites were identified as suitable for the installation of a tube well for irrigation and household uses.

5.3 Groundwater recharging potential and rainwater harvesting suitability with a GIS approach

In recent years, the combination of multi-criteria decision approach, GIS application, and remote sensing has earned significant credibility and surpassed the conventional map overlay. In addition, the suitability model framework, which has adopted the analytical hierarchy process, is one of the spatial decision support systems that can be integrated into a GIS environment using multi-criteria evaluation from expert knowledge, including indigenous knowledge, to produce a decision approach (Malczewski, 2004; Munyao, 2010; Mbilinyi *et al.*, 2007). The RWHS map of the study region was generated by combining the thematic maps, as seen in figure 4.14(a). This map represents clear zones that satisfy all of the established criteria for suitability, as shown in figure 4.14(a,b). Medium potential RWHS level (35.38%) dominates the research region, followed by high, low, and very high suitability levels.

The groundwater recharge prospects are categorized into five zones: very high, high, medium, low, and very low. Low potential areas covered the maximum (30.34%), high potential (21.56%), followed by medium, very low, and very high recharge potential, which are presented in Figures 4.12 and 4.13.

5.4 Streamflow behavior of the Central Kashmir

Streamflow was simulated using the SWAT model for Central Kashmir, and the model performed better during calibration, with R^2 values ranging from 0.56 to 0.97 for the various catchments. During the validation of the model, R^2 ranged from 0.58 to 0.97 for the various catchments of the area. In the prediction of streamflow under all the scenarios of RCP, the average streamflow increased for the Dal catchment in both scenarios. In contrast, other catchments showed decreased flow under RCP 4.5 and increased flow under the RCP 8.5 scenario. Predicted streamflow increase from current levels, mostly due to an increase in precipitation in the future for the Dal catchment, as AMFU Shalimar showed

increased precipitation under both scenarios of RCP. Another catchment's considered the IMD Srinagar station data resulted in decreased streamflow in the future due to reduced precipitation under both scenarios. Some studies pertain to the increased streamflow using the SWAT model (Fentaw *et al.,* 2018) when precipitation increases. Shafi *et al.,* 2020 concluded that increased precipitation led to an increase in discharge in the Leh watershed under the RCP 4.5 and 8.5 scenarios.

Due to the constant land use and soil type, the geographical distribution of runoff will remain the same in all climatic scenarios; however, the strength of runoff will vary due to the variable precipitation across the period. The geographical distribution of annual runoff for various climatic scenarios, which depicts the highest flow in the sub-basin, is mostly due to the absence of adequate agricultural cover and steep gradient. Few sub-basins had the lowest yearly runoff, perhaps due to the solid agricultural cover and moderate slope in most sub-basins (Gull *et al.,* 2017).

5.5 Groundwater behaviors of the Central Kashmir

Estimating the groundwater Flow Budget in response to climate change is crucial for the future management of water resources. Physical-based models have been used by various researchers (Ficklin, 2010; Querner *et al.,* 1997; Allen *et al.*, 2004; Jyrkama and Sykes, 2007; Scibek *et al.*, 2006; Scibek and Allen, 2006, 2006a). However, assigning boundary conditions is difficult in these models, they do not account for changed CO_2 concentration as a result of climate change. In this study, the effects of environmental changes were simulated using a calibrated and validated model for assessing the impact of local environmental change using different statistical techniques and other models used in the GIS domain for the study area.

In many previous studies, a steady-state groundwater model has been used to simulate the effect of climate change on groundwater (Allen *et al.,* 2004;

Woldeamlak *et al.*, 2007), whereas a few (e.g., aforementioned publications by Scibek) run transient simulations. The simulations through the customized groundwater model presented here indicate fluctuation trends in groundwater level in each RCP used for the study. Although there is an overall groundwater extraction during both scenarios, RCP 8.5 discharge is higher than RCP 4.5 compared with baseline. The flow budget for the baseline time period reveals a nearly equilibrium phase in which the quantity of water discharged is comparable to the amount replenished. The drop and declining trend in groundwater levels are ascribed to decreased direct infiltration by rainfall due to changes in LU/LC, leading to reduced groundwater recharge during both scenarios.

The groundwater prediction results should be viewed as trends, not as exact quantitative predictions of hydrological changes (Kaur, 2013). The models were calibrated using present circumstances, therefore, natural or anthropogenic changes in the future groundwater scenario might influence the predictions (Brar *et al.*, 2016). Land-use change may affect overexploitation (Yang *et al.*, 2006). Future greenhouse gas emissions, the GCM employed, and the statistical downscaling performed on the GCM all contribute to the range of uncertainty. The groundwater model parameters were calibrated against uncertain observation data. Model structure, such as the process description applied and the distribution of inputs and parameters, is associated with errors (Kaur, 2013). The current research simply indicates significant change; exact values may not be possible.

5.6 Suggestive conservation measures

In hard rock situations, injection wells are the best choice. Tube well-like construction pumps treated surface water under pressure into an aquifer to augment the groundwater storage capacity (Bhattacharya, 2010). To reduce soil erosion and control runoff, a bench terrace consists of a ridge of earth built over a slope. It involves creating a sequence of flat or almost flat strips or steps over a steep slope. All erosion problems are eliminated since the original slope is turned

into level fields. When runoff water sits on terraces for a lengthy period of time, it increases the amount of water that may permeate into the soil (Bhattacharya, 2010). A large expanse of very permeable ground is submerged under a layer of artificially produced surface water in a percolation tank. The groundwater reserve is refilled by allowing surface runoff to percolate (Mukherjee, 2016). Using contour bunds, slope length decreases, impounds water, and increases runoff seepage to permeate the soil better (Srivastava *et al.*, 2010). Forests have been described as sponges that collect precipitation and gently release it to keep streams and aquifers replenished when the weather is dry (Ilstedt *et al.*, 2016). The macropores in the soil are a network of interconnected channels created by living and decomposing roots. For example, a flow via these macropores may be several hundred times quicker than through the soil matrix (Aubertin, 1971; Chandler and Chappel, 2008). In addition to reducing runoff velocity and preventing it from scoring, the contour trenches shorten the slope. The rainfall collected in the trenches progressively seeps into the soil, increasing the level of recharge (Srivastava *et al.*, 2010).

Chapter-6

SUMMARY AND CONCLUSION

The effect of changing environment on water resources and especially in springshed areas is a complicated process. It would depend on surface and groundwater systems, their geographical location, and changes in hydrological variables. In the Central Kashmir of the Jhelum sub-basin of the Indus basin, the dominant LU/LC is forest followed by snow/glacier in the analyzed time periods. The climate is Temperate cum Mediterranean type. Over the last 30+ years, the average annual T_{max}, $T_{min,}$ and precipitation are 20.02, 7.39 ^{o}C, and 779 mm. Springshed behavior in the future is expected to be changed with a changing environment. Therefore, there is a need to continuously monitor and predict the variability of springshed under changing climate conditions and land use conditions for its proper management.

This study selected and screened five GCM model data while comparing their RMSE value with observed data. HadGEM was the better performing model with RMSE values close to the observed data and was further used for sectoral impacts. The same time period data from 2010 to 2019 HadGEM GCM data was corrected using two simple methods modified difference approach and the linear scaling method. Here, the linear scaling method performed better in correcting the modelled values with RMSE values near the observed one. The correction functions derived using the linear scaling method were used for further investigation in the generation of future scenarios for the two RCP, namely 4.5 and 8.5 scenarios. The developed scenarios were divided into three-time slices in the future viz, near future (NF), mid future (MF), and far future (FF). All these time slices were compared with baseline/observed/station time period for further analysis and inputs to the catchment modelling.

Springsheds with different aquifer characteristics and environmental conditions have been modelled using an integrated framework for hydrogeological

assessment and climate change assessment. Integrated catchment modelling and time series analysis are used in the framework to create model units for the research region based on the available thematic maps like LISS III, ASTER DEM, soil, land use land cover used, and other required information in the GIS environment. Many government agencies provided the required data for integrated catchment modeling and prediction purposes; certain parameters were computed using needed algorithms and equations. For each of the four-time slices (baseline, NF, MF, and FF), a conceptual model was built on the GIS boundary map of the research region, and the necessary inputs, such as packages and layer attributes, were provided.

The framework was used to identify the effects of changing environment on springshed hydrology of Central Kashmir valley. The specific conclusions in the context of changing environment n springshed hydrology are:

1. The climate projections for Agricultural Meteorological Field Unit (AMFU) Shalimar station during the 21st century under the RCP 4.5 scenario using the linear scaling (LS) method indicated that mean annual temperature would increase by 2.71 ^{o}C in NF, 3.19 ^{o}C in MF, and 4.45 ^{o}C in FF.

2. The precipitation under the RCP 4.5 scenario would increase by 317.08 mm (38.45%) during NF, 235.95 mm (28.62%) during MF, and 231.37 mm (28.06%) during FF.

3. The RCP 8.5 scenario model corrected data using the LS method for the AMFU Shalimar showed the average annual temperature would increase by 3.05 ^{o}C in NF, 4.96 ^{o}C in MF, and 6.91 ^{o}C in FF.

4. Under the RCP 8.5 scenario, the precipitation would increase by 389.93 mm (47.29%) during NF, 347.87 mm (42.19%) during MF, and 340.59 mm (41.30%) during FF.

5. The climate projections for the IMD, Srinagar station, under the RCP

4.5 scenario indicated that the average annual temperature would increase by 1.79 ^{o}C in NF, 2.89 ^{o}C in MF, and 3.09 ^{o}C in FF.

6. The precipitation under the RCP 4.5 scenario would decrease by -24.56 mm (-03.34%) during NF, increase by 29.25 mm (03.98%) during MF, and 22.18 mm (03.02%) during FF.

7. Under the RCP 8.5 scenario model corrected data for the IMD, the average annual temperature in Srinagar station would increase by 2.06 ^{o}C in NF, 3.71 ^{o}C in MF, and 5.72 ^{o}C in FF.

8. The precipitation would decrease by -09.95 mm (-01.35%) during NF and then increase by 94.92 mm (12.93%) during MF and 215.98 mm (29.42%) during FF under RCP 8.5 scenario.

9. The average annual streamflow would increase by 135% (RCP 4.5) and 532% (RCP 8.5) in the Dal catchment.

10. The change in maximum groundwater head would be -13 m (RCP 4.5) and -16 m (RCP 8.5), and the change in minimum groundwater head would be -1 m under both scenarios in the Dal Catchment.

11. The average groundwater table drop/decline in the Dal Catchment would be -7 m and -8 m under RCP 4.5 and 8.5, respectively.

12. For the Sindh catchment, the average annual streamflow would decrease by -13% (RCP 4.5) and increase by about 6% (RCP 8.5).

13. The change in maximum groundwater head would be -14 m during RCP 4.5 and -21 m during RCP 8.5, and the change in minimum groundwater head would be -1 m under both scenarios of RCP in the Sindh Catchment.

14. The average groundwater table drop/decline in the Sindh Catchment would be -7.5 m and -11 m under RCP 4.5 and 8.5, respectively.

15. The average annual streamflow of the Dudhganga catchment would

decrease by -20% (RCP 4.5) and increase by 32% (RCP 8.5).

16. The change in maximum groundwater head in the Dudhganga catchment would be -13 m (RCP 4.5) and -16 m (RCP 8.5), and the minimum groundwater head would change by -1 m under both scenarios.

17. The average Groundwater table drop/decline in the Dudhganga Catchment would be -7 m and -8.5 m under RCP 4.5 and RCP 8.5, respectively.

18. In Sukhnag Catchment, the average annual streamflow would decrease by -17% during RCP 4.5 and increase by 16% during the RCP 8.5 scenario.

19. The maximum groundwater head would change by -14 m (RCP 4.5) and -19 m (RCP 8.5), and the change in minimum groundwater head would be -1 m under both scenarios in the Sukhnag Catchment.

20. The average groundwater table drop/decline in the Sukhnag Catchment would be -7.5 m and -10 m under RCP 4.5 and RCP 8.5, respectively.

21. The maximum negative change in LU/LC was seen in Forest (07.30%), and the maximum positive change was seen in Horticulture/Plantation with 5.15%.

22. From the results, it has been inferred that the study area is mostly dominated by low GWRP comprising 30% of the total area, followed by high GWRP comprising 22%, medium GWRP comprising 21%, very low GWRP comprising 17%, and very high GWRP comprising of 10% of the total area.

23. In the case of rainwater harvesting suitability level (WHSL) study area is mainly dominated by medium water harvesting suitability

level comprising 31% of the total area, followed by low WHSL comprising 28%, high WHSL comprising 23%, and very high WHSL comprising 18% of the entire area.

24. Results showed that the average discharge from treated and managed springs in the study area was almost constant throughout the recording period. Some of the springs and wells showed an increase in flow mainly due to the constructed water harvesting structures and fewer LULC changes in the nearby areas.

25. Seasonal variation in spring discharge was also observed in the maximum of the springs under consideration, and few of the springs were found dry during the spring survey.

26. Maximum springs respond to the rainfall in a few hours to days, resulting in a significant increase in spring flow. The reason may be the local area rainfall infiltration and then appear as baseflow from the spring.

27. Discharge from the untreated springs decreases continuously because of the rapid change in LU/LC and the climatic variability.

28. The study also showed a decline in the groundwater table, which will further affect the spring flow in the future.

29. The study showed how GIS could leverage digital data to choose groundwater and rain/snow water harvesting sites. A zonation helps manage water resources, especially springs in the studied region.

30. Identification of GWRP & WHSL in the area can efficiently minimize the time, labor, and money and thereby enables quick decision-making for sustainable water resources management, especially spring rejuvenation, to ensure water security in the water-scarce areas of the Central Kashmir Himalayas.

LITERATURE CITED

Abbaspour, K. C. 2015. SWAT Calibration and Uncertainty programs-a User Manual (SWAT-CUP 2012), *Eawag (Swiss Federal Institute of Aquatic Science and Technology), Zurich, Switzerland.*

Aubertin, G. M. 1971. Nature and extent of macropores in forest soils and their influence on subsurface water movement, *Northeastern Forest Experiment Station, USDA Forest Service* 192.

Aggarwal, P. K. and Mall, R. K. 2002. Climate change and rice yields in diverse agro-environments of India. II. Effect of uncertainties in scenarios and crop models on impact assessment. *Climatic Change* **52**(3): 331-343.

Agarwal, A., Bhatnaga, N. K., Nema, R. K. and Agrawal, N. K. 2012. Rainfall dependence of springs in the Midwestern Himalayan Hills of Uttarakhand. *Mountain Research and Development* **32**(4): 446-455.

Ahmed, I. and Umar, R. 2009. Groundwater flow modeling of Yamuna-Krishni interstream, a part of central Ganga Plain Uttar Pradesh. *Journal of Earth System Science* **118**(5):507-523.

Ahmad, S., Kalra, A. and Stephen, H. 2010. Estimating soil moisture using remote sensing data: A machine learning approach. *Advances in water resources* **33**(1): 69-80.

Ali, S. R. and Khan, J. N. 2021. Climate predictions for central Kashmir of great Himalayas under different emission scenarios of IPCC. *Mausam* **72**(2): 323-330.

Allen, D. M., Mackie, D. C. and Wei, M. 2004. Groundwater and climate change: a sensitivity analysis for the Grand Forks aquifer, southern British Columbia, Canada. *Hydrogeology Journal* **12**(3): 270-290.

Allen, D. M. 2010. Historical trends and future projections of groundwater levels and recharge in costal British Columbia, Canada. *Azores, Portugal SWIM* 21-26.

Al-Adamat, R., Diabat, A. and Shatnawi, G. 2010. Combining GIS with multicriteria decision making for siting water harvesting ponds in Northern Jordan. *Journal of Arid Environments 74*(11): 1471-1477.

Alam, F. and Umar, R. 2013. Groundwater flow modelling of Hindon-Yamuna interfluve region, Western Uttar Pradesh. *Journal of the Geological Society of India* **82**(1): 80-90.

Alford, D. 1992. Streamflow and sediment transport from mountain watersheds of the Chao Phraya Basin, northern Thailand: A reconnaissance study. *Mountain Research and Development* **12**(3): 257-268.

Andreasson, J., Bergstrom, S., Carlsson, B., Graham, L.P. and Lindstrom, G. 2004. Hydrological change-Climate change impact simulation for Sweden. *AMBIO: A Journal of the Human Environment* **33**(4): 228-234.

Arnold, J. G., Srinivasan, R., Muttiah, R. S. and Williams, J. R. 1998. Large-area hydrologic modeling and assessment: Part I. Model development. *Journal of the American Water Resources Association* **34**(1): 73-89.

Arnold, J. G., Muttiah, R. S., Srinivasan, R. and Allen, P. M. 2000. Regional estimation of base flow and groundwater recharge in the upper Mississippi basin. *Journal of Hydrology* **227**(1-4): 21-40.

Arnold, J. G., Potter, K. N., King, K. W. and Allen, P. M. 2005. Estimation of soil cracking and the effect on surface runoff in a Texas Blackland Prairie Watershed. *Hydrological Processes* **19**(3): 589-603.

Babachev, A. A. 2003. IPI2 Win software, http;//geophys.geol.msu.ru

Bhatt, D. K. 1976. Stratigraphical status of Karewa Group of Kashmir, India. *Himalayan Geology* **6**: 197-208.

Bhatt, D. K. 1989. Lithostratigraphy of the Karewa Group, Kashmir valley, India and a critical review of its fossil record. *Memoirs of the Geological Survey of India* **122**:1-85.

Bhatnagar, S., Taloor, A.K., Roy, S. and Bhattacharya, P. 2022. Delineation of aquifers favorable for groundwater development using Schlumberger configuration resistivity survey techniques in Rajouri district of Jammu and Kashmir, India. *Groundwater for Sustainable Development*, **17**:100764.

Bhattacharya, A.K. 2010. Artificial ground water recharge with a special reference to India. *International Journal of Research and Reviews in Applied Sciences* **4**(2): 214-221.

Blanco-Gomez, P., Jimeno-Saez, P., Senent-Aparicio, J. and Perez-Sanchez, J. 2019. Impact of climate change on water balance components and droughts in the Guajoyo River Basin (El Salvador). *Water*, **11**(11): 2360.

Bokar, H., Mariko, A., Bamba, F., Diallo, D., Kamagate, B., Dao, A., Soumare, O. and Kassogue, P. 2012. Impact of climate variability on groundwater resources in Kolondieba Catchment Basin, Sudanese Climate Zone in Mali. *International journal of engineering research and applications* **2**: 1201-1210.

Bruijnzeel, L. A. and Bremmer, C. N. 1989. Highland-lowland interactions in the Ganges Brahmaputra River Basin: A review of published literature. ICIMOD Occassional Paper No. 11. Kathmandu, Nepal: International Centre for Integrated Mountain Development (ICIMOD). *Current Science* 95(12): 1688-1693.

Bouaamlat, I., Larabi, A. and Faouzi, M. 2016. Hydrogeological investigation of an oasis-system aquifer in arid southeastern Morocco by development of a groundwater flow model. *Hydrogeology Journal* **24**(6): 1479-1496.

Brar, M. S., Aggarwal, R. and Kaur, S. 2016. GIS-based investigations on groundwater behavior in Indian Punjab. *Agricultural Research Journal* **53**(4): 519-523.

Brouyere, S., Carabin, G. and Dassargues, A. 2004. Climate change impacts on groundwater resources: modelled deficits in a chalky aquifer, Geer basin, Belgium. *Hydrogeology Journal* **12**(2): 123-134.

Chandler, K. R. and Chappell, N. A. 2008. Influence of individual oak (Quercus robur) trees on saturated hydraulic conductivity. *Forest Ecology and Management*, **256**(5): 1222-1229.

Chandniha, S. K. and Kansal, M. L. 2016. Rainfall estimation using multiple linear regression based statistical downscaling for Piperiya watershed in Chhattisgarh. *Journal of Agrometeorology* **18**(1): 106-112.

Chaturvedi, R. S. 1973. A note on the investigation of ground water resources in westerndistrictsof Uttar Pradesh. *Annual Report. U.P. Irrigation Research Institute, Roorkee* 86-122.

Chaturvedi, R. K., Joshi, J., Jayaraman, M., Bala, G. and Ravindranath, N. H. 2012. Multi-model climate change projections for India under representative concentration pathways. *Current Science* 791-802.

Chapagain, P. S., Ghimire, M. and Shrestha, S. 2019. Status of natural springs in the Melamchi region of the Nepal Himalayas in the context of climate change. *Environment, Development and Sustainability* **21**(1): 263-280.

Chinnasamy, P. 2012. Measuring and modeling water and nutrient flux between a mid-Missouri stream and forested riparian zone in the central US (Doctoral dissertation, University of Missouri--Columbia).

Chinnasamy, P. and Hubbart, J.A. 2014a. Measuring and modeling shallow groundwater flow between a semi-karst border stream and Ozark forested

riparian zone in the central USA. *Journal of Scientific Research and Reports* **3**(6): 844-865.

Chinnasamy, P. and Hubbart, J.A. 2014b. Potential of MODFLOW to model hydrological interactions in a semikarst floodplain of the ozark border forest in the central United States. *Earth Interactions* **18**(20): 1-24.

Chinnasamy, P. and Prathapar, S. A. 2016. Methods to investigate the hydrology of the Himalayan springs: a review. International Water Management Institute (IWMI), 169.

Croley, T. E. and Luukkonen, C. L. 2003. Potential effects of climate change on ground water in Lansing, Michigan. *Journal of the American Water Resources Association* **39**(1): 149-163.

Crosbie, R. S., Scanlon, B. R., Mpelasoka, F. S., Reedy, R. C., Gates, J. B. and Zhang, L. 2013. Potential climate change effects on groundwater recharge in the High Plains Aquifer, USA. *Water Resources Research* **49**(7): 3936-3951.

Copeland, R. E. 2003. Florida spring classification system and spring glossary. Special Publication No. 52:17.

Dar, M. U. D., Aggarwal, R. and Kaur, S. 2018. Comparing bias correction methods in downscaling meteorological variables for climate change impact study in Ludhiana, Punjab. *Journal of Agrometeorology* **20**(2): 126-130.

Dams, J., Woldeamlak, S. T. and Batelaan, O. 2007. Forecasting land-use change and its impact on the groundwater system of the Kleine Nete catchment, Belgium. *Hydrology and Earth System Sciences Discussions* **4**(6): 4265-4295.

Dabiri, D., Alipor, A., Fatahi, A. and Azad, B. 2016. Suitable areas determination for rainwater harvesting (Case study: Kerman Province). *International Journal of Engineering and Advanced Research Technolog* **2**(4): 10-14.

De Roo, A., Odijk, M., Schmuck, G., Koster, E. and Lucieer, A. 2001. Assessing the effects of land use changes on floods in the Meuse and Oder catchment. *Physics and Chemistry of the Earth, Part B: Hydrology, Oceans and Atmosphere* **26**(7): 593-599.

Dickinson, R. E., Errico, R. M., Giorgi, F. and Bates, G. T. 1989. A regional climate model for the western United States. *Climatic change*, **15**(3): 383-422.

Dinesh Kumar, P. K., Gopinath, G. and Seralathan, P. 2007. Application of remote sensing and GIS for the demarcation of GWP zones of a river basin in Kerala, southwest coast of India.*International Journal of Remote Sensing* **28**(24): 5583-5601.

Dolman, A. J., Nabuurs, G. J., Kuikman, P .K., Hutjes, R. W. A., Huygen, J., Verhagen, A. and Vleeshouwers, L. M. 2003. Land use and terrestrial carbon sinks. *Global environmental change and land use* 111-136.

Doummar, J., Sauter, M. and Geyer, T. 2012. Simulation of flow processes in a large scale karst system with an integrated catchment model (Mike She)–Identification of relevant parameters influencing spring discharge. *Journal of Hydrology* **426**: 112-123.

Du Plessis, A. 2017. Freshwater Challenges of South Africa and Its Upper Vaal River Berlin, Germany:29-151.

Eckhardt, K. and Ulbrich, U. 2003. Potential impacts of climate change on groundwater recharge and streamflow in a central European low mountain range. *Journal of Hydrology* **284**(1): 244-252.

El-Baz, F., Himida, I., Kusky, T. and Fielding, L. 1995. Groundwater potential of the Sinai Peninsula, Egypt: United State Agency for International Development, Cairo, Egypt.Project Summery.

Elango, L. and Sivakumar, C. 2008. Regional simulation of a groundwater flow in coastal aquifer, Tamil Nadu, India. *Groundwater Dynamics in Hard Rock Aquifers*:234-242.

El-Yaouti, F., El-Mandour, A., Khattach, D. and Kaufmann, O. 2008. Modelling groundwater flow and advective contaminant transport in the Bou-Areg unconfined aquifer (NE Morocco). *Journal of Hydro-environment Research* **2**(3): 192-209.

Entekhabi, D., Yueh, S., O'Neill, P. E., Kellogg, K. H., Allen, A., Bindlish, R., Brown, M., Chan, S., Colliander, A., Crow, W. T. and Das, N. 2014. SMAP handbook–soil moisture active passive: Mapping soil moisture and freeze/thaw from space.

Famiglietti, J. S. 2014. The global groundwater crisis. *Nature Climate Change* **4**(11): 945-948.

Faramarzie, M., Abbaspour, K. C., Vaghefi, S. A., Farzaneh, M. R., Zehnder, A. J., Srinivasan, R. and Yang, H. 2013. Modeling impacts of climate change on freshwater availability in Africa. *Journal of Hydrology* **480**: 85-101.

Fentaw, F., Mekuria, B. and Arega, A. 2018. Impacts of climate change on the water resources of Guder Catchment, Upper Blue Nile, Ethiopia. *Waters* **1**(1): 16-29.

Fey, M. 2010. Soils of South Africa . Cape Town: CambridgeUniversity Press

Ficklin, D. L., Luedeling, E. and Zhang, M. 2010. Sensitivity of groundwater recharge under irrigated agriculture to changes in climate, CO_2 concentrations and canopy structure. *Agricultural Water Management* **97**(7): 1039-1050.

Fowler, H. J., Blenkinsop, S. and Tebaldi, C. 2007. Linking climate change modelling to impacts studies: recent advances in downscaling techniques for

hydrological modelling. *International Journal of Climatology: A Journal of the Royal Meteorological Society* **27**(12): 1547-1578.

Gaur, S., Chahar, B. R. and Graillot, D. 2011. Combined use of groundwater modeling and potential zone analysis for management of groundwater. *International Journal of Applied Earth Observation and Geoinformation*, **13**(1): 127-139.

Gedebo, A., Appelgren, M., Bjornstad, A. and Tsegaye, A. 2006. Genetic diversity and differentiation of cultivated amochi (Arisaemaschimperianum Schott) in Ethiopia as revealed by AFLP markers. *Hereditas* **143**: 229-235.

Ghimire, M., Chapagain, P. S. and Shrestha, S. 2019. Mapping of groundwater spring potential zone using geospatial techniques in the Central Nepal Himalayas: a case example of Melamchi–Larke area. *Journal of Earth System Science* **128**(2): 1-24.

Ghoraba, S. M. 2015. Hydrological modeling of the Simly Dam watershed (Pakistan) using GIS and SWAT model. *Alexandria Engineering Journal* **54**(3): 583-594.

Giorgi, F. 1990. Simulation of regional climate using a limited area model nested in a general circulation model. *Journal of Climate* **3**(9): 941-963.

Gleick, P. H. 1989. Climate change, hydrology, and water resources. *Reviews of Geophysics* **27**(3): 329-344.

Goyal, M. K. and Ojha, C. S. P. 2010. Evaluation of various linear regression methods for downscaling of mean monthly precipitation in arid Pichola watershed. *Natural Resources* **1**(01): 11-18.

Gosain, A. K., Rao, S. and Basuray, D. 2006, Climate change impact assessment on hydrology of Indian river basins, *Current Science* 90(3): 346-353.

Gull, S., Ahangar, M. A. and Dar, A. M. 2017. Prediction of stream flow and sediment yield of Lolab watershed using SWAT model. *Hydrology:Current Research* **8**(01): 1-9.

Guzman, J. A., Moriasi, D. N., Gowda, P. H., Steiner, J. L., Starks, P. J., Arnold, J. G. and Srinivasan, R. 2015. A model integration framework for linking SWAT and MODFLOW. *Environmental Modelling & Software* **73**: 103-116.

Harbaugh, A. W., Banta, E. R., Hill, M. C. and Mc Donald, M. G. 2000. MODFLOW-2000, The U. S. Geological Survey Modular Ground-Water Model-User Guide to Modularization Concepts and the Ground-Water Flow Process. *Open-file Report. U. S. Geological Survey* **92**: 134.

Hewitson, B. C. and Crane, R. G. 2006. Consensus between GCM climate change projections with empirical downscaling: precipitation downscaling over South Africa. *International Journal of Climatology: A Journal of the Royal Meteorological Society* **26**(10): 1315-1337.

Hostetler, S. W., Bartlein, P. J., Clark, P. U., Small, E. E. and Solomon, A. M. 2000. Simulated influences of Lake Agassiz on the climate of central North America 11,000 years ago. *Nature* **405**(6784): 334-337.

Holman, I. P. 2006. Climate change impacts on groundwater recharge-uncertainty, shortcomings, and the way forward. *Hydrogeology journal* **14**(5): 637–647.

ICIMOD (International Centre for Integrated Mountain Development). 2015. Reviving the drying springs: Reinforcing social development and economic growth in the midhills of Nepal. Issue Brief – February 2015. Kathmandu Nepal: ICIMOD.

Ilstedt, U., Bargues Tobella, A., Bazie, H.R., Bayala, J., Verbeeten, E., Nyberg, G., Sanou, J., Benegas, L., Murdiyarso, D., Laudon, H. and Sheil, D. 2016. Intermediate tree cover can maximize groundwater recharge in the seasonally dry tropics. *Scientific reports* **6**(1): 1-12.

IPCC. 2000. Nebojsa Nakicenovic and Rob Swart (Eds.) Cambridge University Press, UK. pp 570 Available from Cambridge University Press.

IPCC. 2001. Climate Change 2001: The Scientific Basis. Contribution of Working Group I to the Third Assessment Report of the Intergovernmental Panel on Climate Change.

IPCC. 2014. Climate change 2014 synthesis report. *IPCC: Geneva, Szwitzerland*.

Ines, A. V. and Hansen, J. W. 2006. Bias correction of daily GCM rainfall for crop simulation studies. *Agricultural and forest meteorology* **138**(1-4): 44-53.

Jalota, S. K., Kaur, H., Ray, S. S., Tripathi, R., Vashisht, B. B. and Bal, S. K. 2012. Mitigating future climate change effects by shifting planting dates of crops in rice–wheat cropping system. *Regional Environmental Change* **12**(4): 913-922.

Jones, P. G. and Thornton, P. K. 2013. Generating downscaled weather data from a suite of climate models for agricultural modelling applications. *Agricultural Systems* **114**: 1-5.

Jyrkama, M. I. and Sykes, J. F. 2007. The impact of climate change on spatially varying groundwater recharge in the grand river watershed (Ontario). *Journal of Hydrology* **338**(3): 237-250.

Karanth, K. R. 1987. Ground Water Assessment Development and Management New York: McGraw-Hill.

Kaur, H., Jalota, S. K., Kanwar, R. and Bhushan Vashisht, B. 2012. Climate change impacts on yield, evapotranspiration and nitrogen uptake in irrigated maize (Zea mays)-wheat (Triticum aestivum) cropping system: A simulation analysis. *Indian Journal of Agricultural Sciences* 82(3): 213.

Kaur, S. 2013.Modeling the impact of climate change on groundwater resources in central Punjab. Ph.D. Dissertation, Punjab Agricultural University, Ludhiana, Punjab, India.

Khan, S., Rana, T., Ullah, K., Christen, E. and Nafees, M. 2003. Investigating conjunctive water management options using a dynamic surface-groundwater modelling approach: a case study of Rechna Doab.

Kirshen, P. H. 2002. Potential impacts of global warming on groundwater in eastern Massachusetts. *Journal of Water Resources Planning and Management* **128**(3): 216-226.

Kim, N. W., Chung, I. M., Won, Y. S. and Arnold, J. G. 2008. Development and application of the integrated SWAT–MODFLOW model. *Journal of hydrology* **356**(1-2): 1-16.

Kouchi, D. H., Esmaili, K., Faridhosseini, A., Sanaeinejad, S. H., Khalili, D., Abbaspour, K. C. 2017. Sensitivity of calibrated parameters and water resource estimates on different objective functions and optimization algorithms. *Water* **9**(6): 384.

Krishnamurthy, J. and Srinivas, G. 1995. Role of geological and geomorphological factors in groundwater exploration: A study using IRS LISS II data. *International Journal of Remote Sensing* **16**(14): 2595-2618.

Krois, J. and Schulte, A. 2013. Modeling the hydrological response of soil and water conservation measures in the Ronquillo watershed in the Northern Andes of Peru. *6th International conference on water resources and environment research*: 147-184.

Kumar, A., Tomar, S. and Prasad, L. B. 1999. Analysis of fractures inferred from DBTM and remotely sensed data for Groundwater development in Godavari sub-watershed, Giridih, Bihar. *Journal of Indian Society of Remote Sensing* **27**(2): 105-114.

Kumar, K. R., Sahai, A. K., Kumar, K. K., Patwardhan, S. K., Mishra, P. K., Revadekar, J. V., Kamala, K. and Pant, G.B. 2006. High-resolution climate change scenarios for India for the 21st century. *Current science*: 334-345.

Kumar, K. K., Patwardhan, S. K., Kulkarni, A., Kamala, K., Rao, K. K. and Jones, R. 2011. Simulated projections for summer monsoon climate over India by a high-resolution regional climate model (PRECIS). *Current Science*: 312-326.

Kumar, S. N., Aggarwal, P. K., Rani, S., Jain, S., Saxena, R. and Chauhan, N. 2011. Impact of climate change on crop productivity in Western Ghats, coastal and northeastern regions of India. *Current Science*: 332-341.

Kumar, C. P. 2012. Assessment of Impact of Climate Change on Groundwater Resources. *Water and Energy International* **69**(8): 25-31.

Kumar, C. P. 2013. Numerical modelling of Groundwater flow using MODFLOW. *Indian Journal of Science* 2: 86-92.

Kumar, V. and Sen, S. 2020. Assessment of spring potential for sustainable agriculture: a case study in lesser Himalayas. *Applied engineering in agriculture* **36**(1): 11-24.

Kushwaha, R. K., Pandit, M. K. and Goyal, R. 2009. MODFLOW based groundwater resource evaluation and prediction in Mendha sub-basin, NE Rajasthan. *Journal of the Geological Society of India* **74**(4): 449-458.

Lenderink, G., Buishand, A. and Van Deursen, W. 2007. Estimates of future discharges of the river Rhine using two scenario methodologies: direct versus delta approach. *Hydrology and Earth System Sciences*, **11**(3): 1145-1159.

Leander, R. and Buishand, T.A. 2007. Resampling of regional climate model output for the simulation of extreme river flows. *Journal of Hydrology* **332**(3-4): 487-496.

Liu, J., Chen, S., Li, L. and Li, J. 2017. Statistical downscaling and projection of future air temperature changes in Yunnan Province, China. *Advances in Meteorology* 2017: 1-11.

Limbrick, K. J., Whitehead, P. G., Butterfield, D. and Reynard, N. 2000. Assessing the potential impacts of various climate change scenarios on the hydrological regime of the River Kennet at Theale, Berkshire, south-central England, UK: an application and evaluation of the new semi-distributed model, INCA. *Science of the total environment* **251**: 539-555.

Loaiciga, H. A., Maidment, D. R. and Valdes, J. B. 2000. Climate-change impacts in a regional karst aquifer, Texas, USA. *Journal of Hydrology* **227**(1): 173-194.

Loke, M. H. and Barker, R. D. 1996. Rapid least-squares inversion of apparent resistivity pseudosections by a quasi-Newton method1. *Geophysical prospecting* **44**(1): 131-152.

Malczewski, J. 2004. GIS-based land-use suitability analysis: a critical overview. *Progress in planning* 62(1): 3-65.

Mahamuni, K. and Kulkarni, H. 2012. Groundwater resources and spring hydrogeology in South Sikkim, with special reference to climate change. *Climate change in Sikkim-Patterns, impacts and initiatives*: 261-274.

Mall, R. K., Singh, R., Gupta, A., Srinivasan, G. and Rathore, L.S. 2006. Impact of climate change on Indian agriculture: a review. *Climatic change* **78**(2): 445-478.

Maurer, E. P. and Hidalgo, H. G. 2008. Utility of daily vs. monthly large scale climate data: An intercomparison of two statistical downscaling methods. *Hydrology and Earth System Sciences* 12: 551-63.

Mwega, W. B., Mati, B. M., Mulwa, J. K. and Kituu, G. M. 2013. Identification of groundwater potential zones using remote sensing and GIS in Lake Chala watershed, Kenya. *Proceedings of Sustainable Research and Innovation Conference* 42-46.

Mbilinyi, B. P., Tumbo, S. D., Mahoo, H. and Mkiramwinyi, F. O. 2007. GIS-based decision support system for identifying potential sites for rainwater harvesting. *Physics and Chemistry of the Earth, Parts A/B/C* **32**(15-18): 1074-1081.

McDonald, M. G. and Harbaugh, A. W., 1988. A modular three-dimensional finite-difference ground-water flow model. *US Geological Survey* , Book 6, Chapter A1.

Mousavi, S. M., Golkarian, A., Naghibi, S. A., Kalantar, B. and Pradhan, B. 2017. GIS-based groundwater spring potential mapping using data mining boosted regression tree and probabilistic frequency ratio models in Iran. *AIMS Geosciences* **3**(1): 91-115.

McGuffie, K. and Henderson, S. A. 1997. A climate modeling primer. John Wiley & Sons Ltd, Chuchester: 253.

Miglani, P., Aggarwal, R. and Kaur, S. 2015. Groundwater Simulation Model for Sirhind Canal Tract of Punjab. *Journal of Engineering and Technology* **5**(1): 31.

Millennium Ecosystem Assessment, 2005. Ecosystems and Human Well-being: Synthesis. *Island Press, Washington, DC*.

Moscrip, A. L. and Montgomery, D. R. 1997.Urbanization flood frequency and salmon abundance in Puget Lowlan Streams. *Journal of American Water Resources Association* **33**(6): 1289- 1297.

Moss, R. 2010. A new approach to scenario development for the IPCC Fifth Assessment Report. *Nature* 463: 747-756.

Molobela, I. P. and Sinha, P. 2011. Management of water resources in South Africa: A review. *African Journal of Environmental Science and Technology* **5**(12): 993-1002.

Mukherjee, D. 2016. A review on artificial groundwater recharge in India. *SSRG International Journal of Civil Engineering* **3**(1): 57.

Munyao, J. N., Mannaerts, C. M. M. and Krol, M. 2010. Use of satellite products to assess water harvesting potential in remote areas of Africa. *Land Degradation & Development* **22**: 359-372.

Nag, S. K. and Ghosh, P. 2013. Delineation of groundwater potential zone in Chhatna Block, Bankura District, West Bengal, India using remote sensing and GIS techniques. *Environmental earth sciences* **70**(5): 2115-2127.

NDF (Nordic Development Fund). 2014. Strategic technical assistance to support the building climate resilience of watersheds in mountain eco-regions project. Finland: Nordic Development Fund (NDF).

Negi, G. C. 2002. Hydrological research in the Indian Himalayan mountains: Soil and water conservation. *Current Science*: 974-980.

Negi, H. S., Thakur, N. K. and Mishra, V. D. 2007. Estimation and validation of snow surface temperature using MODIS data for snow-avalanche studies in NW-Himalaya. *Journal of the Indian Society of Remote Sensing* **35**(4): 287-299.

Neff, R., Chang, H., Knight, C. G., Najjar, R. G., Yarnal, B. and Walker, H.A. 2000. Impact of climate variation and change on Mid-Atlantic Region hydrology and water resources. *Climate Research* **14**(3): 207-218.

NITI, Aayog. 2017. Report of Working Group I - Inventory and revival of springs in the Himalayas for water security. NITI Aayog India.

Onta, P. R. and Gupta, A. D. 1995. Regional management modeling of a complex groundwater system for land subsidence control. *Water resources management* **9**(1): 1-25.

Orellena, E. and Mooney, H. M. 1966. Master tables and curves of vertical electrical sounding over layered structures, *Interciencia, Madrid, Spain*: 150-166.

Osman, Y. Z. and Bruen, M. P. 2002. Modelling stream–aquifer seepage in an alluvial aquifer: an improved loosing-stream package for MODFLOW. *Journal of Hydrology* **264**(1): 69-86.

Pandit, B. H., Wagley, M. P., Neupane, R. P. and Adhikary, B. R. 2007. Watershed management and livelihoods: Lessons from Nepal. *Journal of Forest and Livelihood* **6**(2): 67-75.

Parmar, M. K. Negi, R. S. and Purohit, K. 2016. Geohydrology of springs in a mountain watershed: A case study of Takoli Gad watershed Garhwal Himalay. *I.J. of Current Engineering and Technolog* **6**(1): 26-30.

Piani, C., Haerter, J.O. and Coppola, E. 2010. Statistical bias correction for daily precipitation in regional climate models over Europe. *Theoretical and Applied Climatology* **99**(1): 187-192.

Querner, E. P., Tallaksen, L. M., Kasparek, L. and Van-Lanen, H. A. J. 1997. Impact of land-use, climate change and groundwater abstraction on streamflow droughts using physically-based models. *IAHS publication*: 171-180.

Rana, S. and Gupta, V. 2009. Watershed management in the Indian Himalayan region: Issues and challenges. In *World Environmental and Water Resources Congress, Great Rivers*: 1-12.

Ranjan, P., Kazama, S. and Sawamoto, M. 2006. Effects of climate change on coastal fresh groundwater resources. *Global Environmental Change* **16**(4): 388-399.

Rao, J. P., Harikrishna, R. and Rao, B. S. 2004. An integrated study on groundwater resources of PeddaGedda watershed. *Journal of Indian Society of Remote Sensing* **32**(3): 307-311.

Rawat, P. K., Tiwari, P. C. and Pant, C. C., 2011. Climate change accelerating hydrological hazards and risks in Himalaya: A case study through remote sensing and GIS modeling. *International Journal of Geomatics and Geosciences*, **1**(4): 678.

Reeve, A. S., Warzocha, J., Glaser, P. H., and Siegel, D. I. 2001. Regional ground-water flow modeling of the Glacial Lake Agassiz Peatlands, Minnesota. *Journal of Hydrology* **243**(1): 91-100.

Rosenberg, N. J., Epstein, D. J., Wang, D., Vail, L., Srinivasan, R. and Arnold, J. G. 1999. Possible impacts of global warming on the hydrology of the Ogallala aquifer region. *Climatic Change* **42** (4): 677-692.

Saha, A. K., Arora, M. K., Csaplovics, E. and Gupta, R. P. 2005. Land cover classification using IRS LISS III image and DEM in a rugged terrain: a case study in Himalayas. *Geocarto International* **20**(2): 33-40.

Saraf, A. K. and Choudhury, P. R. 1998. Integrated remote sensing and GIS for groundwater exploration and identification of artificial recharge sites. *International journal of Remote sensing* **19**(10): 1825-1841.

Sarkar, B. C., Deota, B. S., Raju, P. L. N. and Jugran, D. K. 2001. A geographic information system approach to evaluation of groundwater potentiality of Shamri micro-watershed in the Shimla Taluk, Himachal Pradesh. *Journal of the Indian Society of Remote sensing* **29**(3): 151-164.

Sitender, R. 2010. Delineation of groundwater potential zones in Mewat District, Haryana, India. *International journal of geomatics and geosciences* **2**(1): 270-281.

Schuol, J., Abbaspour, K. C., Yang, H., Srinivasan, R. and Zehnder, A. J. 2008. Modeling blue and green water availability in Africa. *Water resources research* **44**(7).

Scibek, J. and Allen, D. M. 2006a. Comparing modelled responses of two high-permeability, unconfined aquifers to predicted climate change. *Global and Planetary Change* **50**(1): 50-62.

Scibek, J. and Allen, D. M. 2006. Modeled impacts of predicted climate change on recharge and groundwater levels. *Water Resources Research* **42**(11): 405-423.

Scibek, J., Allen, D. M., Cannon, A. J. and Whitfield, P. 2006. Groundwater surface water interaction under scenarios of climate change using a high resolution transient groundwater model. *Journal of Hydrology* **333**(2-4): 165-181.

Senanayake, I. P., Dissanayake, D. M., Mayadunna, B. B. and Weerasekera, W. L. 2016. An approach to delineate groundwater recharge potential sites in Ambalantota, Sri Lanka using GIS techniques. *Geoscience Frontiers* **7**(1): 115-124.

Senthilkumar, M. and Elango, L. 2004. Three-dimensional mathematical model to simulate groundwater flow in the lower Palar River basin, southern India. *Hydrogeology Journal* **12**(2): 197-208.

Setegn, S. G., Srinivasan, R. and Dargahi, B. 2008. Hydrological modelling in the Lake Tana Basin, Ethiopia using SWAT model. *The Open Hydrology Journal* **2**(1).

Setegn, S. G., Rayner, D., Melesse, A. M., Dargahi, B. and Srinivasan, R. 2011. Impact of climate change on the hydroclimatology of Lake Tana Basin, Ethiopia. *Water Resources Research* **47**(4).

Sherif, M. M. and Singh, V. P. 1999. Effect of climate change on sea water intrusion in coastal aquifers. *Hydrological Processes* **13**(8): 1277-1287.

Shams, S., Chen, D., Arevalo, J., Leone, A. and Moreno, C. C. 2013. Water balance study: an application of WPS technologies training manual. *European Commission, Luxembourg*.

Shafi, M. 2020. Assessment of climate change impacts on runoff and sediment yield of Leh watershed using SWAT model. *M.Tech Thesis, SKUAST Kashmir*.

Singh, A. and Gosain, A. K. 2011. Scenario generation using geographical information system (GIS) based hydrological modelling for a multijurisdictional Indian River basin. *Journal of Oceanography and Marine Science* **2**(6): 140-147.

Singh, S. and Kumar, C. P. 2011. Impact of Climate Change on Dynamic Groundwater System in a Drought Prone Area: part-II. National Institute of Hydrology (Roorkee).

Singhal, B. B. S. and Gupta, R. P. 2010. *Applied hydrogeology of fractured rocks*. Springer Science & Business Media.

Singhal, D. C., Israil, M., Sharma, V. K. and Kumar, B. 2010. Evaluation of groundwater resource and estimation of its potential in Pathri Rao watershed, district Haridwar (Uttarakhand). *Current Science*: 162-170.

Siarkos, I. and Latinopoulos, P. 2012. Delineation of wellhead protection zones for the control of point pollution sources in the aquifer of N. Moudania, Greece.

Srinivas, G. and Naik, G. M. 2017. Hydrological Modeling of Musi River Basin, India and Sensitive Parameterization of Stream Flow Using SWAT CUP. *Journal of Hydrogeology and Hydrologic Engineering* **6**: 2-10.

Srivastava, R. K., Sharma, H. C. and Raina, A. K. 2010. Suitability of soil and water conservation measures for watershed management using geographical information system. *Journal of Soil and Water Conservation* **9**(3): 148-153.

Sokolov, A. A. and Chapman, T. G. 1974. Methods for water balance computations;an international guide for research and practice-a contribution to the International Hydrological Decade. *Paris, France: the UNESCO Press*.

Sudhakar, S., Verma. M. K, and Singha. S. 2016. Application of GIS and MODFLOW to Ground Water Hydrology-A Review. *Int. Journal of Engineering Research and Applications* **6**: 36-42.

Suryabhagavan, K. V. 2017. Application of remote sensing and GIS for groundwater potential zones identification in Bata river basin, Himachal Pradesh, India. *Indian Society of Geomatics*, **11**(1).

Tambe, S., Kharel, G., Arrawatia, M. L., Kulkarni, H., Mahamuni, K. and Ganeriwala, A.K. 2012. Reviving dying springs: climate change adaptation experiments from the Sikkim Himalaya. *Mountain Research and Development* **32**(1): 62-72.

Tesfaye, T. 2010. Groundwater potential evaluation based on integrated GIS and RS techniques in Bilate river catchment, South rift valley of Ethiopia. *American Scientific Research Journal for Engineering Technology and Sciences* **10**(1): 85-120.

Toews, M. W. and Allen, D. M. 2009. Simulated response of groundwater to predicted recharge in a semi-arid region using a scenario of modelled climate change. *Environmental Research Letters* **4**(3): 035003.

UNESCO, 2011. The impact of global change on water resources: The response of UNESCO's international hydrological program. *UNESCO Paris, France.*

UNCCD (United Nations Convention to Combat Desertification). 2017. *The global land outlook, first edition. Bonn, Germany.*

Valdiya, K. S. and Bartarya, S. K., 1989. Diminishing discharges of mountain springs in a part of Kumaun Himalaya. *Current science* **58**(8): 417-426.

Vandam, J. C., and Meulankamp, J. J. 1967. Some results of geoelectrical resistivity method in groundwater investigations in the Netherlands. *Geophysical Prospecting* **15**: 92-115.

Vashisht, A. K. and Sharma, H. C. 2007. Study on hydrological behaviour of a natural spring. *Current Science*: 837-840.

Vashisht, A. K. 2008. Ingenious techniques for irrigation sustainability in Himalayan and Shiwalik foothill regions. *Current Science*: 1688-1693.

Wadia, D. N. 1975. Geology of India, 4th edition, Tenth reprint (1989) *Tata McGrawHill Publishing Co., New Delhi*.

Wilby, R. L. and Wigley, T. M. 1997. Downscaling general circulation model output: a review of methods and limitations. *Progress in physical geography* **21**(4): 530-548.

Wilby, R. L., Troni, J., Biot, Y., Tedd, L., Hewitson, B. C., Smith, D. M. and Sutton, R. T. 2009. A review of climate risk information for adaptation and development planning. *International Journal of Climatology: A Journal of the Royal Meteorological Society* **29**(9): 1193-1215.

Wilkinson, W. B. and Cooper, D. M. 1993. The response of idealized aquifer/river systems to climate change. *Hydrological sciences journal 38*(5): 379-390.

Wood, A. W., Leung, L. R., Sridhar, V. and Lettenmaier, D. P. 2004. Hydrologic implications of dynamical and statistical approaches to downscaling climate model outputs. *Climatic change* **62**(1): 189-216.

Woldeamlak, S. T., Batelaan, O. and De Smedt, F. 2007. Effects of climate change on the groundwater system in the Grote-Nete catchment, Belgium. *Hydrogeology Journal* **15**(5): 891-901.

Xu, C. Y. 2000. Climate change and hydrologic models: A review of existing gaps and recent research developments. *Water Resources Management* **13**(5): 369-382.

Xu, X., Huang, G., Zhan, H., Qu, Z. and Huang, Q. 2012. Integration of SWAP and MODFLOW-2000 for modeling groundwater dynamics in shallow water table areas. *Journal of Hydrology* **412**: 170-181.

Yang, Y., Watanabe, M., Zhang, X., Hao, X. and Zhang, J. 2006. Estimation of groundwater use by crop production simulated by DSSAT-wheat and DSSAT-maize models in the piedmont region of the North China Plain. *Hydrological Processes: An International Journal* **20**(13): 2787-2802.

Zandi, J., Ghazvinei, P. T., Hashim, R., Yusof, K. B. W., Ariffin, J. and Motamedi, S. 2016. Mapping of regional potential groundwater springs using logistic regression statistical method. *Water Resources* **43**(1): 48-57.

Sher-e-Kashmir
University of Agricultural Sciences and Technology of Kashmir
Division of Soil & Water Conservation Engineering
College of Agriculture Engineering & Technology,
Faculty of Horticulture

C E R T I F I C A T E

Certified that all the corrections/amendments as suggested by External Examiner **Dr. Manzoor Ahmad Ahanger,** Professor & Head**,** National Institute of Technology, Srinagar, during Viva-Voce examination held on 20-10-2022, have been incorporated in the manuscript entitled **"Assessment of Hydrogeological Characterization and Modelling of Springsheds in a Changing Environment of Central Kashmir"** submitted by **Mr. Syed Rouhullah Ali (Regd. No. 2018-815-D).**

(Dr. Junaid N. Khan)
Chairman
Advisory Committee